Quantitative evaluation of debris flow hazard using depth-integrated particle method and satellite image

July 2015

Ni Zhang

Quantitative evaluation of debris flow hazard using depth-integrated particle method and satellite image

Graduate School of Systems and Information Engineering

University of Tsukuba

July ２０１５

Ni Zhang

ABSTRACT

Debris flow is one of common and disastrous geo-hazards in mountainous area around the world. There are thousands of fatalities who were killed by debris flow every year. Due to its worldwide, destructive nature, complex material composition, wide occurrence area and long travel distance as well as uncertainty and unknown parameters, it's still a critical problem both theoretically and practically. It urged us to quantitative evaluate debris flow hazard to provide adequate prevention and mitigation measures.

In the present study, the mixing model based on two-step evaluation scheme was proposed to quantitatively evaluate the debris flow hazards in terms of affect areas, flow path, travel distance, critical slope of deposition, velocity, concentration and hydrograph in Zhouqu and Wenchuan earthquake-stricken areas using depth-integrated particle method and satellite images. The conclusions are summarized from the depth-integrated particle method, the mixing model, satellite image, parametric studies, and quantitative evaluation of debris flow hazards in Zhouqu and Wenchuan earthquake-stricken areas.

The depth-integrated particle method is a very simple and efficient method with only two parameters to simulate debris flows. The modified depth-integrated particle method was verified by two simple flows in 1-D. It can be applied to quantitatively evaluate actual debris flow hazards based on detailed DEM. The mixing model based on two-step evaluation scheme can efficiently evaluate the debris flows according to the diffusion equation. In the present model, diffusion coefficient was assumed to a constant in the whole simulation process. And one fitting coefficient was assumed to build the relationship between the critical deposition slope and concentration.

The satellite image of ALOS is characterized by wide coverage area and high spatial resolution. The images can be processed into detailed DEM with the resolution is less than 10m combined control points from the Google earth. The error of control points was evaluated in comparison with the topographic map, and it was acceptable in this study. The good quality images that were observed shortly after the earthquake are precious data for the sequence evaluation of disasters as well as reconstruction in the earthquake-stricken areas. It's available to check the location of debris sources by satellite image, but it's very hard to evaluate the volume of debris source only depending on satellite image.

By parametric studies, it's found that the accurate topographic data played a critical role in quantitative evaluating debris flow hazards in terms of affect area, travel distance, flow path. The discharge strongly governed the flow behavior on the deposition fan, while Manning coefficient influenced the velocity of debris flow. The critical slope of deposition and flow volume significant determined the travel distance and the extent of deposition.

The debris sources in Zhouqu debris flows were evaluated in terms of location and thickness

combined the post-event satellite image and filed survey. It's reasonable to evaluate debris sources in Zhouqu region by setting critical failure slope and repose of angle is 60º and 26º respectively. By assuming the initial particle height is 1.0m, the thickness of debris sources ranged 0-8m. Re-initiation model and mixing model were adopted to evaluate the Zhouqu debris flow hazard. It's found that the re-initiation model is very efficient with small particles, while the mixing model is rather time-consuming because of more than 2 or 3 times of solid particles were increased as water particles to initiate debris flow. The re-initiation model is suitable to evaluate the extent of deposition area and flow path on the deposition fan. Although two more additional parameters (diffusion coefficient and fitting coefficient for the relationship between critical deposition slope and concentration) were taken into account in the mixing model, it's reasonable to evaluate debris flow hazard to consider the physical properties of particles. Moreover, more local concentration-related phenomenon is also described in the mixing model. Affected area was evaluated using re-initiation model, the agreement is good on SYY and LJY deposition fan if the critical failure slope is set to 60º and 61.5º. The debris sources were initiated when the mean rainfall was 29.03mm at the upstream of valley and the diffusion coefficient was set to 0.1. A series of simulation results showed the difference of discharge on both valleys strongly influenced the debris flow hazard on deposition fan. Advantage topographic features, rich debris sources and rainstorm together triggered this debris flow event. The failure of some countermeasure structures and high population density enlarged the destructive nature to large extent.

Quantitative evaluation of debris flow hazards in the Wenchuan earthquake-stricken areas, it's found that almost every valley has potential high-risk to occur debris flow. The evaluation of earthquake-induced debris sources was focused on the Beichuan region, while the simulation concentrated on blocking river in the area from Yingxiu to Wenchuan along the Min River. It's hard to evaluate debris sources by a single critical failure slope in a wide region, particularly, an active fault crosses the research area. The evaluation results of debris sources strongly influenced the evaluation of regional debris flow hazards. The topographic features determined the debris flows in the ranges along Min River are easy to flow the river and the watershed features demonstrated that the debris flows are extremely easy to block river and form barrier lake due to 60% cross-angles ranged 80°-100°. Two patterns of blocking river were simulated and the coupling effect of multiple debris flows and two opposite debris flows occurred simultaneously are also evaluated. The simulation results indicated that such phenomenon would increase the possibility of blocking river. It must take measures to avoid such disasters to occur.

The parameters of quantitative evaluation of debris flow in terms of velocity, hydrograph, the extent of deposition, travel distance and flow path are favor to provide adequate protective measures to prevent and mitigate the disasters in practical engineering.

Content

List of Figures

List of Table

CHAPTER 1 INTRODUCTION

1.1 Research background

Debris flow is gravity-driven, highly concentrated mixtures of sediment and water commonly composed of poorly sorted rock, soil, organic matter, and sundry debris (Major, 1997). It usually occurred by rainfall, snowmelt, typhoon, earthquake, etc. in steep mountainous area around the world. It is often characterized by traveling hundreds of meters to tens of kilometers from initiation to final deposition, regarding occurrence process. Meanwhile, this process is a very important land shaping process in mountainous area because of frequent and intermittent erosion and deposition along the whole flow path. Considering its destructive nature, it usually destroyed humankind and fundamental infrastructures in mostly events. There are thousands of fatalities who were killed by debris flow every year. In particular, such as China (Zhouqu and Sichuan, 2010), Japan (Hiroshima, 2014), Brazil (Rio de Janeiro, 2010, 2011), Venezuela (Vargas State, 1999), Nepal (Seti River, 2012), India (Kedarnath, 2013), as well as France and Switzerland, it behaved more seriously in such mountainous or/and rich rainstorm countries. Figure 1.1 showed the distribution map of landslide occurrence frequency around the world (http://www.preventionweb.net/english/). Here, landslides contain debris flow, mud flow, mud slide, rock fall, slide, lahar, rock slide and topple

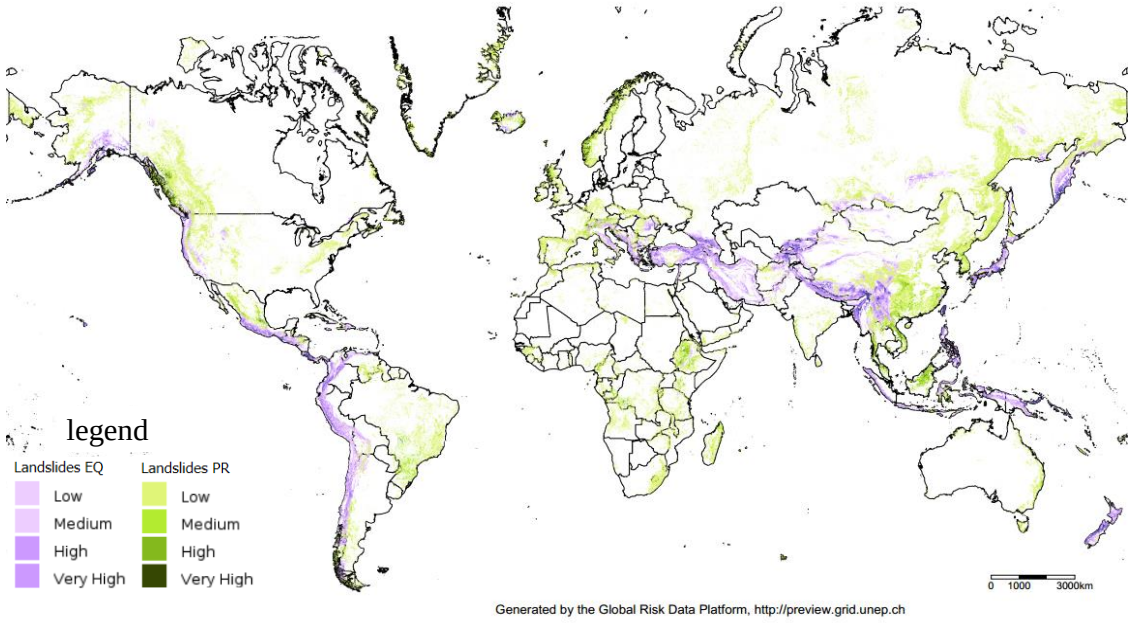

Note: Landslides EQ means the landslides frequency triggered by earthquake, while landslides PR means the landslides frequency triggered by precipitation.

Fig.1.1 The distribution map of landslides around the world

According to the occurrence factors of debris flow, where the overlapped areas by

high-frequency occurrence of both earthquake and precipitation high are extremely dangerous places, such as the southwest China, Japan. Actually, these areas will still face the seriously destroys in the future. As illustrated in the figure 1.2, the event number of kinds of catastrophes is still increasing, according to the number of events of natural catastrophes worldwide among 1980-2012 (http://www.preventionweb.net/english/). The geophysical events and hydrological events increased more rapidly than the other two types. However, the earthquake, tsunami and volcanic eruption are close relation to landslide, debris flows, etc. Such as, the 2008 Wenchuan Earthquake caused more than 30,000 landslides and rock falls, the 2011 Tohoku Earthquake triggered tsunami and further flooded very wide areas.

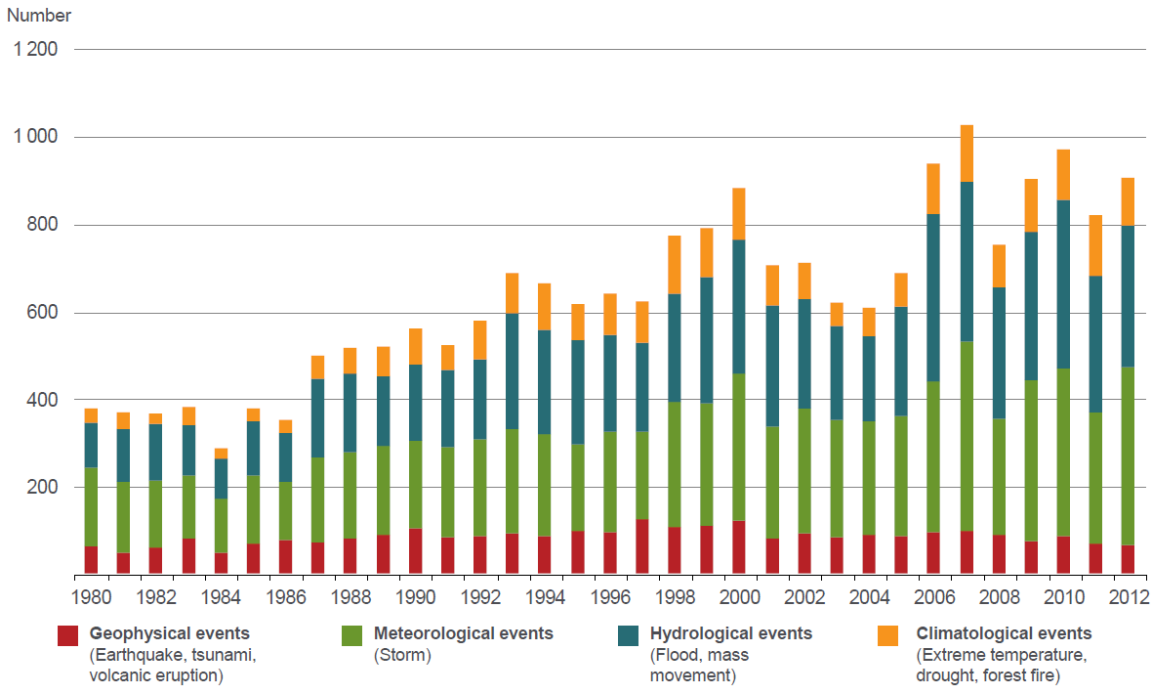

Fig.1.2 The number of events of natural catastrophes worldwide among 1980-2012

Due to its worldwide, destructive nature, complex material composition, wide occurrence area and long travel distance as well as uncertainty and unknown parameters, it's still a critical problem both theoretically and practically. It urged us to quantitative evaluate debris flow hazard to provide adequately prevention and mitigation measures. Nowadays the detailed digital elevation model is gradually available even in the remote mountainous area, such as aerial photos and satellite image. However, the simulation cost becomes expensive with such data, and an efficient numerical tool suitable for such simulation is required.

1.2 Current research of debris flow

In last century 30s, Chinese scientists began to realize the debris flow hazard, until 60s' they started

to wide study the essential physical properties of debris flow (Du, 1995). When the phenomenon of debris flows were recognized in Canada in the 1940s, however, most studies of the topic have been carried out since the early 1980s (Vandine & Bovis, 2002). In Japan, the scientific investigations of debris flow began in the1950s and full investigations were not undertaken until the 1970s (Takahashi, 2009). With the increasing of enormous threaten of natural geological disasters, the research work of debris flow is widely operated and gradually improved in the worldwide. The most comprehensive and detailed observations and mathematical-physical studies firstly have been conducted in Japan and China (Huttcr, 1996), especially in field observing and experiment research work.

1.2.1 Field survey and monitoring

Field survey is an original and direct way to understand the phenomenon of debris flow. Field surveys had been executed after the disaster. However, the surveys had supplied only the data of the results of erosion, deposition and damages brought about by debris flows in many single points. There was no actual data of debris flow motion. Furthermore, it's really a hard work because the observation place located in mountains and the ranges are wide Therefore monitoring of actual debris flows was required to obtain dynamic data for designing new effective countermeasure structures against the debris flows.

Field monitoring is one more effective way to help humankind recognize the entire process of debris flow. Meanwhile, it's a very important method to attain parameters of motion, deposition and destruction. Here I will briefly review on the development as well as outcomes of field monitoring by mainly introducing some contributions of two of famous field monitor stations for debris flow. One is the Yakedake monitoring station of Disaster Prevention Research Institute in Japan, and the other one is the Dongchuan debris flow observation and research station in China.

(1) Yakedake monitoring station

After a succession of serious debris-flow disasters in Japan in the late 60's, the practical importance of further attempts to understand the mechanics of debris flows is forced researchers to promote studies on debris flow. In order to monitor the actual phenomena of debris flow, Disaster Prevention Research Institute (DPRI) was constructed at Kamikamihorizawa Creek on the eastern slope of Mount Yakedake by Kyoto University and Matsumoto Sabo Construction Office of Ministry of Construction in 1970 (Suwa et al., 2011). The Mount Yakedake is a high frequency occurrence area of debris flow and there were large amount of volcano debris. During the last 40 years, they mainly monitored several topics, such as rheological type, pulsation, mass and boulder focusing, ground tremor and sound, test of moderation of debris flow discharge, etc. from 91 debris flow events that contained more than 200 episodes of debris-flow surges. Studies from the data supplied a general concept of the debris-flows and their geomorphic effects at volcanic slopes as follows. Such as, debris flows are triggered by a large intensity of rainfall in a short duration as much as 10 minute; threshold of rainfall intensity for debris flows increases with time after the end of volcanic eruption,

while it drastically decreases with the eruption (Suwa et al., 2011).

The DPRI also monitored other many areas cooperating with several countries. Such as with China (1991-1998), Indonesia (1991-1995), Pakistan (2000), etc. (Suwa et al., 2011). Large amount of monitoring works in wide and different zones provide much richer parameters and phenomenon characteristics to improve the research.

(2) Dongchuan debris flow observation and research station

The Dongchuan Debris Flow Observation and Research Station (DDFORS) is a facility of the institute of mountain hazards and environment, Chinese academy of science. The Jiangjia valley has provided an ideal site to explore debris flow formation and initiation in combination with a background of loose materials and rainfall. This is important for forecasting debris flow. The debris flows occurred more or less 11 times every year. Each debris flow event in the Jiangjia valley was consisted of tens of hundreds of surges, providing a wide variety of phenomenon that are rarely seen in other areas of the world. Observation data and videos of living debris flows in the Jiangjia valley are the most unique resource with contributing to future studies in the field.

The primary contribution of Jiangjia valley debris flow behaved on the following respects: relationships between rainfall and debris flow; dynamic properties (velocity, impact forces, super-elevation in channel bends); static properties (density and concentration, composition); sediment transportation and influence on the main river; deposition etc. (Cui, 2005).

In the last 40 years, two famous of monitoring stations provided much valuable videos which contribute us to analyze the motion of debris flow, and also obtained many important parameters, such as early cumulative rainfall, rainfall intensity, velocity, frontal velocity, peak velocity, peak flow depth, peak discharge and total discharge (Rickenmann, 2006), etc. The research results of flow behavior, characteristics, etc. were published in terms of papers, reports, books. The large amount of monitoring data improved the systematic research on debris flow. The existing researches illustrated that the observation results of both stations usually are used as a benchmark to validate the study results around the world. For the evaluation of debris flow hazards, many empirical equations were summarized or proposed to apply in practical engineering.

However, the majority of these studies put their large efforts on understanding the general characters of debris-flow travel processes. A systematic monitoring of debris-flow initiation, motion, inundation and deposition in the fan needs to be improved. Most of observation results, such as data from the Dongchuan observation station, haven’t been analyzed deeply. Although it’s possible to install advanced equipment on everywhere and observe the process of debris flow, a delimited direction and only surface characteristic is observed. Even some devastating incidents usually occurred in the evening, nothing was observed. The existing observation works only recorded in small places where they occurred frequently, and vertical variables such as total flow depth, vertical velocity distribution, and vertical variation of material composition have not yet been measured in a

moving debris flow (Davis, 1990).

Debris flow is a complex phenomenon, which strongly influenced by topographic characteristic, the amount and distribution features of debris sources and rainfall. It's not enough to observe the limited individual event and/or valley to study the general characteristics of debris flows. In particular, it's not possible to install monitoring equipment in every potential debris flow valley in developing countries at least nowadays. So far, the field observation only observe a limited section and instant phenomenon. It's hard to apply the results of observation to a wide area or a different region.

1.2.2 Experiment

As one of traditional and essential methods in exploring the unsolved questions and phenomena, experiment plays a significant role in studying debris flow. The experiment is mainly divided into laboratory experiment and field experiment.

Lots of different scale laboratory experiments and even field experiment were operated. As mentioned in the definition and characteristics of debris flow, it's composed of water and sedimentation that wide range from clay to boulder. The existing research demonstrated that the debris flow behavior was significant controlled by larger grains (Davies, 1990). The scale of laboratory experiment usually is very small and used particles distribution is monotonous. It also usually initiated on the steep place of mountain and transported even dozens of kilometers along a various channel. However, a simple channel was often adopted on a very small experiment zone. Perhaps, these works contribute us to understand the local features of debris flow, but it ignored the scaling effect and topographic features.

Field experiment scale is larger than laboratory experiments. One of famous field experiments is debris-flow flume experiment in U.S. The U.S. Geological Survey (USGS) debris-flow flume, a steep concrete channel 95 m long, 2 m wide, and 1.2 m deep (Iverson et al., 1992; Iverson and Lahusen, 1993a) (Fig.1.3). The channel slopes 31° along its upper 88m and gradually flattens over the lower 7 m to adjoin a concrete runout surface that slopes 3°. To create a debris flow, sediment was loaded behind a steel gate at the head of the flume, soaked with water, and abruptly released.

In last dozens of years, they did large amounts of experiments about debris flow and dam breach, meanwhile, they obtained many valuable conclusions. Detailed references can see Richard M. Iverson. He and Matthew Logan summarized the output of experiment videos and opened a set of videos presents about 17 hours of footage documenting the 146 experiments conducted at the USGS debris-flow flume from 1992 to 2013. However, the flume size is rather small compared natural debris flow event. Moreover, the topographic characteristic is too simple and boundary condition is restriction due to the smaller width of flume. Deposition characteristics were detailed analyzed (Major, 1990; Major & Iverson, 1999; Major, 2000), and some empirical equations were concluded, such as the relation between hazardous area and flow volume.

Fig.1.3 Experimental debris flow descending U.S. Geological Survey debris-flow flume

A high proportion of the studies designed to occur debris flow on a relatively small scale. Davis (1986) pointed that the degree of understanding involved is quite limited, and the small scale channel experiment can't well describe the characteristics and mechanics of the larger and more destructive phenomenon during actual debris flow events. Furthermore, he agreed that the obvious characteristics (e.g. boulder transport, deep bed erosion, intermittent jamming) can be explained if debris flows are treated as a macro-viscous flow of large stones in a slurry of fine solids in water.

From the field observation and experiment, lots of empirical equations were summarized, such as runout distance, depositional area (Iverson, 2014), etc. but there is still a gap between empirical equations and accurate predict and prevent actual debris flow. Over the past 50 years, studies of debris flows have matured into rigorous scientific investigations combining field measurements, controlled experiments, and mechanistic analyses (Iverson, 2014). The International Decade for Natural Disaster Reduction (IDNDR) (beginning on 1 January 1990, was launched by the United Nations) promoted the research of debris flow and landslide effectively. By statistics of current state of landslide and debris flow by SCIE papers included on Thomson Data Analyzer (TDA) and Ucinet from 1902-2010 (An et al., 2011), it's demonstrated that GIS, tsunami, numerical simulation and submarine landslide are new topics in recent 10 years as well as modeling is always a main method to study geological disaster.

Although some techniques make limited use of analytical and experimental results (Takahashi, 1981), current methods for evaluation of debris flow hazards rely largely on empirical data and field

survey (Ikeya, 1981; Iverson, 2014). Davis (1990) proposed that the best prospect for eventual explanation and prediction of debris flow behavior is numerical simulation of individual grain dynamics, in combination with empirical models. What the purpose of study debris flow is to evaluate potential disaster and effectively prevent it. Considering complex and various topographic features, it's rarely possible to survey and monitor every potential debris flow valley. The only way is numerical simulation, which can come true of evaluating every debris flow valley.

1.2.3 Numerical simulation

Numerical simulation provides an alternative tool of scientific investigation, instead of carrying out time-consuming and heavy work in both field survey and experiments. The numerical tools are often more useful than the traditional experimental methods in terms of providing insightful and complete information that cannot be directly measured or observed, or difficult to acquire via other means.

Since 1990, numerical simulation began to widely been applied to study debris flow as a new method, with the improving of recognize to the physical and disaster mechanism of debris flow in the field of experiments and field survey. To furtherly explore the mechanism of debris flow and help humankind well recognize its natural phenomenon, a number of models are developed so far. Hakuno & Uchida (1991) developed a modification of distinct element method in which the effect of water present between particles is taken into account, and simulated the deposition process after the debris flow reached a levee area. The simulation of simplified models appears to be a reasonable first step towards a systematic application and evaluation of simulation models. Due to the complexity and constitute ranges clay to boulders, the models usually simplified to a single-phase model with a simplified topography, such as muddy flow, granular flow, and most of which can't explain the natural debris flow and parts will get a rough result on the basis of empirical data. The application is very limited.

With the development of numerical simulation, there emerged lots of mathematical and numerical modelling of studying the debris flow. Hutter (1996) reviewed on debris flow modeling from a survey of the existing literature and works on debris flows, and proposed that typical features of debris flow should be incorporated in general into any model, such as dilatancy, internal friction, cohesion, fluidization and particle segregation. Boulder is considered as one of the most important factors to cause disaster. However, what force supported it to move so long distance from the mouth of valley is always an obscure problem. Cohesive strength, buoyancy and dispersive stress of debris flow have ever been regarded as the main forces to transport it. But Davies (1986) concluded that both cohesive strength and buoyancy can't support grain to move and only if the shearing of grains in the inter-granular slurry was viscous, dispersive stress would carry larger material. Kinds of factors (e.g., velocity, depth, concentration, clay content and coarse particles, discharge, friction angle, yield stress, etc.) are considered by different proposes due to uncertainty. The yield stress or the basal friction angle is considered to govern the depositional behavior to large extent

(Rickenmanm, 2006).

The pre-existing simulation models almost based on a simple inclined slope or used the simplified topographic data, which rarely reflect the actual topographic characteristic and can't be applied in practical engineering. Furthermore, oversimplified representation of the topographic features might modify forces acting on debris flow. The input topographic data should be accurate enough to obtain reasonable results, because the gravity and frictional forces are heavily dependent on the inclination of the sliding base (Chen & Lee, 2000). How to efficiently validate it and further reproduce the natural debris flows?

Over more than 20 years, numerical simulation in debris flow experienced a series of exploring process, one phase to two phase, solid to flow, one-dimension to three-dimension, simplified model to actual model. One of main improvements is obtained, which is the accurate representation of natural topographic data played a critical role in flow behavior (Fannin et al., 2001; Rickenmann et al., 2006). Iverson (2014) emphasized the importance of natural events characteristics in simulation research work, such as the poorly constrained initial and boundary conditions and unmeasured material properties. Meanwhile, he also argued that it can fail to predict the behavior of a natural debris flow if adequate knowledge of the initial conditions, terrain or material properties is lacking, even if a model is entirely sound physically, mathematically and computationally (Iverson, 2014). Although kinds of novel models are continuously built and gradually applied into the practical engineering, empirical methods continue to play an important role in debris-flow hazard assessment (Iverson, 2014), because of the lack of accurate representation of topography.

So far, there are three main models to consider realistic topography in numerical simulation of debris flow. They are numerical models based on geographic information system (GIS), the FLO-2D and depth-integrated particle method. Both GIS and FLO-2D are two commercial software.

With the developing and widespread using of geographic information system (GIS), it has been recognized as a useful tool to process spatial data and display results for both hazard mapping and risk assessment. One dominant advantage of numerical simulation coupled with GIS is that the grid networks for simulation can be extracted from GIS raster data. All of calculated results can be directly displayed in GIS and used to the hazard mapping (Wu et al., 2013). Mergili et al. (2012) described a method for integrated modelling of debris flows (from triggering to deposition) based on the software GRASS GIS, in which 5-m digital elevation models (DEMs) for the study areas were created by aerial photographs (scale 1:20,000 and 1:60,000) and SPOT satellite imagery (cell size: 2.5 m). Although infiltration and surface runoff, detachment and sediment transport, slope stability, debris flow mobilization, and travel distance and deposition were discussed, it's demonstrated there are some limitations about parameters. Wu et al. (2013) developed a debris flow simulation program incorporating with GIS by deriving the computation networks from GIS raster data, following a derivation of the debris flow model considering both erosion and deposition processes. And verified

the model is rational and effective by simulating a well-documented Amamioshima debris flow in Japan. But it seems that the accuracy of simulation results is not high. Based on the GIS platform, it's available to consider more factors about topographic features, vegetation, lithology, rainfall, etc. However, what need to do is how to combine an efficient numerical model into this advantage platform.

The FLO-2D computer model was developed at the Colorado State University and is a quadratic friction law, which is a combination of yield, viscous, collision and turbulent stress components. Hübl (2001), Rickenmann et al. (2006), Stolz & Huggel (2008) and Matthias et al. (2013) simulated debris flows by FLO-2Dcomputer model on the base of topographic data. It's found that FLO-2D computer model enables the simulation of velocities, depth and runout distance of debris flows even in catchments. The application of the FLO-2D mode1 requires high quality input data, especially a digital elevation mode1 and rheological parameters of the debris flow material. Noted that it will never be possible to calibrate even high sophisticated numerical models if lack the real-time documentation of debris flows. The inaccuracy of the model was summarized from both systematic topographic errors and simplification of the real multi-surge event by a single triangular hydrograph (Rickenmann et al., 2006).

FLO-2D simulation code solves the equations using a finite difference method (FDM) on a fixed rectangular grid. Although it's popular for practical application as a commercial software, it still exists some limitations. Determining the precise locations of the in homogeneities, free surfaces, deformable boundaries and moving interfaces within the frame of the fixed Eulerian grid is a formidable task (Liu & Liu, 2003). Furthermore, a laminar flow resistance coefficient was brought for smooth, wide rectangular channels. Its value is supposed to increase with roughness and irregular cross-section geometry (Rickenmann et al., 2006). Additionally, the mesh-based method is limited to the analysis of relatively small displacements due to mesh distortion, it's hard to correctly evaluate the affect areas and travel distance.

Although many models were concentrated on the simulation of natural debris flows based detailed topographic information from topographic map, aerial photographs, etc. It seems that the simulation results were not good enough, besides some researches are lack of validation among of experimental data, theoretical solutions, or the exact results from other established methods for benchmark problems or actual engineering problems. Because the generic type and spatial resolution of DEMs have a main influence on the results of debris flow modeling (Stolz & Huggel, 2008). Additionally, both Stevens (2002) and Huggel (2008) found that the generic DEM type was responsible for a larger difference in debris-flow modeling results than grid spacing.

Depth-integrated method is a nice comprise between accuracy and computation time. In 2008, Pastor et al. proposed a depth-integrated SPH model to evaluate flow-like landslide basing on an actual topographic data. Hoang et al. (2009) also proposed a depth-integrated particle method that is

a simple and efficient model to simulate debris flow in a wide area based on detailed topographic data. Therefore, it's available to evaluate debris flow in a wide area taking into account actual topographic characteristics using a mesh-free method.

So far, the study of debris flows still rely on field survey and monitoring, experiments and numerical simulation, due to the complexity of the debris flow process (Rickenmann, 1999). The purpose of numerical simulation is to evaluate the actual debris flow event and apply in practical engineering. Debris flow is a gravity- driven, free surface and boundary flow. Its occurrence mainly contained three factors, advantage topography, rainfall and rich debris source. Therefore, it is necessary to build a reasonable and effective model based on a natural topographic data to quantitative evaluate the debris flow hazard.

1.3 Research contents in this study

1.3.1 Method

To reproduce the natural debris flow, it must consider realistic topographic features. From the aforementioned literatures, it becomes available to obtain topographic data, such as from aerial photos, satellite image, topographic maps, etc.

Recently, the development of computer capability enables us to carry out a wide range of debris flow simulation with taking account of the detailed topographic data (Pastor et al., 2009 and 2014; Safeland 2013), and still, an efficient numerical scheme is a key issue. A depth-integrated particle method is a powerful method for this purpose, and various versions have been proposed so far. Among them, Hoang et al. (2009) developed a simple and still efficient particle method, in which the pair-wise particle interaction is modeled basing on the hydraulic gradient. This simplification makes the simulation very efficient and stable as well. Another advantage of this method is the small number of parameters as described in the governing equations. Furthermore, it's available to reproduce a natural debris flow based on detailed representation of topography (Nakata et al., 2014; Zhang et al., 2014a). Therefore, I also adopt this method in the present study.

As illustrated in the figure 1.4, the evaluation of debris flow hazard adopted there models. Hoang et al. (2009) proposed the depth-integrated particle method and adopted the original model to evaluate debris flow hazard. In the original model, slope failure directly transformed into debris flow and moved down. The several case studies of slope failure triggered debris flows demonstrated that the initial volume of slope failure were insignificant in comparison with the whole volume of the events (Theule et al., 2012). Actually, debris sources located on the both sides of valley channel and sedimentation on the channel bed played an important role in occurring debris flow and increasing the magnitude of debris flow. The generation time of such debris source is not the same period with the debris flow. Therefore, two-step simulation scheme was proposed (Zhang et al., 2014b). In this scheme, the debris sources can be quantitative evaluated in step 1. Step 2 is simulation of debris flow.

In the step 2, two models are also proposed. It's assumed that the debris flow was initiated at the valley by directly changing the parameters of debris sources that were generated in the step 1 in the re-initiation model. Actually, it's hard to be initiated on the valley channel with none of external force. To more reasonable and realistic initiate the debris flow in step 2, the mixing model was proposed.

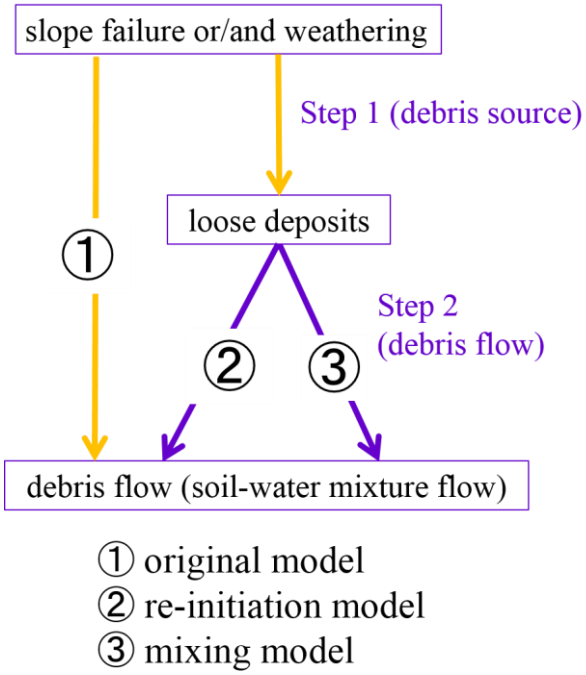

Fig.1.4 The scheme of evaluation

The detailed description of the depth-integrated particle method and the mixing model will be shown in Chapter 2.

1.3.2 Satellite images

The aforementioned that the generic type has large influence for simulation results. In this study, we choose satellite image from the ALOS satellite. The choosing debris flow events mainly occurred on 2008 to 2011, and the ALOS satellite was just observed in this period. We will download the images for our research propose. Generally, the pre-disaster image is used to provide the detailed DEM for simulation after processing, while the post-disaster image is mainly used to evaluate the simulation results.

From the pre-existing researches about numerical simulation based on DEM, it's revealed that the accurate topographic data played a critical role in numerical simulation. Therefore, how to obtain an accurate DEM from the satellite image and how to evaluate the accuracy of processed DEM will be detailed described in Chapter 3.

1.3.3 Quantitative evaluation of debris flows

China is a fast developing country since 1980. As a unique and typical mountainous geo-hazard, debris flow hazards are very seriously in China (Fig.1.1 and Fig.1.5) because the 2/3 areas belong to mountainous area. As illustrated in the figure 1.5, the occurrce density of debris flow is very high in southwest China. It mainly because the complex geological condition and special weather condition. Natural condition determines mostly zones of China belong to high frequency occurrence areas of debris flow. Furthermore, numerous of human-activities with the rapidly increasing of the population is also one of important factors to trigger the disaster of debris flow. The development of policy led to more and more people rushed into city, even though small city and town. Such as, the Zhouqu debris flow on 7 August 2010, led to a debris flow disaster killed more than 1700 lives due to large population density.

The 2008 Wenchuan Earthquake seriously destroyed wide zones of the southwest China. After that, several more earthquakes occurred in the southwest China, such as Lushan Earthquake in 2013, earthquakes in Yunnan Province in last five years. Meanwhile, extremely rich geo-hazards were triggered in these regions. The existing researches demonstrate such geo-hazards (e.g., debris flows, landslides) will last more than dozens of years (Nakamura et al., 2000; Huang, 2011).

Overall, the southwest China is one of best regions to study debris flow by considering many factors. Another advantage is there are kinds types of debris flows and where also have rich monitoring data. In last 5 years, there occurred many typical large-scale debris flows and led to seriously damages. Therefore, Zhouqu and Wenchuan earthquake-stricken region are chosen to quatitative evaluate the debris flows in this study.

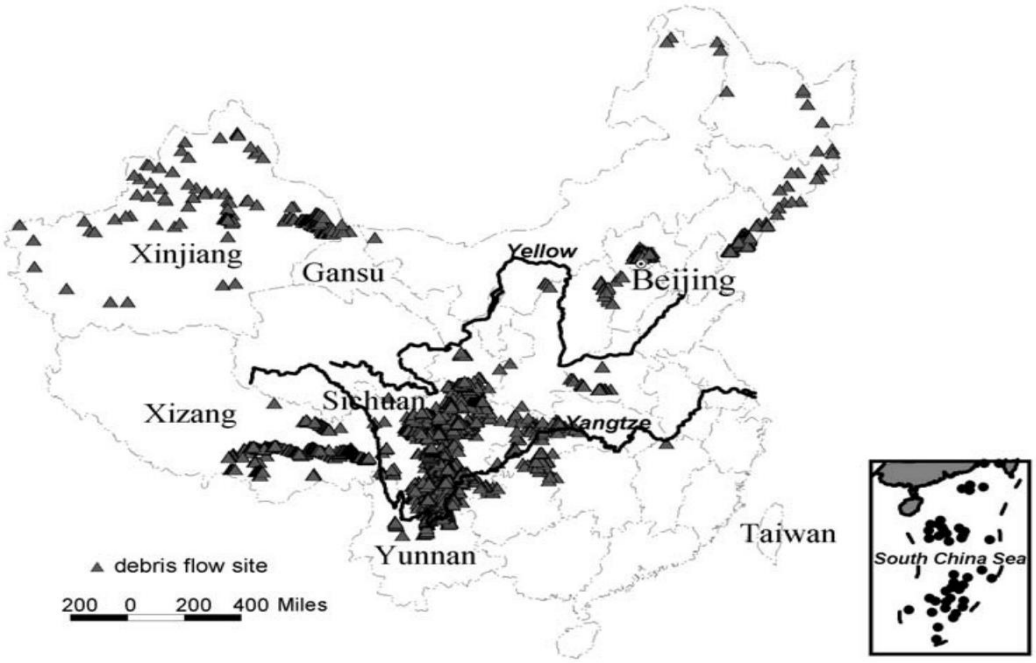

Fig.1.5 The distribution map of debris flow in China (Cui et al., 2005)

With the simplicity and efficient of the aforementioned method, the debris flow in Zhouqu and debris flows in the Wenchuan earthquake-stricken areas are evaluated as an individual debris flow hazard and regional debris flows hazards. The main evaluation works contain three section.

Firstly, mesh size and the factors of both parameters in the model (Manning coefficient and critical slope of deposition) and flow properties (discharge and flow volume) were evaluated in terms of affected area, travel distance, velocity and spatial patterns of debris flow deposition.

Then, quantitative evaluation of works focus on identification of debris source, analysis on initiation and transportation processes as well as deposition features for an individual debris flow hazard in Zhouqu. The mixing model was proposed to initiate debris flow by controlling volume concentration. The disaster mechanism of debris flow on 7 Aug. 2010 is also analyzed. The detailed information see Chapter 4.

Finally, regional debris flows in the earthquake-stricken areas are quantitative evaluated in the chapter 5. The main works concentrate on the following parts: the surface damaged features of earthquake-stricken areas are estimated by satellite images; review on the post-earthquake debris flows; and two regions (Beichuan region and the region from Yingxiu to Wenchuan along the Min River) are selected to evaluate regional debris flow hazards. Beichuan debris flows focused on the identification of debris sources on the base of surface damaged features of image. Both concentration and velocity distribution features varied with the simulation process are also estimated. Regional debris flows in the region from Yingxiu to Wenchuan along the Min River focus on the evaluation of typical features of debris flows, such as blocking river by multiple debris flows occurrence simultaneously and two opposite debris flow occurrence. Simple countermeasure structures are evaluated on the topographic data of Hongchun valley as a case study.

As illustrated in the figure 1.6, this study concentrates on the quantitative evaluation of debris flow hazards in Zhouqu region and Wenchuan earthquake-stricken areas using depth-integrated particle method and satellite images.

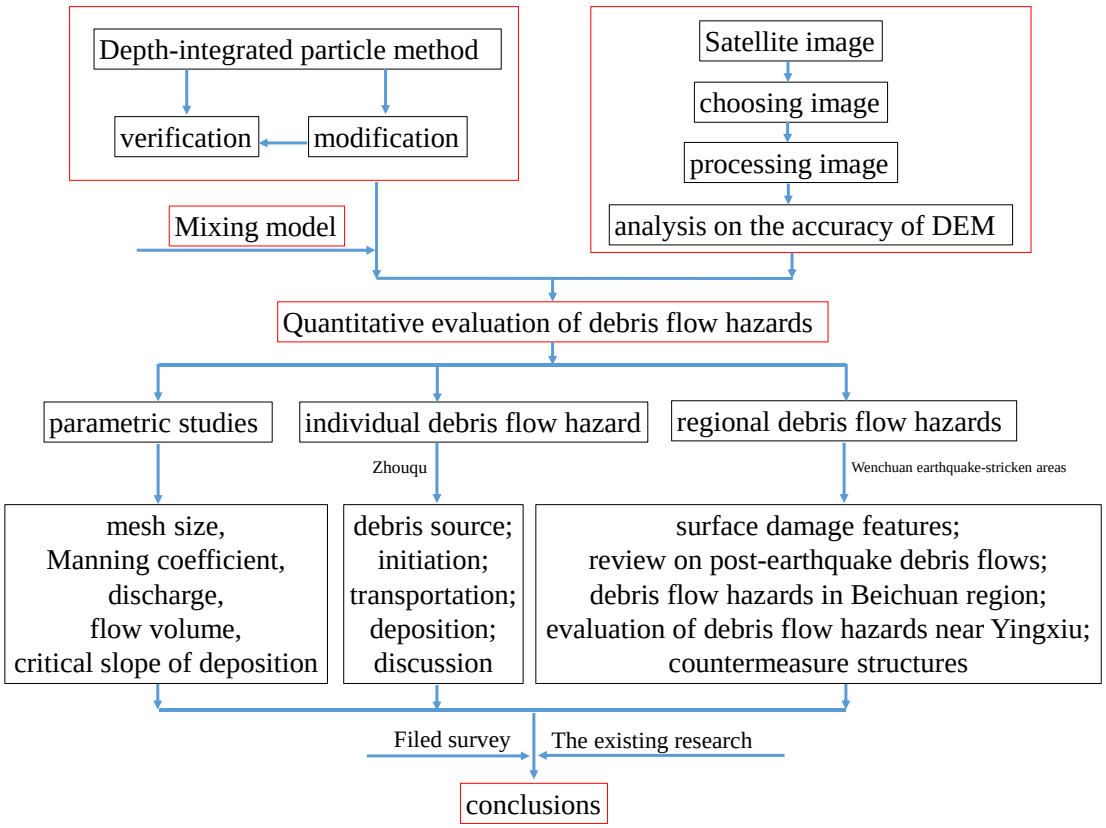

Fig.1.6 Flow chart of this study

CHAPTER 2 DEPTH-INTEGRATED PARTICLE METHOD

2.1 Mesh-free particle method

Facing many difficulties and limitations (large deformation, large inhomogeneities, moving material interfaces, deformable boundaries, and free surfaces. complex mesh generation, mesh adaptively, and multi-scale resolution) in grid-meshed method, a series of mesh-free methods have begun to be developed in recent years. The key idea of the mesh-free methods is to provide accurate and stable numerical solutions for integral equations or partial differential equations with all kinds of possible boundary conditions with a set of arbitrarily distributed nodes (or particles) without using any mesh that provides the connectivity of these nodes or particles. By different numerical discretization techniques (weak form, strong form, particle methods), there are basically three types of mesh-free methods: methods based on strong form formulations, methods based on weak form formulations, and particle methods. Here, I'll focus on mesh-free particle method (MPM).

A MPM in general refers to the class of mesh-free methods that employ a set of finite number of discrete particles to represent the state of a system and to record the movement of the system. Each particle can either be directly associated with one discrete physical object, or be generated to represent a part of the continuum problem domain. Initially, MPM was developed for systems with discrete particles. So far, there are also some applications in continuum media by generating the initial distribution of particles. As a MPM, mostly are inherently Lagrangian methods, in which the particles represent the physical system moving in the Lagrangian frame according to the internal interactions and external force, and thus evolve the system in time.

In the MPMs, there is no need to prescribe the connectivity between the particles. All one needs is an initial distribution or generation of the particles that represent the problem domain, if the problem domain is not initially in discrete particle form. Different ways of generating particles for continuous domains can be employed. Since mesh generation algorithms (e.g. triangulation algorithm) are readily available for both the 2D and 3D space. The neighboring particles within the support domain of a particle provide all the necessary and sufficient information for the field variable approximations at the particle.

There are several large advantages for MPM: treatment of large deformation is relatively much easier; discretization of complex geometry is simpler, and only an initial discretization is required; pressure is available to compute from the neighboring particles; identifying free surfaces, moving interfaces and deformable boundaries is very easy to obtain.

Kinds of particle methods, such as DEM, SPH, which have large advance in applying to geotechnical engineering. Recently, the development of computer capability enables us to carry out a wide range of debris flow simulation with taking account of the detailed topographic data (Pastor et

al., 2014; Safeland 2013), and still, an efficient numerical scheme is a key issue. Considering on the special features of debris flow (wide area, long distance), a simpler and more efficient particle method, which was developed by Hoang et al. (2009), will be used to evaluate the debris flow hazards.

2.2 Depth-integrated particle method

The flow depth is small compared to the length of the channel, so it's reasonable to consider debris flow as a kind of shallow water flow. Hoang et al. (2009) had developed an efficient numerical simulation method based on shallow water equation, which called the depth-integrated particle method. Such method is a mesh-free method, in which the governing equations are discretized over a set of arbitrary distributed particles or columns moving in a Lagrangian coordination. It's suitable for the simulation of long-distance debris flow or the entire geo-hazard evaluation of very wide area with the detailed topographic information (Nakata et al., 2014, Zhang et al, 2014).

2.2.1 Governing equation

The equations are derived from depth-integrating the Navier-Stokes equations, in the case where the horizontal length scale is much greater than the vertical length scale. Under this condition, the horizontal velocity field is constant throughout the depth of the fluid, while vertically integrating allows the vertical velocity to be removed from the equations.

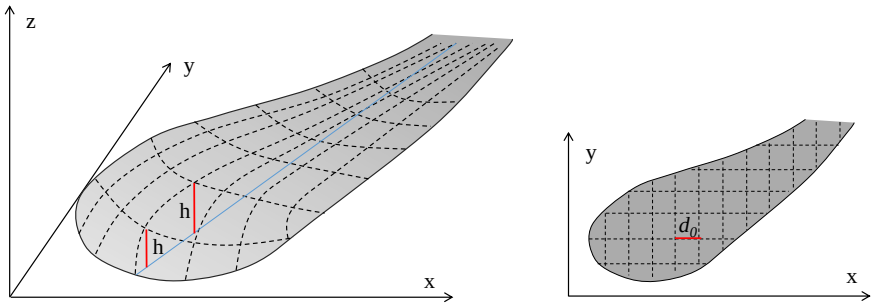

Fig.2.1 The schematic illustration of shallow water equation

The shallow water equation is commonly described as follows:

$$\frac{\partial v_x}{\partial t}+v_x\frac{\partial v_x}{\partial x}+v_y\frac{\partial v_x}{\partial y}=g_x-\frac{\partial p}{\rho\partial x}-\frac{\tau_{bx}}{\rho h}$$
$$\frac{\partial v_y}{\partial t}+v_x\frac{\partial v_y}{\partial x}+v_y\frac{\partial v_y}{\partial y}=g_y-\frac{\partial p}{\rho\partial y}-\frac{\tau_{by}}{\rho h} \quad (1)$$

where, $v=(v_x,v_y)$ is a depth-integrated flow velocity vector, h is the surface height of debris flow, $\boldsymbol{\tau_b}=(\tau_{bx},\tau_{by})$ is the bottom shear stress vector, ρ is the density of the debris flow, p is the

hydraulic pressure, and (g_x,g_y) is the component of gravitational acceleration parallel to the base slope. Note that the mass conservation equation is not necessary in Lagrangian particle methods.

2.2.2 Hydraulic pressure

The hydraulic pressure is calculated from the hydraulic gradient, which is discretized by the difference of the height between the neighboring particles (Fig.2.2). Here we assume only a pair-wise particle interaction, in which the height of each particle is computed from the inter-particle distance by assuming the constant particle volume. The hydraulic pressure is modeled by the following inter-particle force (Hoang et al., 2009):

$$\nabla \mathbf{p} = \begin{cases} -\rho g \dfrac{h_0}{d_0}\left(\dfrac{1-\|\mathbf{d}\|/d_0}{1+\|\mathbf{d}\|/d_0}\right)\dfrac{\mathbf{d}}{\|\mathbf{d}\|} & (\|\mathbf{d}\| < d_0) \\ -\dfrac{1}{2}\rho g \dfrac{h_0}{d_0}\left[\left(\dfrac{\|\mathbf{d}\|}{d_0}-\dfrac{3}{2}\right)^2-\dfrac{1}{8}\right]\dfrac{\mathbf{d}}{\|\mathbf{d}\|} & (d_0 \le \|\mathbf{d}\| < 2d_0) \\ 0 & (\|\mathbf{d}\| \ge 2d_0) \end{cases} \tag{2}$$

where, h_0 is the initial height of the debris flow layer, d_0 is the bottom width of the debris 'particle' or 'column', **d** is the distance vector between two interacting particles. In this computed model, the effective influence distance was assumed to $2.0d_0$. That means there will have no interaction between two particles which the distance is larger than $2.0d_0$. The shape of eq.(2) is shown in figure 2.3. This equation demonstrated that repulsive force played a major role in both particles when the two particles closer than the initial distance d_0, while the attraction force acts on the pairwise particle if the distance is larger than d_0.

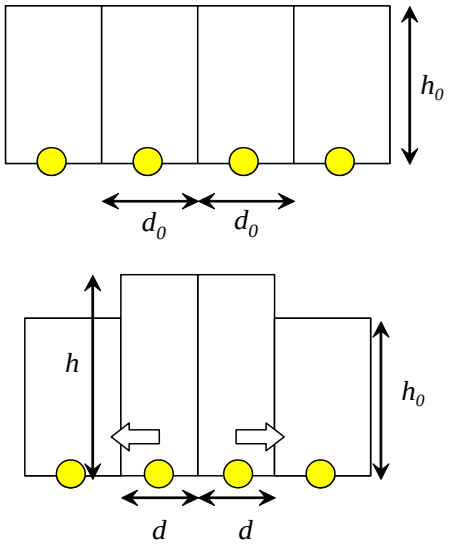

Fig.2.2 The calculation model of hydraulic pressure

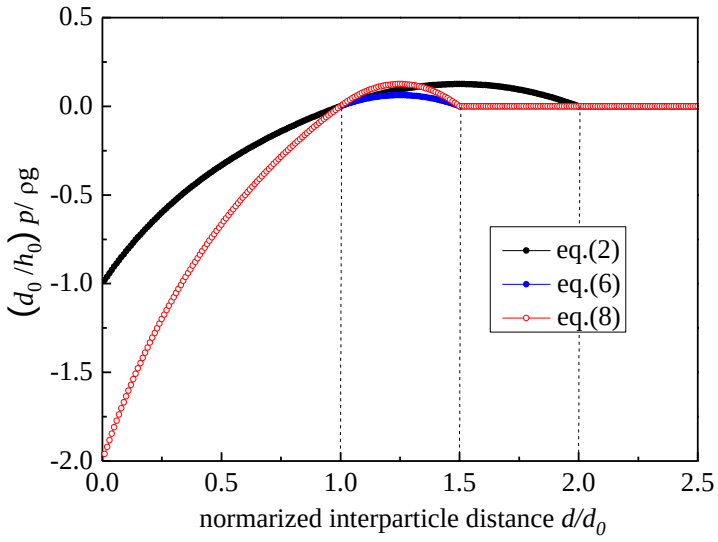

Fig.2.3 Hydraulic pressure

2.2.3 Bottom shear stress

The bottom shear stress is expressed as follows:

$$\boldsymbol{\tau}_b = \left(\tau_{cr} \|\mathbf{v}\|^m + \rho g \frac{n^2}{R_h^{1/3}} \|\mathbf{v}\|^2 \right) \frac{\mathbf{v}}{\|\mathbf{v}\|}$$

$$\tau_{cr} = \rho g R_h i_{cr} \qquad (3)$$

where, n is Manning coefficient, R_h is hydraulic radius (assumed to be equal to d_0) andi_{cr} is the critical slope of deposition. Additionally, a numerical parameter m is introduced for smoothing Bingham fluid model as shown in Fig.2.4. In the present study, m is set to 0.01.

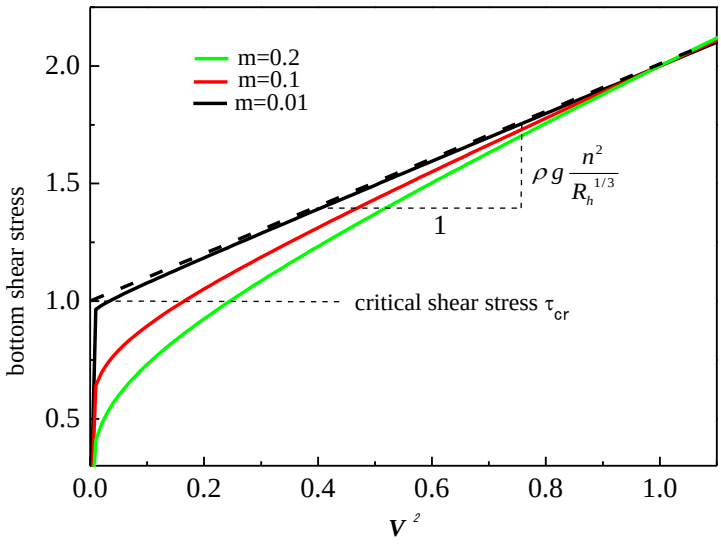

Fig.2.4 Bottom shear stress varied with velocity

This simplified depth-integrated particle model enables us to carry out debris flow simulation with relatively small number of particles based on accurate topographic data. This feature leads to the drastic reduction of computational cost. It is also worth mentioning that there are only two major parameters to control the flow behavior, Manning coefficient and critical slope of deposition. They kept constant in computation time in the present study.

The flowchart of depth-integrated particle method program used in present paper showed in the table 2.1.

Table 2.1 Flowchart of depth-integrated particle method program used in present study

(1) Start
(2) Input data-file reading
(3) Input topographic data
(4) Calculation of the topographic slope
(5) Step 1: generation of debris sources
(6) Slope failure judgment and put particles on the slope failure position
(7) fall down and deposit with the repose of angle
(8) Step 2: simulation of debris flow
(9) Use the position information of debris sources
(10) Loop for calculation steps
(11) Loop for each particle calculation steps
(12) Loop for neighboring particles
(13) Inter-particle distance judgment: if larger the maximum influence distance, go to (15)
(14) Calculation of hydraulic pressure
(15) Next neighboring particle: go to (12)
(16) Next particle: go to (11)
(17) Calculation of gravitational force and
(18) Critical slope judgment and calculation of bottom shear stress
(19) Sum up the total forces
(20) Solve the equation of motion and obtain the next position of particles
(21) Next calculation step: go to (10)
(22) Repeat (10)-(21)
(23) Output
(24) End

2.3 Verification of the modified method

Two simple examples of flow under 1D, wave propagation on the flat surface and flow behavior in

the hollow place, have been simulated to verify and validate the accuracy of the proposed depth-integrated particle method.

2.3.1 Wave propagation on a flat surface

Under 1D and slope angle is 0°, the equation of motion is:

$$\frac{\partial v}{\partial t} = -\frac{\partial p}{\rho \partial x}$$
$$\frac{\partial p}{\partial x} = -\rho g \frac{\partial h}{\partial x} \tag{4}$$

18 flow particles were set on a flat surface in a line, and stable one particle on each side (particle 1 and particle 18) (Fig.4). Firstly, we give a minor disturbance by giving a small velocity (v_0') to the particle 2. Then we observe the wave propagation and record the location of every particle in each time step (*nstep*) under the whole process (Fig.2.5). Finally, calculate the simulated wave velocity by wavelength (L) and time (eq.(5)).

$$c = \frac{L}{nstep \times dt} \tag{5}$$

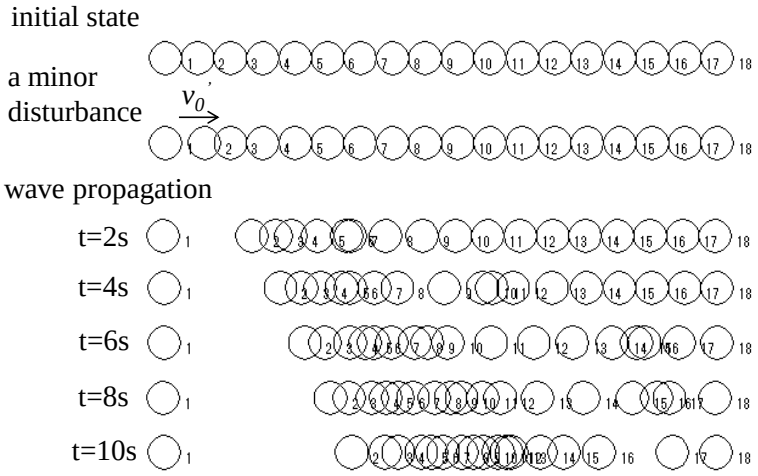

Fig.2.5 The model for wave propagation on a flat surface by the eq.(2)

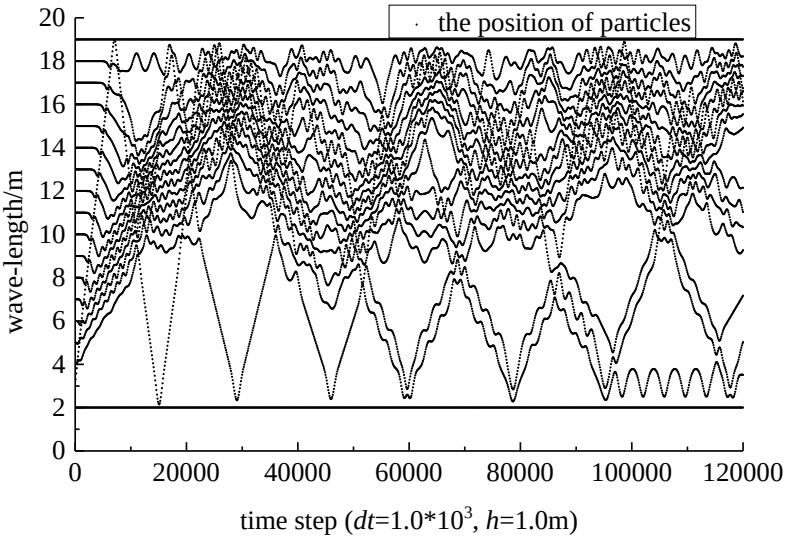

Fig.2.6 Wave propagation on a flat surface with eq.(2)

It seems that the effective influence distance limited in $2.0d_0$ is too large to get a good wave propagation result by figure 2.5 and figure 2.6. Therefore, we modified the eq.(2) to simulate the wave propagation by reducing the effective influence distance. Here, three cases of simulation results were shown under the effective influence distance with $1.7d_0$,$1.5d_0$ and $1.3d_0$ (Fig.2.7 and Fig.2.8).

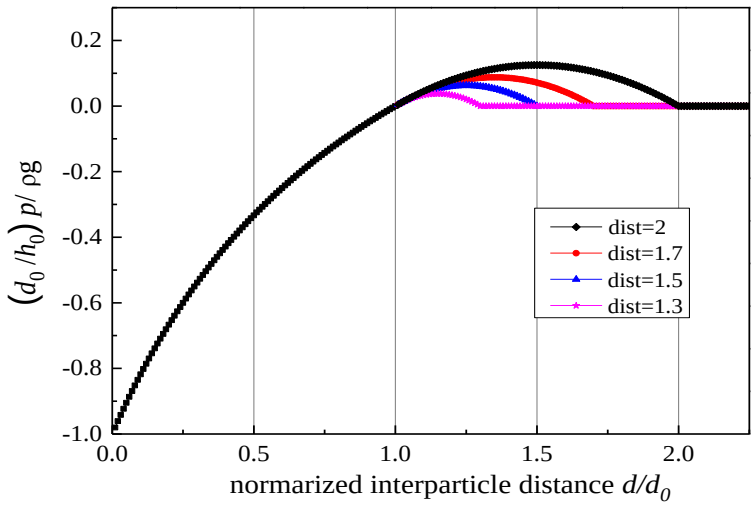

Fig.2.7 The model of hydraulic pressure under different effective influence distance

It's found that there is a good wave propagation result if the effective influence distance was assumed to $1.7d_0$, $1.5d_0$ and $1.3d_0$.However, the wave propagation becomes unstable gradually with the increase of effective influence distance. We must consider the stability of simulation, meanwhile, the effective influence distance is as large as possible. So, we assumed the effective influence distance is $1.5d_0$, and the hydraulic pressure is calculated by the following equation,

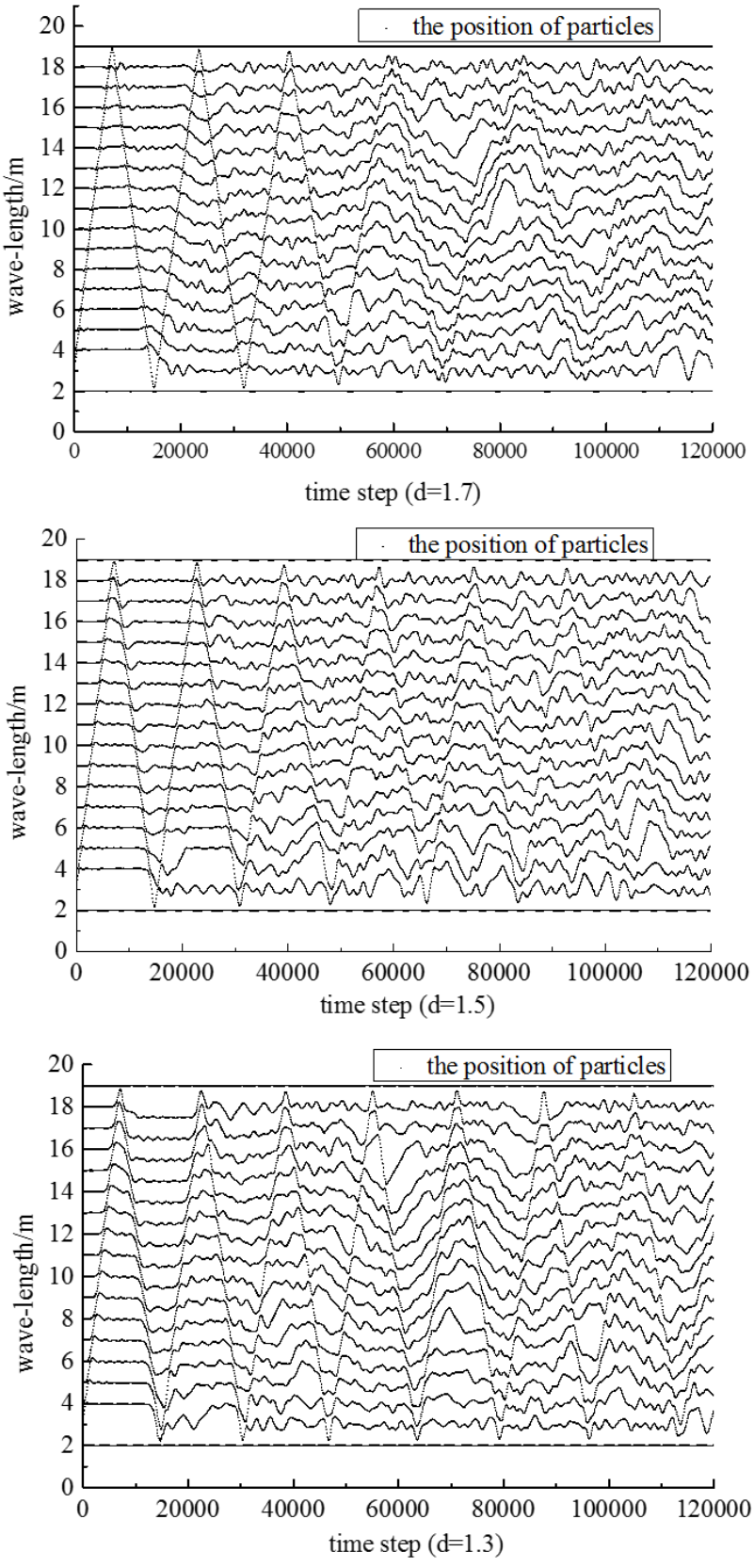

Fig.2.8 Wave propagation on a flat surface under different effective influence distance

$$\nabla \mathbf{p} = \rho g \nabla h = \begin{cases} -\rho g \dfrac{h_0}{d_0}\left(\dfrac{1-\|\mathbf{d}\|/d_0}{1+\|\mathbf{d}\|/d_0}\right)\dfrac{\mathbf{d}}{\|\mathbf{d}\|} & (\|\mathbf{d}\| < d_0) \\ -\rho g \dfrac{h_0}{d_0}\left[\left(\dfrac{\|\mathbf{d}\|}{d_0}-\dfrac{5}{4}\right)^2 - \dfrac{1}{16}\right]\dfrac{\mathbf{d}}{\|\mathbf{d}\|} & (d_0 \le \|\mathbf{d}\| < 1.5d_0) \\ 0 & (\|\mathbf{d}\| \ge 1.5d_0) \end{cases} \tag{6}$$

Then, simulate a series of wave velocity with different flow depth, and validate the accuracy of the calculated model of hydraulic pressure. The simulated wave velocity is calculated by eq.(5), and compared the results with the theoretical value.

In theory, wave velocity is expressed:

$$c = v_0 \pm \sqrt{g h_0} \tag{7}$$

where, c is wave velocity, v_0 is the flow velocity and $h_0$is the flow depth.

In the simple model, the flow velocity is 0, and the flow depth equals particle height.

Compared simulated wave velocity with theoretical value to verify the accuracy of the proposed method. It's not good the calculated wave velocity had a good trends with the increasing the flow depth compared with theoretical curve, but its value is smaller than the theoretical value. It maybe the described hydraulic pressure is smaller than the actual value. Analysis of numerous simulations, it's found that the simulation results matched well with the theoretical curve (Fig.2.10) if the hydraulic pressure increased to twice of eq.(6). So, the reasonable and correct hydraulic pressure is calculated by the eq.(8). And one wave propagation result was shown in figure 2.9, in which the wave propagation looks very good and fairly stable.

$$\nabla \mathbf{p} = \rho g \nabla h = \begin{cases} -2\rho g h_0\left(\dfrac{1-\|\mathbf{d}\|/d_0}{1+\|\mathbf{d}\|/d_0}\right)\dfrac{\mathbf{d}}{\|\mathbf{d}\|} & (\|\mathbf{d}\| < d_0) \\ -2\rho g h_0\left[\left(\dfrac{\|\mathbf{d}\|}{d_0}-\dfrac{5}{4}\right)^2 - \dfrac{1}{16}\right]\dfrac{\mathbf{d}}{\|\mathbf{d}\|} & (d_0 \le \|\mathbf{d}\| < 1.5d_0) \\ 0 & (\|\mathbf{d}\| \ge 1.5d_0) \end{cases} \tag{8}$$

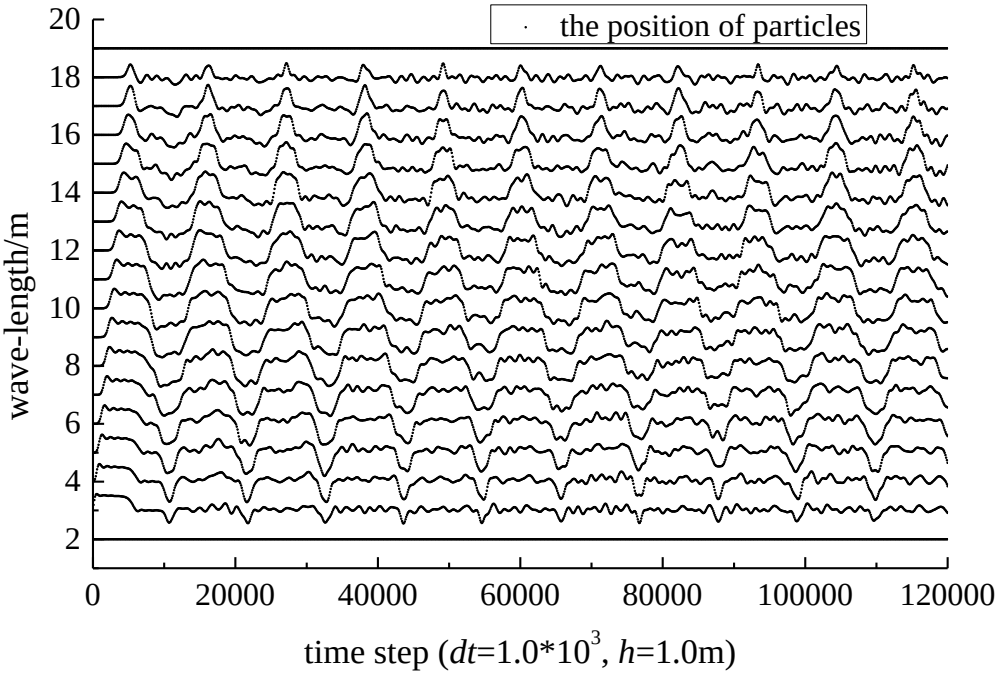

Fig.2.9 Wave propagation on a flat surface with modified hydraulic pressure (eq.(8))

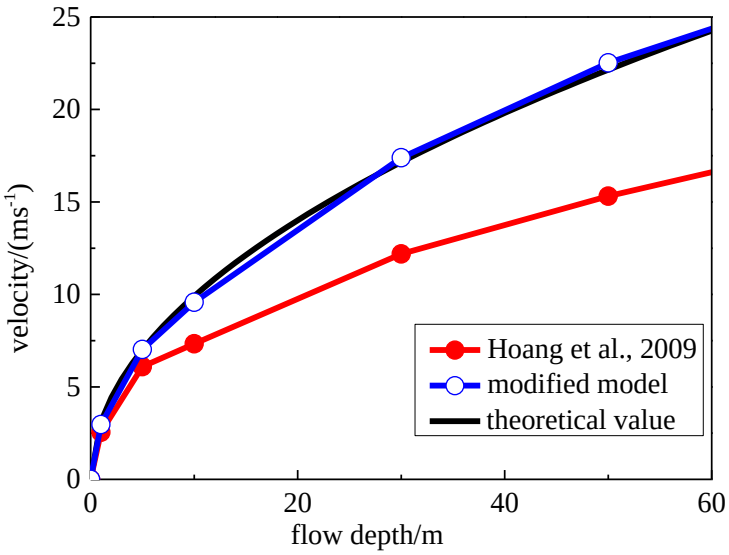

Fig.2.10 The relation between wave velocity and flow depth

By simulating a series of flow behaviors, it found that the simulated wave velocity kept the consistence with theoretical value (Fig.2.10). Therefore, we think the eq.(8) is accurate and can be used to describe the flow behavior well.

2.3.2 Flow behavior on a V-shape slope

The equation of motion

$$\frac{\partial v}{\partial t} = g - \frac{\partial p}{\rho \partial x} - \frac{\tau_b}{\rho h} \tag{9}$$

The volume keeps constant,

$$dh = d_0 h_0 = const. \tag{10}$$

58 flow particles with 5.0m height were averagely distributed on a V-shape slope, which slope angle is 60° (Fig.2.11). Here, the hydraulic pressure is calculated by the eq.(8). Then the flow particles flowed down according to the equation of motion (eq.(9)). In the whole process, the particle volume keeps the constant (eq.(10)).

(1) Critical slope of deposition is 0°

The simulation results showed that particles flowed into V-shape hollow place and the deposition height tends to lever. Furthermore, the location and height of deposition had a good agreement with theory results (Fig.2.11).

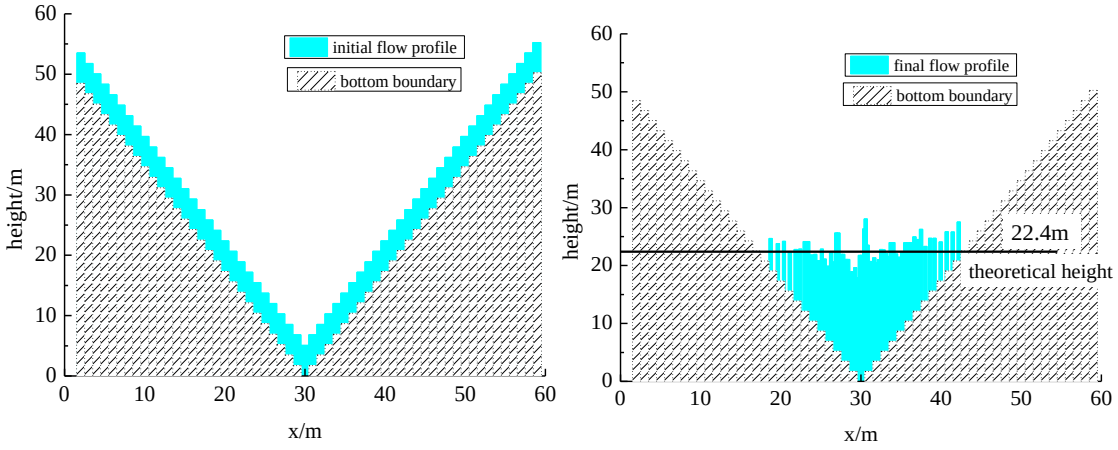

Fig.2.11 The model for flow motion on a non-flat slope

By simulating two simple flows, the accuracy of the modified hydraulic pressure model was verified, and we think it can be applied to simulate actual debris flow accurately.

(2) Critical slope of deposition is not 0°

The slope of V-shape is set to 30°. Three cases for critical slope of deposition are simulated on 30°, 25° and 32°. As illustrated in the figure 2.12, the model can describe flow behavior well with different critical slope of deposition on a non-flat slope.

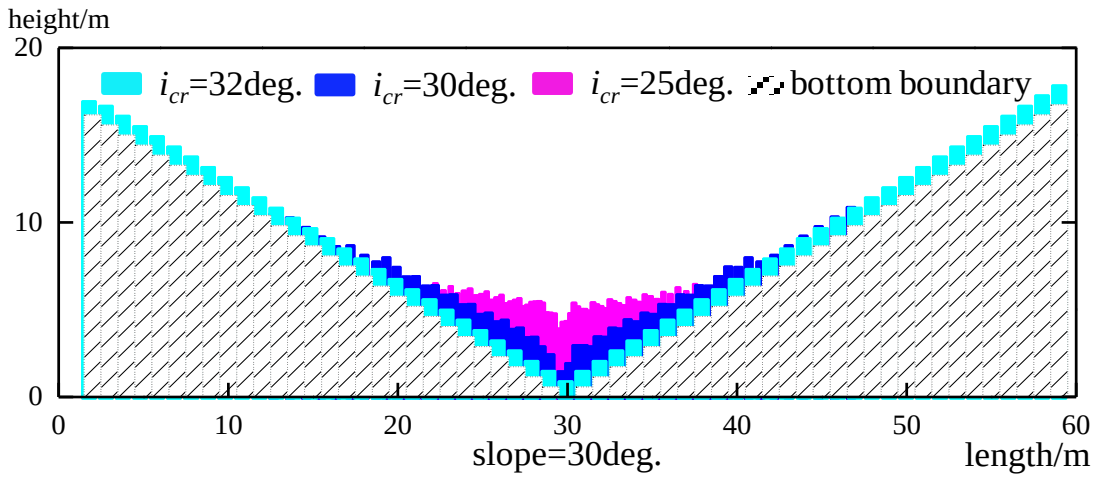

Fig.2.12 The simple flow behavior on a V-shape slope and the critical slope of deposition is not 0°

2.4 Mixing model

In the mixing model, it is assumed that a water particle initiated a solid particle by changing solid particle concentration according to the diffusion equation, if the distance of both particles is less than one initial distance. The mixing model showed in the figure 2.13.

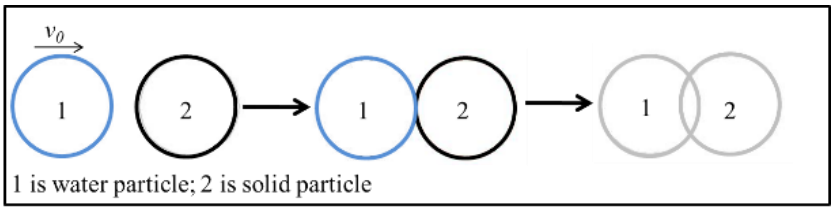

Fig.2.13 The initiation model of pair-wise particle

The diffusion equation is

$$\frac{\partial c}{\partial t} = D\frac{\partial c}{\partial x} \tag{11}$$

where, D is diffusion coefficient, which determined the initiate rate. Its value ranged 0 to 1. In the present study, the diffusion coefficient is set to a constant in the whole simulation process. At the initial state, assumed

$$\begin{aligned} c_s &= 1 \\ c_w &= 0 \end{aligned} \tag{12}$$

By discretize the diffusion equation (11), the concentration increment is calculated by

$$\frac{\Delta c}{\Delta t} = D\frac{\Delta c}{\Delta x^2} \tag{13}$$

So, the concentration of both particles varied with computation time by the following equations:

$$c_{s(t+\Delta t)} = c_{s(t)} - \Delta c$$
$$c_{w(t+\Delta t)} = c_{w(t)} + \Delta c \tag{14}$$

The simulation results of concentration variation of pair-wise particle under different diffusion coefficient is showed in figure 2.14.The diffusion coefficient strongly influenced the initiation time.

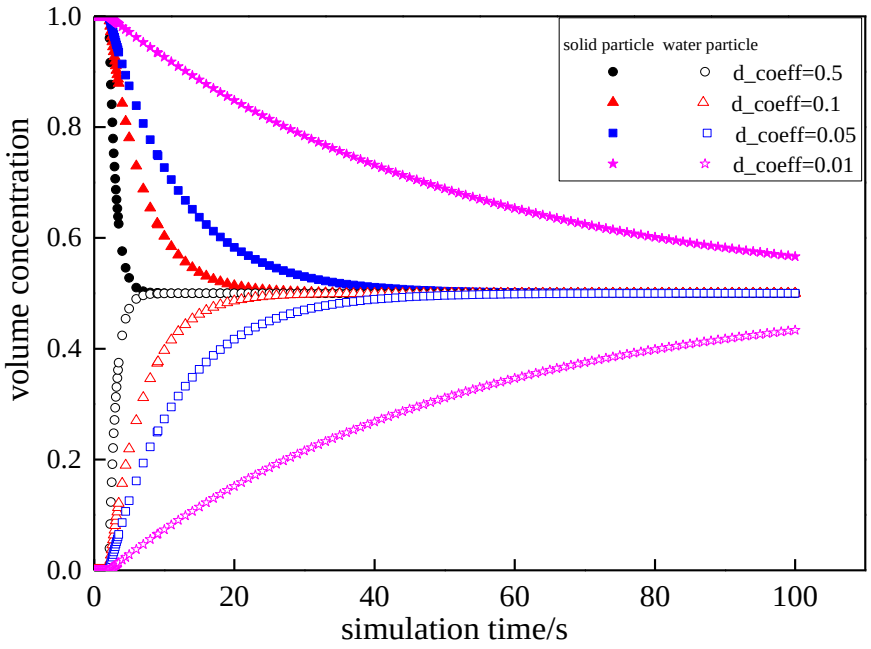

Fig.2.14 The concentration of both particles varied with computation time under different diffusion coefficient

(1) Critical slope of deposition

In the mixing model, there are three types of particles, water particle, debris flow particle and solid particle. It's no doubt that the critical deposition slopes of water particle and solid particle are 0° and repose angle of solid particles. However, what's the critical deposition slope of debris flows? Three relationships between critical deposition slope and volume concentration are assumed as illustrated in the figure. In three assumed relations, i_{cr}_s is the critical deposition slope of solid particles, while *icr_f* is the critical deposition slope of debris flows. Two critical volume concentration (c_critical and c_max) are also assumed in the three relationships. It's not hard to define the c_max value according to the existing research. Mostly researchers agreed that the maximum concentration ranged 0.6 to 0.64 if the uniform particles deposited. However, the data of filed observation demonstrates that the largest concentration can up to 0.83 (Fei & Shu, 2004). So far, there is not a clear definition for flood and debris flow. Therefore, in the present study, it's assumed that the critical concentration for the solid particle is initiated and entrained to debris flow is not larger than 0.83, while the critical concentration of water particle becomes debris flow is larger than 0.35. The

simulation results showed in the figure 2.16.

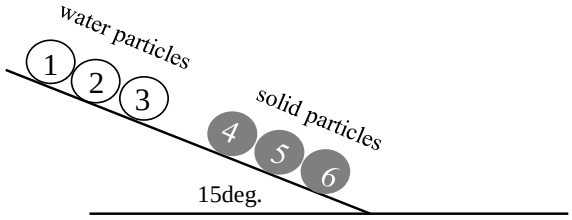

Simple mixing case

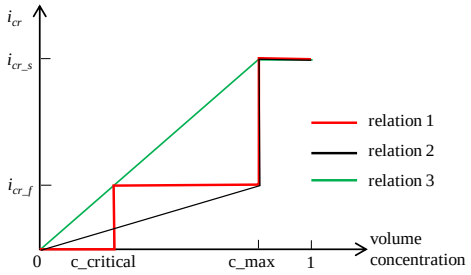

the relationship between critical deposition slope and volume concentration

Fig.2.15 The simple mixing case study and the assumed relationship between critical deposition slope and volume concentration

Due to the two critical values of deposition slope in the relation 1, it seems that the volume concentration is not stable in the present mixing model. It becomes better in the relation 2, but the volume concentration didn't vary with computed time smoothly. The relation 3 showed the volume concentration varied with computed time smoothly and stable. However, the large volume concentration of debris flows are always observed on the very flat slopes with 1°-3° in the filed survey. Therefore, a relationship between critical deposition slope and volume concentration (eq.(15)) is proposed with avoiding several critical values.

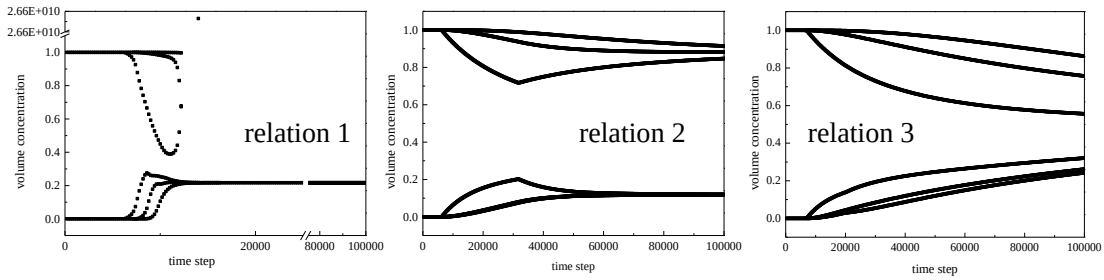

Fig.2.16 The volume concentration varied with the computed time under three cases of i_{cr}-c

$$i_{cr} = \begin{cases} \alpha(e^{\beta c} - 1) & (c \le 0.75) \\ -2\alpha\beta e^{0.75\beta}(c-1)^2 + \tan 30° & (c > 0.75) \end{cases} \qquad (15)$$

$$\alpha = \tan 30° / (e^{0.75\beta}(1 + 0.125\beta) - 1)$$

In the equation, α and β are two fitting parameters. α determines the inclination of relation curve. The relations showed in the figure under different β value. The simulation results (Fig.2.18) showed the volume concentration varied with computed time smoothly. In the present study, the β value varied with the topographic features.

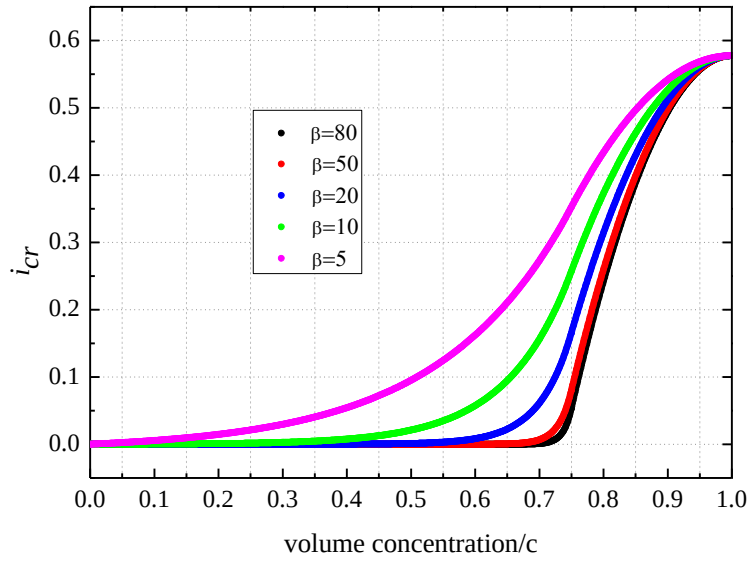

Fig.2.17 The proposed relationship between critical deposition slope and volume concentration

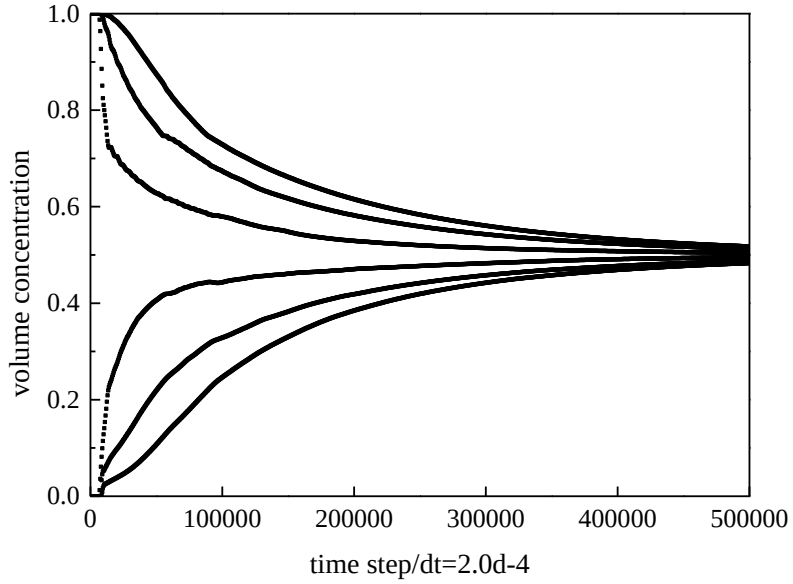

Fig.2.18 The volume concentration varied with computed time (β=10)

Such simple mixing model is not only used to initiate the solid particles, and also applied to reproduce some concentration-related phenomenon in the initiation and deposition processes.

(2) Verification

In the present model, diffusion coefficient was assumed to a constant in the whole computed time. Two cases (Fig.2.19) under three different diffusion coefficient are shown the effect of diffusion coefficient. In case 1, it is assumed that the water flow came from the upstream of valley. The water particles are assumed to distribute averagely in the whole research area in case 2.

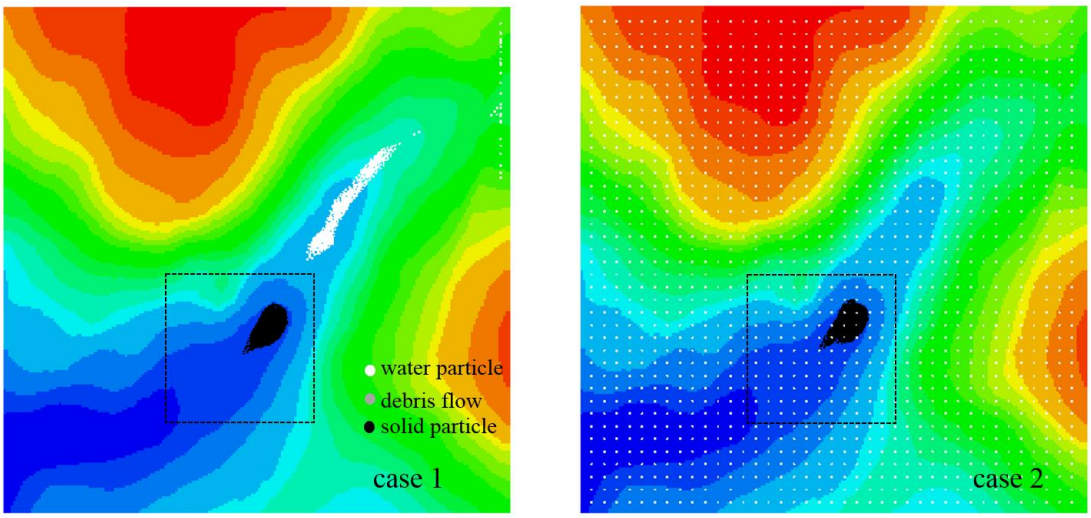

Fig.2.19 Two cases for evaluating the effect of diffusion coefficient

In the case 1 (Fig.2.20 and Fig.2.21), flow behavior clearly varied with the diffusion coefficient. As the diffusion coefficient is set to 0.001, the solid particles were mixed fast along the flow direction and debris flow washed out the landslide dam around 260s. Small solid particles with large concentration larger than 0.75 were moved to the downstream of valley together with debris flow (at 320s). After 380s, there remained many solid particles on the both sides of flow path near landslide dam under the diffusion coefficient is 0.001. The flow particles mixed solid particles along the marginal of landslide dam and finally more than one half of landslide dam were entrained to debris flow and flowed down if the diffusion coefficient is set to 0.01. Due to the large diffusion coefficient, the entire landslide dam was entrained to debris flow and was moved down with the diffusion coefficient equals to 0.1.

After 500s, the entrainment rate is 31.55%, 49.03% and 100% if the diffusion coefficient is set to 0.001, 0.01 and 0.1 respectively.

In the case 2 (Fig.2.22), water particles were averagely distributed in the whole research area and the direction of water flow was completely determined by the topographic feature. It means that there might be several different flows around the landslide dam, while the water flow only came from the upstream of valley in the case 1. The flow behavior also varied with the diffusion coefficient. Although the solid particles were mixed around the whole landslide dam at the initial state, the water flow coming from the upstream of valley channel played a primary role in mixing solid materials. Large diffusion coefficient inferred that flow had large entrain capability to move solid particles.

The flow behavior varied with the diffusion coefficient and water flow (direction, volume) in comparison with simulation results of both cases under three different diffusion coefficient. It inferred that the initiation mechanism influenced the flow behavior, discharge, volume, concentration, etc.

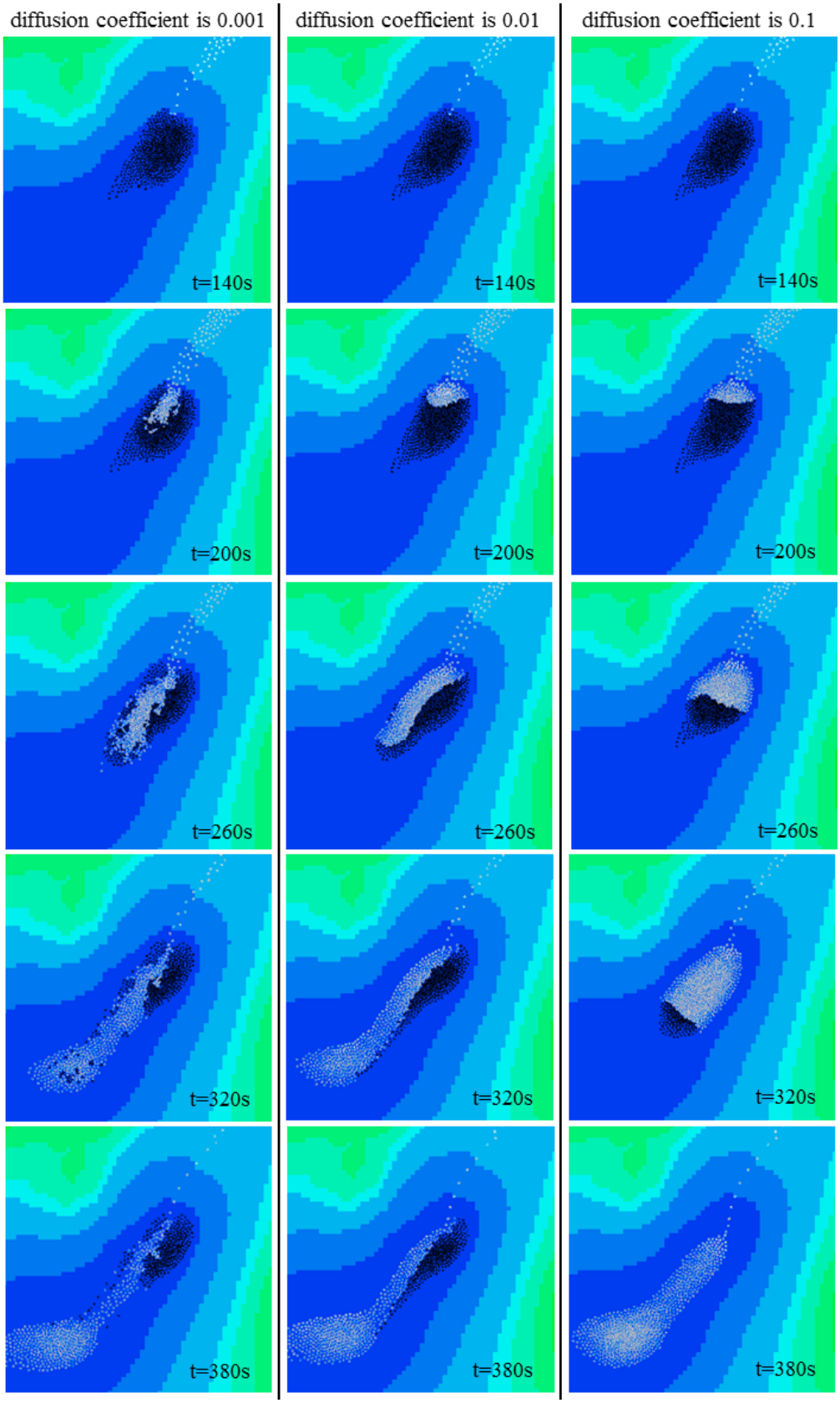

Fig.2.20 Flow behavior under three different diffusion coefficient in case 1

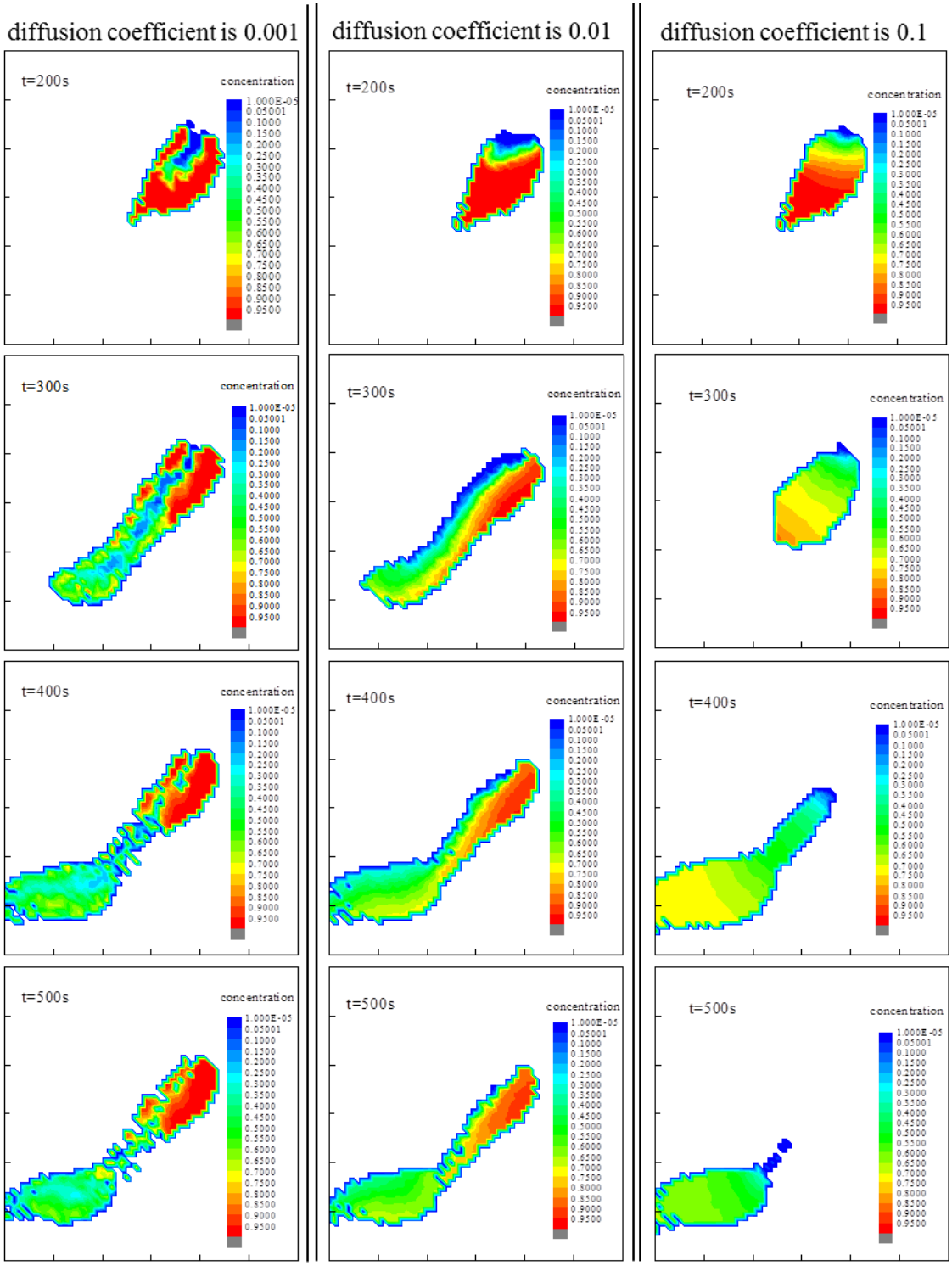

Fig.2.21 Volume concentration varied with simulation time in case 1

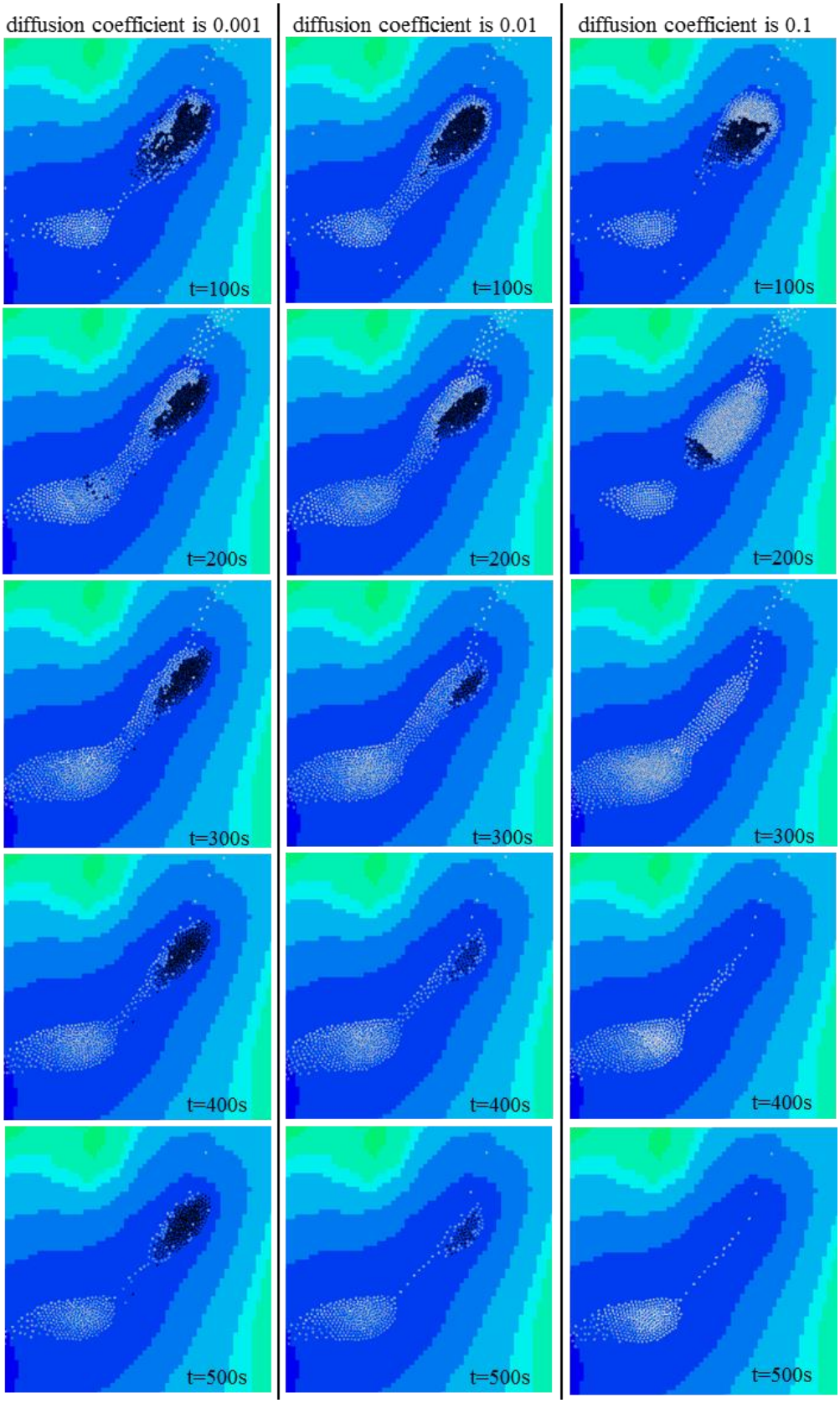

Fig.2.22 Flow behavior under three different diffusion coefficient in case 2

CHAPTER 3 SATELLITE IMAGES

Geographic Information System (GIS) is an efficient tool enabling to integrate information on environment, resources and human activities through digital base maps. It has been widely applied into kinds of fields, particularly, in geo-hazard assessment. Nowadays, kinds of images (such as aerial photos, topographic maps, and satellite images) are also be available to apply in assessing geo-hazards by processing to DEM. Satellite imagery has advantages in generating DEM because the measurement techniques are relatively established and elevation data are not likely to change so frequently. Combination of DEM and satellite imagery will contribute to the development of global spatial data infrastructure. We obtained satellite image from ALOS satellite in this study, I will make a detailed description in this chapter.

3.1 The Advanced Land Observing Satellite

The Advanced Land Observing Satellite (ALOS) "Daichi" was operated on 24 January 2006 to12 May 2011. The ALOS was expected to contribute to society in numerous ways, such as cartography, regional observation, disaster monitoring and resource surveying, etc. The introduction of ALOS cited the user handbook of earth observation research center in Japan aerospace exploration agency.

The ALOS has three remote-sensing instruments: the Panchromatic Remote-sensing Instrument for Stereo Mapping (PRISM) consists of three panchromatic radiometers and is used to derive a digital surface model (DSM) with high spatial resolution, which is an objective of the ALOS mission; Advanced Visible and Near Infrared Radiometer type 2 (AVNIR-2) has four radiometric bands from blue to near infrared, which are used for precise land coverage observation, such as investigating regional environment issues such as land-use and land-cover classifications, and disaster monitoring; Phased Array type L-band Synthetic Aperture Radar (PALSAR) for day-and-night and all-weather land observation.

Because PRISM extracted data will provide a highly accurate digital surface model (DSM), therefore, we downloaded satellite image from PRISM sensor in this study. The PRISM has three independent optical systems for viewing nadir, forward and backward producing a stereoscopic image along the track of satellite. Each telescope consists of three mirrors and several CCD detectors for push-broom scanning. The nadir-viewing telescope covers a width of 70km; forward and backward telescopes all cover 35km each. The telescopes are installed on the sides of the optical bench with precise temperature control. Forward and backward telescopes are inclined +24 and -24 degrees from nadir to realize a base-to-height ratio of 1.0. The wide field of view of PRISM provides three fully overlapped stereo (triplet) images of a 35km width without mechanical scanning or yaw steering of the satellite. Without this wide field of view, forward, nadir, and backward images would

not overlap each other due to the rotation of Earth. (Figure 3.1, Figure 3.2, Table 3.1, Table 3.2)

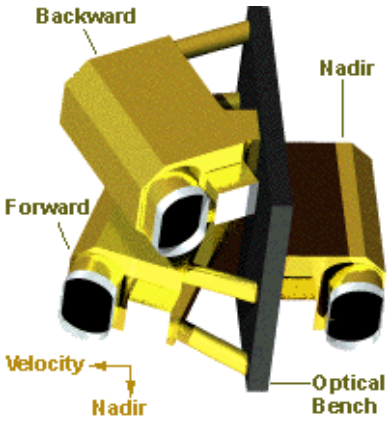

Fig.3.1 Overview of PRISM

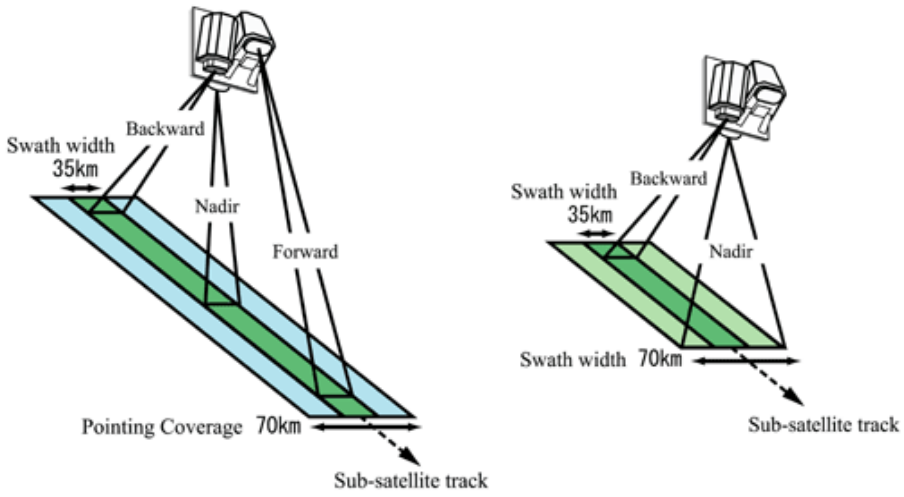

Fig.3.2 PRISM Observation Modes

Table 3.1 PRISM characteristics

Number of bands	1 (panchromatic)
wavelength	0.52 to 0.77 micrometers
Number of optics	3 (nadir, forward, backward)
Base-to-height ratio	1.0 (between forward and backward view)
Spatial resolution	2.5m (at nadir)
Swath width	70km(nadir only) / 35km (triplet mode)
S/N	>70
MTF	>0.2
Number of detectors	28000 /band (swath width 70km); 14000 /band (swath width 35km)
Pointing angle	-1.5 to +1.5 degrees (triplet mode, cross-track dirction)
Bit length	8 bits

Table 3.2 Observation modes

Mode 1	Triplet observation mode using forward, nadir and backward views (swath width is 35km)
Mode 2	nadir (70km) +backward (35km)
Mode 3	nadir (70km)
Mode 4	nadir (35km) +forward (35km)
Mode 5	nadir (35km) +backward (35km)
Mode 6	forward (35km) +backward (35km)
Mode 7	nadir (35km)
Mode 8	forward (35km)
Mode 9	backward (35km)

3.2 Choosing satellite images

In order to choose high-quality satellite image for special research area, it mainly ruled three criterions: observation time, cloud coverage and observation mode. Due to Zhouqu debris flow event and Wenchuan Earthquake occurred in 2010 and 2008 respectively, which all occurred during the ALOS work period. Therefore, it's completely available to obtain pre- and post-event images in observation time. Secondly, the image quality depends on cloud and snow coverage to large extents. Actually, it's very hard to control this factor, because there are large uncertainties about the location of cloud coverage and the type of cloud before obtaining the image. Generally, cloud coverage problem is more seriously in summer than in winter, while snow coverage mainly appeared on the images which observed in winter. In addition, in order to obtain DEM we must choose a pairs of images. Therefore, we have five choices from all of observation modes (Table 3.2). However, it's better to choose observation mode 1 and 2 because there are more observation images and also that overlap area is largest.

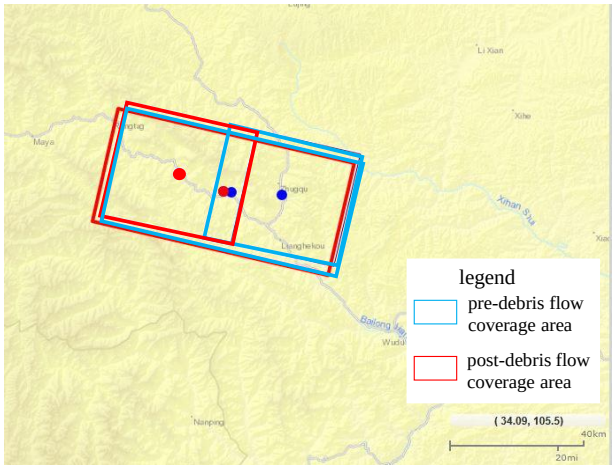

Fig.3.3 The location of pre- and post-debris flow satellite images

Table 3.3 The information of Satellite images for Zhouqu region

Scene ID	Obs. Date	Pds_Product ID	Img_Center coordinate Lat.	Lon.	Img_Cloud quantity	Pdi_No of pixels	note
ALPSMB212982975	20100123	O1B1_B	33.774	104.526	1	4928	pre-
ALPSMW212982920	20100123	O1B1_W	33.787	104.364	0	4992	disaster
ALPSMB273372975	20110313	O1B1_B	33.837	104.191	1	4928	post-
ALPSMW273372920	20110313	O1B1_W	33.790	104.337	2	4992	disaster

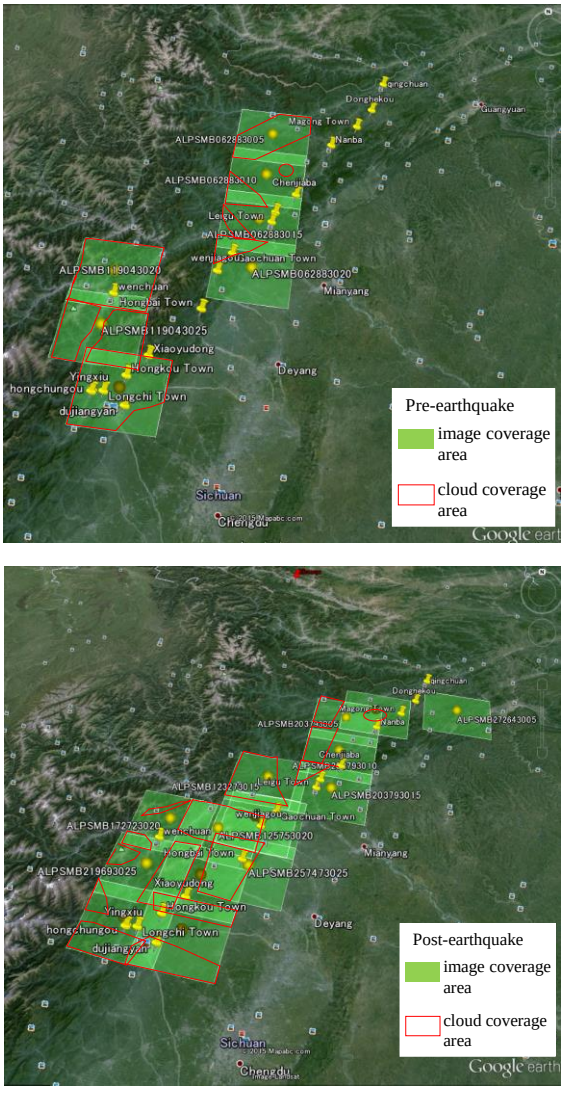

Fig.3.4 Pre- and post-earthquake satellite image in Wenchuan earthquake-stricken areas

Considering various factors, 24 pairs of images in two zones were downloaded. And 22 pairs of images covered the Wenchuan, Pingwu, Qingchuan, Beichuan, Anxian, Maoxian, Dujiangyan, etc., where mainly along the main faults and were seriously damaged during the earthquake. Mostly images are derived from observation mode 2, there is one more uncertainty about overlap area.

Because of the uncertainty of cloud coverage, special weather and topographic conditions, the quality of many pairs of images are very bad and can't be processed into DEM (Table 3.4 and Fig. 3.4). Therefore, we only determined study areas according to the existing images which quality is good enough to be processed into DEM, particularly in Wenchuan earthquake zone.

Table 3.4 The information of Satellite images for Wenchuan earthquake zone

Scene ID	Obs. date	Pds_Product ID	Img_Center coordinate		Img_	Img_Cloud	note
			Lat.	Lon.	Pixels	quantity	
ALPSMB072073030	20070602	O1B2R_UB	31.082	103.635	16188	4	Yingxiu
ALPSMW072072975	20070602	O1B2R_UW	31.068	103.628	29310	5	(×)
ALPSMB119043025	20080419	O1B2R_UB	31.362	103.538	16172	5	Yingxiu_
ALPSMN119042970	20080419	O1B2R_UN	31.347	103.531	14646	5	Wenchuan(×)
ALPSMB119043020	20080419	O1B2R_UB	31.609	103.603	16171	4	Wenchuan_
ALPSMF119042910	20080419	O1B2R_UF	31.576	103.610	16283	3	Maowen
ALPSMN119042965	20080419	O1B2R_UN	31.595	103.596	14647	4	(×)
ALPSMB062883020	20070331	O1B2R_UB	31.577	104.314	16188	1	Xiaoyudong
ALPSMW062882965	20070331	O1B2R_UW	31.562	104.306	29307	1	
ALPSMB062883015	20070331	O1B2R_UB	31.824	104.380	16186	1	Beichuan_Leigu
ALPSMW062882960	20070331	O1B2R_UW	31.810	104.373	29310	1	
ALPSMB062883010	20070331	O1B2R_UB	32.072	104.447	16187	1	Nanba_Magong
ALPSMW062882955	20070331	O1B2R_UW	32.057	104.439	29313	1	Town
ALPSMB062883005	20070331	O1B2R_UB	32.319	104.513	16190	3	Pingwu
ALPSMW062882950	20070331	O1B2R_UW	32.304	104.505	29314	2	(×)
ALPSMW219692975	20100310	O1B2R_UW	31.068	103.627	29309	1	Yingxiu
ALPSMB219693030	20100310	O1B2R_UB	31.111	103.485	16172	2	
ALPSMB219693025	20100310	O1B2R_UB	31.359	103.550	16172	2	Yingxiu_
ALPSMW219692970	20100310	O1B2R_UW	31.315	103.692	29310	2	Wenchuan
ALPSMB172723020	20090422	O1B2R_UB	31.604	103.635	16173	2	Wenchuan_
ALPSMW172722965	20090422	O1B2R_UW	31.560	103.778	29313	5	Maowen
ALPSMB125753020	20080604	O1B2R_UB	31.551	103.901	16212	4	Maowen-Qingping
ALPSMF125752910	20080604	O1B2R_UF	31.520	103.907	16248	4	(×)
ALPSMN125752965	20080604	O1B2R_UN	31.536	103.893	14635	4	
ALPSMB125753025	20080604	O1B2R_UB	31.304	103.834	16211	2	Xiaoyudong
ALPSMN125752970	20080604	O1B2R_UN	31.289	103.827	14635	2	(×)
ALPSMB125753030	20080604	O1B2R_UB	31.056	103.769	16211	1	Dujiangyan
ALPSMF125752920	20080604	O1B2R_UF	31.026	103.775	16245	1	(×)
ALPSMN125752975	20080604	O1B2R_UN	31.042	103.761	14634	1	
ALPSMB257473025	20101124	O1B2R_UB	31.361	104.070	16170	5	Mianzhu
ALPSMW257472970	20101124	O1B2R_UW	31.316	104.213	29307	3	(×)
ALPSMW123272960	20080518	O1B2R_UW	31.814	104.346	29306	2	Beichuan
ALPSMB123273015	20080518	O1B2R_UB	31.866	104.165	16171	1	(×)
ALPSMB203793015	20091121	O1B2R_UB	31.795	104.529	16213	0	Beichuan-Leigu
ALPSMW203792960	20091121	O1B2R_UW	31.809	104.370	29312	1	
ALPSMB203793010	20091121	O1B2R_UB	32.043	104.596	16214	2	Chenjiaba
ALPSMW203792955	20091121	O1B2R_UW	32.056	104.437	29313	2	
ALPSMB203793005	20091121	O1B2R_UB	32.290	104.663	16213	2	Pingwu
ALPSMW203792950	20091121	O1B2R_UW	32.303	104.503	29314	2	
ALPSMB268413005	20110207	O1B2R_UB	32.352	104.864	16171	0	Nanba, Magong
ALPSMW268412950	20110207	O1B2R_UW	32.307	105.007	29309	2	
ALPSMB272643005	20110308	O1B2R_UB	32.352	105.397	16171	0	Qingchuan
ALPSMW272642950	20110308	O1B2R_UW	32.307	105.541	29311	0	

Note: (×)-the image quality is very bad, and can't be processed into accurate DEM.

3.3 Image processing

In this study, we process satellite image into DEM using a commercial software that is MapMatrix. MapMatrix is a new digital photogrammetry platform developed by Wuhan Visiontek Inc. It can be applied in the field of 4D products production, disaster evaluation, emergency survey, forestry, water and national defense. It is often used to process kinds of images (e.g. aerial photos, satellite images) and attain DEM and DOM product. One of main features is high efficient image matching and image correction function; support data customization and dxf, dgn, txt and other popular formats data and coordinate system conversion.

The key procedure of processing image is selection of control points, which determined the absolute coordinate information. It's rarely available to get control point by measuring the absolute coordinate on site, we get control point from the Google Earth. Although the accuracy of Google Earth in China is not very high, it's an available and simple way to get control point. Generally, it needs five control points for a pair of images. Such control points should cover the whole overlap area, meanwhile, it's better to distribute in different geomorphology, such as flat lower place, summit, etc. It's noted that the cloud and snow coverage areas need to avoid. Even though the small coverage area has a strongly influence with the processed results. In the figure 3.5, it's very clearly that cloud coverage areas can't be processed correctly. It seems that the processed results are not bad beyond the cloud coverage area.

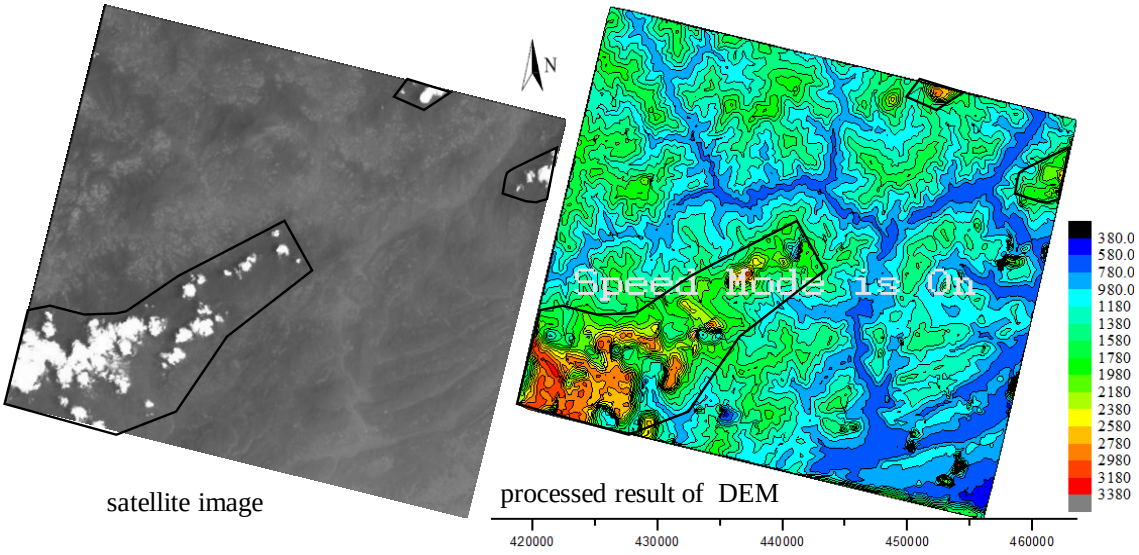

Fig.3.5 The effect of cloud coverage area to processed DEM

The resolution of such image is 2.5m. Considering the compatible between computation time and accuracy of topographic data, the pre-event satellite images are processed to 10m resolution digital elevation models for the present simulation.

3.4 Analysis on the accuracy of DEM

(1) Zhouqu

Compared topographic data from Google Earth and topographic map (1969), it's found that it's not a good choice to select control points on transition zone between lower-elevation area and summit to process satellite images. The error is very large, particular for elevation. We mainly chose control points from flat area and summit where rarely change in long period to attain more accuracy DEM and avoid additional error. The last update of Google Earth didn't cover the research area, but covered the vicinity area (point_03 and point_05). Therefore, five pairs of points were chosen from the topographic map and Google earth to check the accuracy of control points which obtained from the Google earth. The longitude and the latitude error is less than 3 seconds, and the error of elevation less than 50m except point_01. It's mentioning that the elevation error on flat lower-elevation zone is smaller than in summit. The process mechanism is interpolation. Therefore, it's better to choose control points both in lower elevation zone and high elevation zone, such as point_02 and point_04.

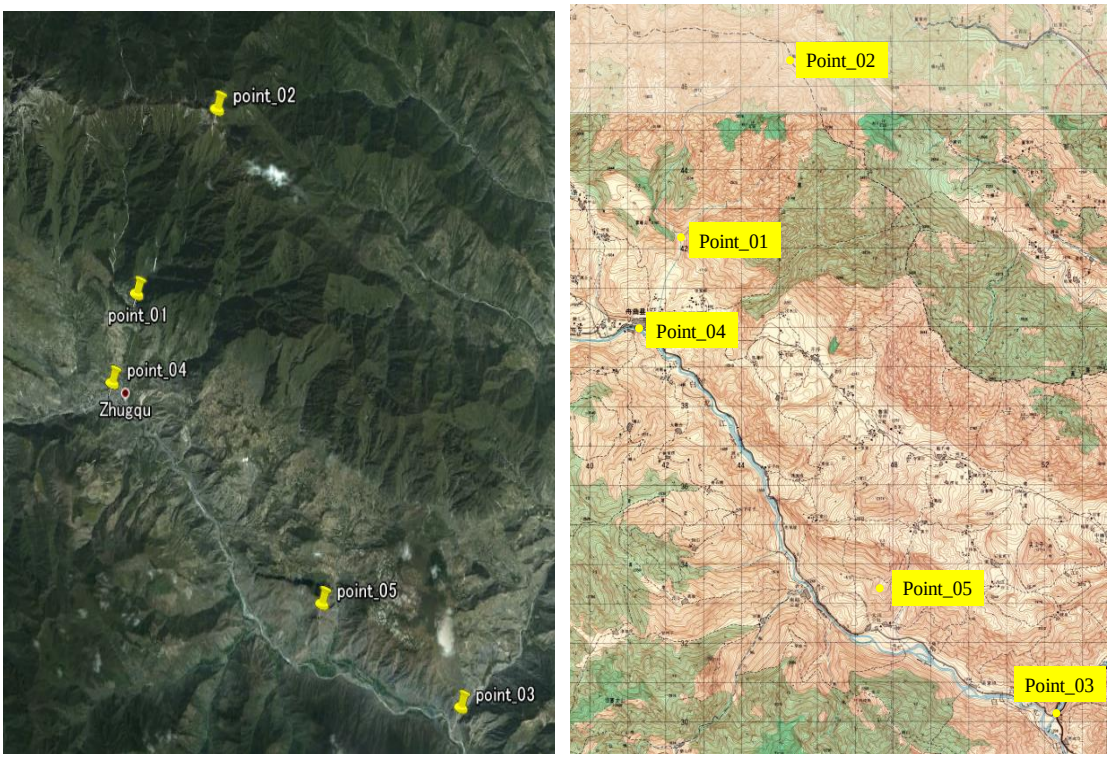

Fig.3.6 Choosing control points

Table 3.2 Comparison of the error of control points

Point	data source	longitude	/error	latitude	/error	elev./m	/error
Point_01	Topographic map	104°22'39"	2.36"	33°48'17.7"	0.87"	1585	-227
	Google earth	104°22'36.24"		33°48'16.83"		1812	
Point_02	Topographic map	104°24' 32.22"	-2.47"	33°50'37.24"	0.62"	3820	42
	Google earth	104°24'34.69"		33°50'36.62"		3778	
Point_03	Topographic map	104°29'9"	-0.34"	33°41'45"	-2.34"	1240	1
	Google earth	104°29'9.34"		33°41'47.34"		1239	
Point_04	Topographic map	104°21'53.4"	-1.07"	33°47'5.67"	2.26"	1340	3
	Google earth	104°21'54.47"		33°47'3.41"		1337	
Point_05	Topographic map	104°26'11.33"	-0.85"	33°43'31.52"	-1.28"	1880	38
	Google earth	104°26'12.18"		33°43'32.80"		1842	

It's note that all of coordinate information is obtained by interpolation according to several control points. Therefore, the error is gradually decreased in the whole processed area. We check the processed results with topographic map (by China National Mapping Bureau, 1969), it's indicated that it's reasonable to use Google Earth to decide control points if ignore small error which occurred by different coordinate system.

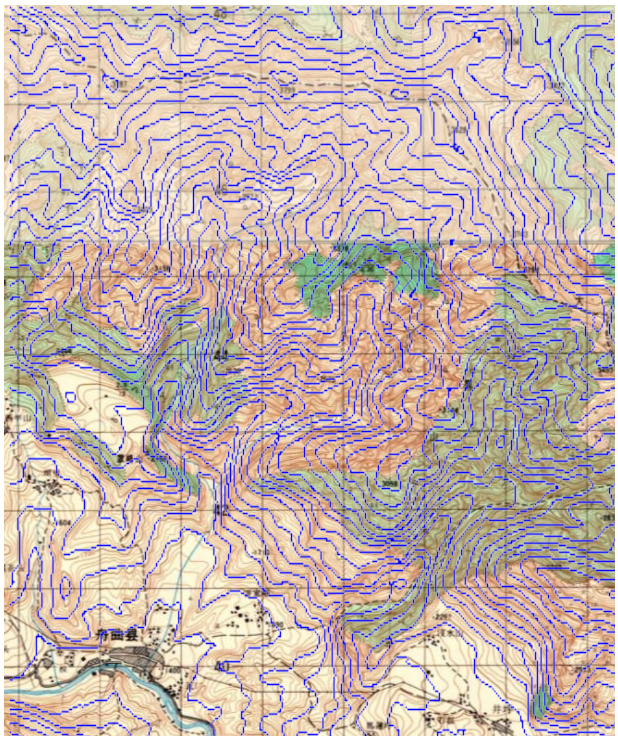

Fig.3.7 The overlap results between processed DEM and topographic map

(2) Wenchuan

The images of the earthquake-stricken areas are adopted to analyze post-earthquake debris flows in a wide region. Therefore, the topographic data of Google map was used to roughly check the processed results of DEM. In the figure 3.8, the region from Wenchuan to Caopo was showen in terms of satellite image, processed results of DEM and Google map, respectively. The satellite image showed that snow covered on the higher-elevation zones, while there are rarely snow or cloud in the lower-elevation zones. Therefore, only lower-elevation zones were selected and processed. It's rarely available to obtain an accurate point from Google map. Only main topographic features, such as valley channel, river, were roughly checked with the Google map. It's seems that the valley channels and river matched well with each other. In addition, three small areas were selected to check the elevation. It's found that the snow had a little influence for the elevation of lower-elevation zones.

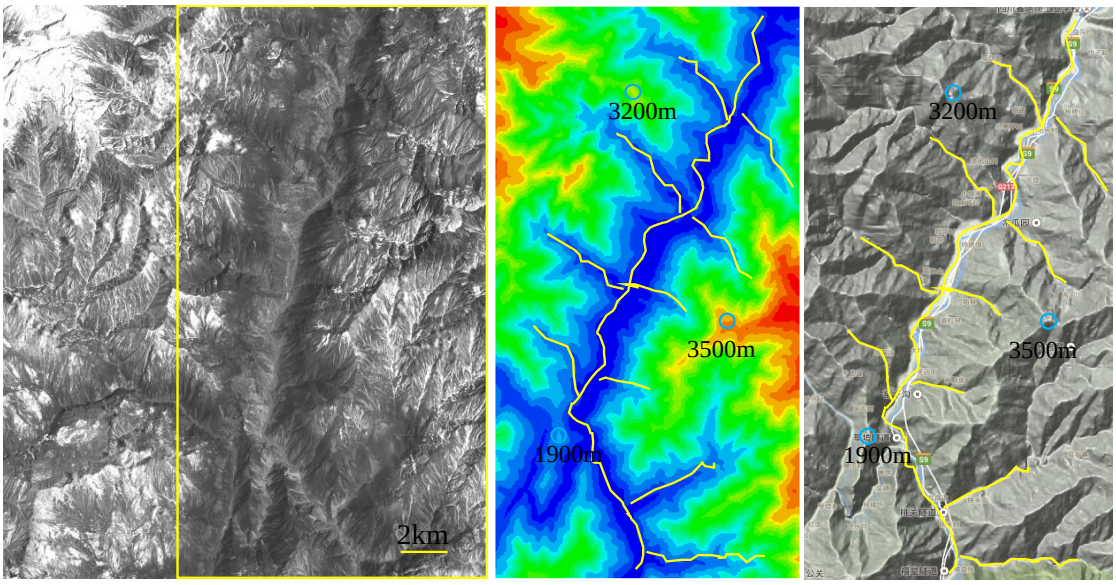

satellite image processed result of DEM from Google map

Fig.3.8 Roughly check the accuracy of DEM by Google map in Wenchuan region

CHAPTER 4 A DEBRIS FLOW EVENT IN ZHOUQU COUNTY

4.1 Geological setting

Zhouqu, located in the southern of Gansu province, China. It belongs to the transitional mountainous region between the southeastern edge of the Tibetan Plateau and the Qinling-Longmen mountain ranges. Due to Indosinian, Yanshan and the Himalayan orogenic affected, the geology structure is rather complex and faults activity are very frequently (Fig.4.1). New tectonic is also very active, the topography of this region is characterized by rugged mountains with elevations between 1000m and 4000m and deeply incised valleys (Hu et al., 2010). The region of Zhouqu, where situated in Zhouqu-Wudu earthquake zone, is an active earthquake region and the seismic intensity is Ⅶ. According to seismological monitoring of Zhouqu county, there were more than 200 times earthquake which intensity less than Ⅳ, and in particular the intensity ranged Ⅱ-Ⅳ up to 60 times from 1990-2008. Due to the Tibet plateau uplift, the earthquake occurred frequently in the western of China, and Zhouqu experienced several important earthquake in history (Table 4.1). By history records and literatures, the Wudu earthquake in 1879 caused large collapses in Zhouqu area, especially in Sanyanyu (SYY) and Luojiayu (LJY) catchments. And the 2008 Wenchuan earthquake had also some influence to Zhouqu, but there wasn't any new collapse and landslide in both SYY and LJY catchments by field investigation and Tang et al. (2011) also indicated that no significant landslides were triggered by this earthquake. The geology lithology of this area consists of Silurian slates and phillites, Permian limestones, and Devonian limestones and slates. Quaternary deposits mainly distributed on river terraces and alluvial fans. The surface of the bedrock is deeply fractured and highly weathered (Tang et al., 2011).

Table 4.1 Statistical results of main earthquakes in Zhouqu and its adjacent areas (Li et al. 2011)

Time	Epicenter	intensity
BC186	Wudu	6-7
1634	Northern of Wenxian	6
1677	Wudu	5.5
29 June 1879	Southern of Wudu	5.7
1 July 1879	Wudu	8
3 February 1960	Zhouqu	5.2
22/23 August 1976	Songpan	6.7/7.2
8 January 1987	Diebu	5.9
12 May 2008.	Wenchuan	8

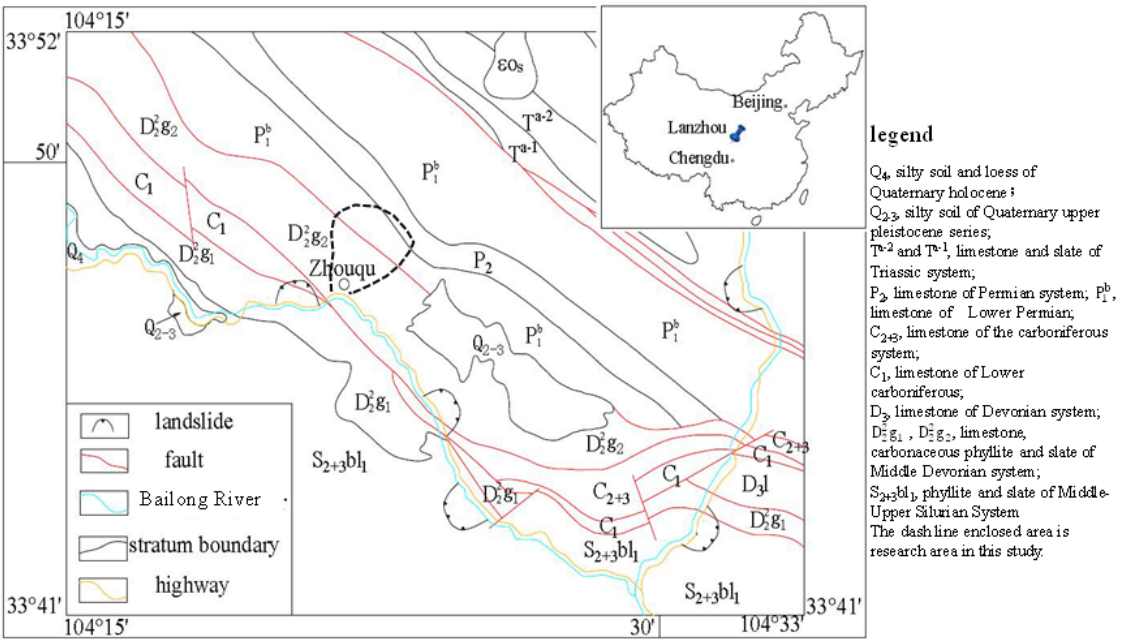

Fig.4.1 Geological map of Zhouqu region

This area has a semi-arid to arid climate with an annual mean precipitation of 434mm. On average, 75% of the annual precipitation falls largely concentrated in the period from June to September. There geological disasters occur frequently due to complex geological setting, special climate condition and human activities. Landslide and debris flow are the most common patterns of geo-hazards in this zone. They always threat local resident and influence the traffic system seriously.

4.2 Debris flow

On midnight of 7 August 2010, two giant debris-flows developed by a rainstorm in the SYY and LJY catchments, in the northern direction of the Zhouqu City. They killed 1765 people living on the existing alluvial fan and caused huge economic losses. Furthermore, more than 5500 houses along their flow paths were damaged. In addition, the debris flows rushed into the Bailong River and formed a barrier lake about 550 m in length and 70 m in width (across the river) which flooded the 1/3 of the city for several days.

According to the existing literature (Wang et al., 2011), SYY valley is a frequently and active debris flow valley which occurred dozens of times (Table 4.2) since 1823 recorded and almost every event caused different damage to local resident, infrastructures, farmland, lifeline projects, etc., while LJY valley is a low-frequency and inactive debris flow valley.

(1) Topographic features

The topographic characteristics of both SYY and LJY catchments are rather complex. Both sides of valley channels are very steep and the valley channels are very narrow (Fig.4.2). It is noted that the

slope angle of both sides of valley channel ranged 55° to 74°. The shape of whole catchment area looks like a fan, of which the upstream is very wide and the mouth of valley is rather narrow (Fig.4.2, Table 4.3). Such topographic characteristics are very easy to confluence in short time if it rains. The discharge will be increased drastically at the mouth of valley due to the width of flow cross-section must decrease at the mouth of valley. The slope of valley channel in most parts is larger than 15°. Takahashi (1980) indicated that channel slope was greater than 15° and of which was favor for triggering debris flow. It means that the original topography is favor for generating debris flow under reasonable rain condition if there are sufficient debris sources in both catchments.

Table 4.2 The history of SYY debris flow valley

Time	casualties	buildings	farmland ($10^4 m^2$)	economic loss (10^4 RMB)	Others
1823, 1879, 1904	▲	▲	▲	▲	▲
1916	> 60	>90	20	▲	▲
Jul. 1943	46	140	32	▲	damaged 8 bridges
1961	28	160	36	43.4	traffic interruption 45 days, blocked the Bailong river
Jul. 1978	58	98	43.33	42	traffic interruption 12 days
May 1989	51	360	63.67	1000	damaged 10 bridges and other infrastructures
30 Apr. and 4 Jun. 1992	87	344	87.73	1260	damaged infrastructures
13 Jul.1993	▲	40	20.66	▲	▲

Note: ▲ means not detailed recordings.

Table 4.3 Main morphometric parameters of research area

Valley	catchment area	length	relative elevation	width of valley mouth
SYY	$25.75 km^2$	10.4km	2488m	50m
LJY	$16.14 km^2$	9.5km	2460m	7-8m

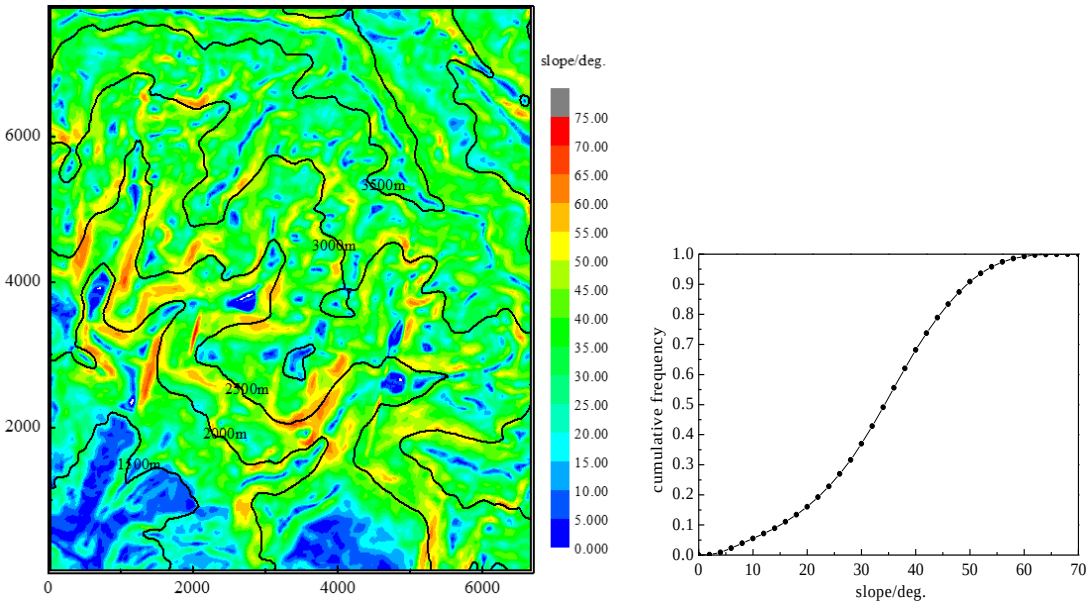

Fig.4.2 Slope distribution features in the Zhouqu region

(2) Debris sources

By filed survey, it's found that there are very rich debris sources in both valleys (Fig.4.3). It mainly originated from three kinds of sources, such as large landslide dams, weathering deposits on both sides of valley channel and sediment on the channel bed. The peak discharge of the debris flow increased at least 60% due to the breaching of the landslide dams in the SYY valley (Yu et al., 2010). The debris flow tracks widened from the original 2-4m to the present 5-9m in the upstream rills of the initiation area of the SYY valley and the incision depth of channel is 0.5-1.5m (Tang et al., 2011). Debris source was also significant in LJY valley. It is estimated that the erosion depth was up to 1-3 m, and the erosion width and length was about 20-40m and 2-3km respectively. The mobilized channel-bed material continually scoured and entrained additional debris and progressively increased the solid concentration of the flow transforming it into a debris flow. Tang's research showed that colluvium deposits were mainly present along and near torrents exposed by erosion triggered by channel incision. The basin behind check dams had been filled half or even totally before the event. All of check dams were destroyed during this catastrophic event and all materials stored behind check dams supplied 10-15% materials due to the dam failure.

The large landslide dams were originated from the rock-fall due to the provious earthquake (Ma & Qi, 1997), therefore, there were many huge boulders on deposition fan near mouth of valley after debris flow disaster. It's noted that the height of landslide dams up to 80-280m and the volume is about $2800\times10^4 m^3$, of which recharge rate is 68%. Due to the scale of landslide dam is large and boulders usually larger than 10cm and the largest can up to 12-14m, debris flow washed out and eroded the margin of landslide dam, and caused some part of margin would collapse and composed

main debris source for debris flow further. The recharge of solid loose material is about $2693.84\times10^4m^3$ and the recharge rate up to 65%.

Fig.4.3 Debris sources in both valleys

Table 4.4 Types of debris source for debris flow at SYY valley (Tang et al., 2011)

type of debris source	landslide dams	landslide	channel deposits	slope debris	unstable rock mass	amount
storage of solid loose material/10^4m^3	2829.4	94.9	840.12	315	64.1	4143.52
recharge of solid loose material/10^4m^3	1926.4	52.6	523.8	141.5	49.3	2693.6

The volume of sediment in debris flow was transported out of valley which was estimated at $97.7\times10^4m^3$, however, there are still large amount of loose debris materials remain in the valley.

(3) Rainfall

Rainfall plays a critical role in triggering debris flow. However, it was always mild rain in Zhouqu city from debris flow initiation to finally deposition on the deposition fan. The nearest rain gauge station (Zhao, 2010) in Zhouqu city monitored the rainfall was only 2.4mm and the early cumulative rainfall was less than 5mm at 0:00 on 8 August 2010. But the destructive debris flows had occurred at 23:20. According to the recordings of rainfall stations near Zhouqu (Fig.4.4), the existing research (Yu et al., 2010; Zhao et al., 2010; Tang et al., 2011) agreed that the event rainfall was 77.3mm during 45min from Dongshan rain station.

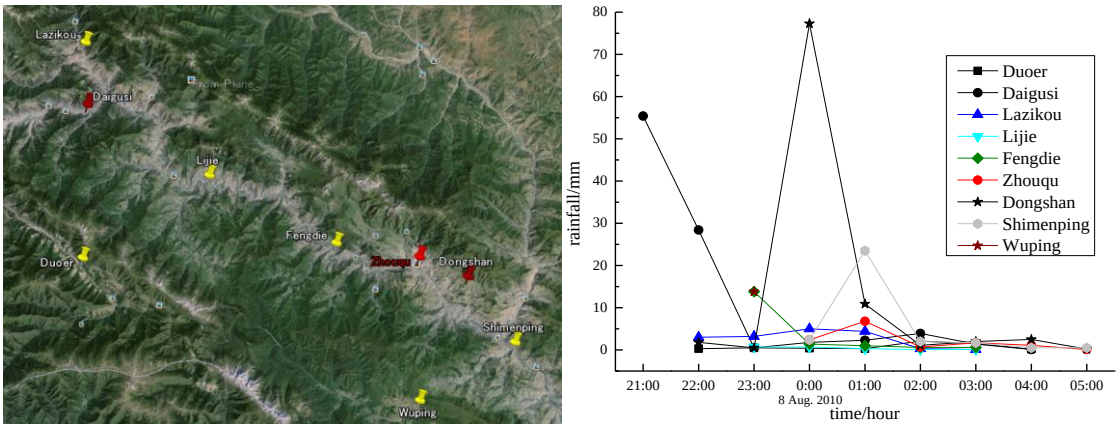

Fig.4.4 The rainfall features from rain gauge stations in the vicinity of Zhouqu City

From the rainfall features for previous debris flow events in SYY valley (Table 4.5), it's found that basically more than 30mm rainfall in one hour can trigger debris flow. Therefore, it seems reasonable to agree the disaster was an unexpected incident from Zhouqu rain gauge station. It's revealed that rainstorm concentrated on upstream and middle part of SYY and LJY catchment before 23:00. From the recordings of eight rain gauge stations near Zhouqu, it's demonstrated that there had a large difference for local rainfall features in a wide catchment. Therefore, rainfall was a trigger factor and can't be used to evaluate the disaster because of its uncertainty and diversity. It's also inferred that the forecast of geo-hazards is not mature in the rural mountain areas, due to the shortage of equipment and technology.

Table 4.5 The rainfall features for previous debris flow events in SYY valley

date	rainfall/mm	duration
15 July 1978	37.4	1h
18 June 1982	46.8	1h
10 May 1989	47.0	1h
4 June 1992	38.4	45min
7 August 1994	63.3	2h

Advantage topographic features, rich debris sources and rainstorm played a fundamental role in generating debris flow. However, why the discharge and magnitude of the debris flow was increased suddenly compared the history events according to LIGC and TSIG in 1982 (Tang et al., 2011) with not clearly change on topography and debris sources? And what's the rainfall intensity to trigger the disaster in that time? Therefore, it's necessary to quantitative evaluate the disastrous mechanism to avoid sequence potential debris flow disasters.

4.3 Basic results

4.3.1 Parametric studies

In this section we discuss the effect of some parameters including mesh size, Manning coefficient, critical slope of deposition, flow volume and discharge on the overall debris flow behavior. A series of simulations were simulated to discuss about five factors in terms of the spatial pattern of deposition, travel distance and extent of deposition. By recording the location information of every particle in the whole simulation process, and then the affected areas were mapped to analyze the influence of kinds of factors. In the simulation process, debris flow particles were set to generate automatically near the valley mouth by a constant discharge except evaluation of mesh size.

(1)Mesh size

The input topographic data should be accurate enough to obtain reasonable results, because the gravity and frictional forces are heavily dependent on the inclination of the sliding base (Chen & Lee, 2000). The existing study demonstrated that DEM quality and grid resolution were crucial for the resulting delineation of potentially affected areas and thus for hazard assessment and mapping (Stolz & Huggel, 2008). Accurate and more detailed spatial resolution of topography is especially important to reproduce the natural debris flows. Due to the dynamic characters of debris flows, the user must verify whether the DEM used for modeling applications actually represents the current surface and morphology in the investigation area, especially the high-resolution DEM is better. It is available to reproduce the actual events on the basis of accurate topographic data. However, facing the contradictions between topographic accuracy and computation capacity, it's necessary to evaluate its effect before simulating actual debris flow.

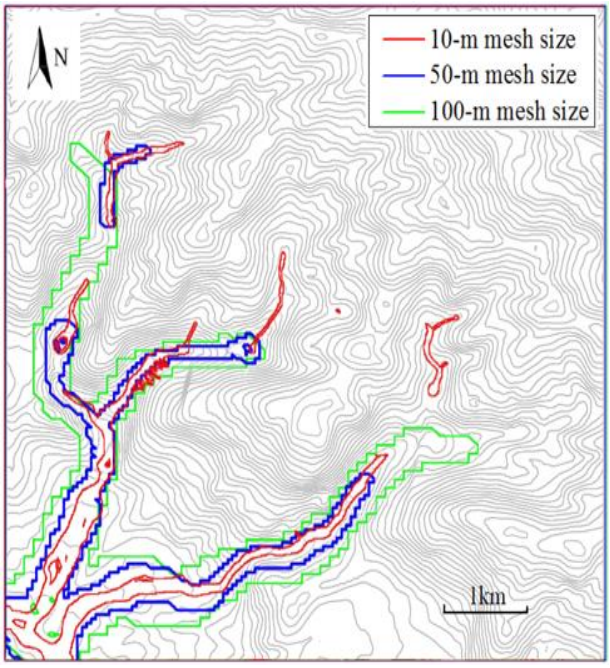

Fig.4.5 Simulated affected area under different mesh size

At the initial state before simulation of debris flows, the research area is discretized by the mesh size, it stands for the high resolution of topographic data to large extent. Figure 4.5 showed the resulting flow areas obtained by various mesh size with the same condition except mesh size. It is observed that the flow area increases with increasing mesh size. It is primarily because the loss of topographic details leads to less disturbance of the flow. Furthermore, the numerical particles themselves become larger and the number of particles becomes smaller by increasing mesh size, which may reduce the energy dissipation due to particle interaction.

According to the comparison results of mesh size in terms of affected area, the affected area by the smaller mesh size is more close the reasonable results. The affected area by 50m mesh size and 100m mesh size is 2.2 times and 4.6 times respectively of the smallest affected area. It seems that the travel distance is sensitive to the smaller mesh size. Because larger mesh size only roughly showed the topographic features and ignored the detailed local information. It demonstrated that larger mesh size is only adopted to give an approximate estimation of the potential affect zones for evaluation of regional debris flows, while the smallest mesh size is adopted to quantitative evaluation of individual debris flow. Therefore, the mesh size will be adopted 10m in the sequence simulation. The mesh size also influences the maximum velocity of the debris flow, and its effect will be discussed in the following sector in detail.

(2) Manning coefficient

Figure 4.6 shows the maximum velocity during the entire flow in the simulation in terms of mesh size and Manning coefficient. It was found that the maximum velocity of simulated debris flow is within the range of realistic value (15-5m/s) under the commonly-used Manning coefficient range (0.1-0.3) if the 10m mesh is adopted. The maximum velocity with 50m and 100m mesh size increased by 127% and 189% comparing with 10m mesh size, respectively, which may be not realistic range. Since the flow velocity is not only very sensitive to impact force acting on the structure in the flow, and its value also influenced the entrainment of solid materials in the initiation process, it is important to validate it by the parametric study.

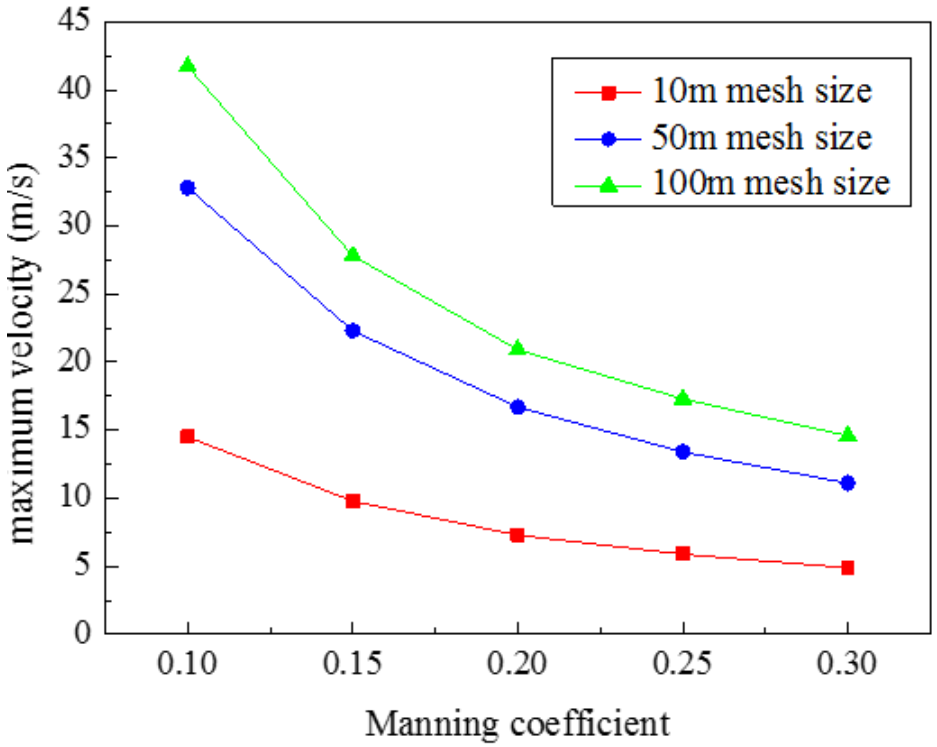

Fig.4.6 Maximum velocity varies with Manning coefficient under different mesh size

parameter	Q=1000m³/s	Q=200m³/s	Q=50m³/s
n=0.1			
n=0.2		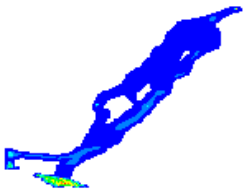	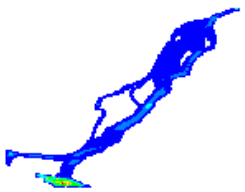
n=0.3			

Fig.4.7 Simulation results under discharge and Manning coefficient

Manning coefficient not only influenced the velocity of debris flow, it also influenced the deposition features. The effect of Manning coefficient and discharge in figure 4.7. In this series of simulations, 10m mesh size was adopted and the critical slope of deposition was set to 1°. The simulation results under discharge and Manning coefficient showed that Manning coefficient has a little influence with deposition if the discharge is set larger than 200 m^3/s. If the discharge is set to 50 m^3/s, it's found that Manning coefficient influenced the spatial patterns of deposition and extent of deposition.

(3) Critical slope of deposition, flow volume and discharge

The effects of critical slope of deposition, flow volume and discharge are illustrated in figure 4.8. In this series of simulations, 10m mesh size was adopted and the Manning coefficient was set to 0.1. When critical slope of deposition was set to 3°, affected area and travel distance clearly became smaller than the case with critical slope of deposition was set to 1°. When the critical slope of deposition was set to 5°, the affected area and travel distance became much smaller. It's demonstrated that the critical slope of deposition mainly governed the travel distance. The travel distance reduced rapidly with the increasing of critical slope of deposition. It's also found that discharge strongly influenced the spatial patterns of debris flow deposition as well as the extent of deposition if critical slope of deposition is set to 1°. The extent of deposition is clearly decreased with decreasing the discharge. Such influence will be reduced with increasing the critical slope of deposition. It's inferred that smaller critical slope of deposition played a significantly role in deposition features if the discharge is also small. It's observed that the flow volume influenced the travel distance and extent of deposition. The travel distance and extent of deposition are all increased with increasing flow volume.

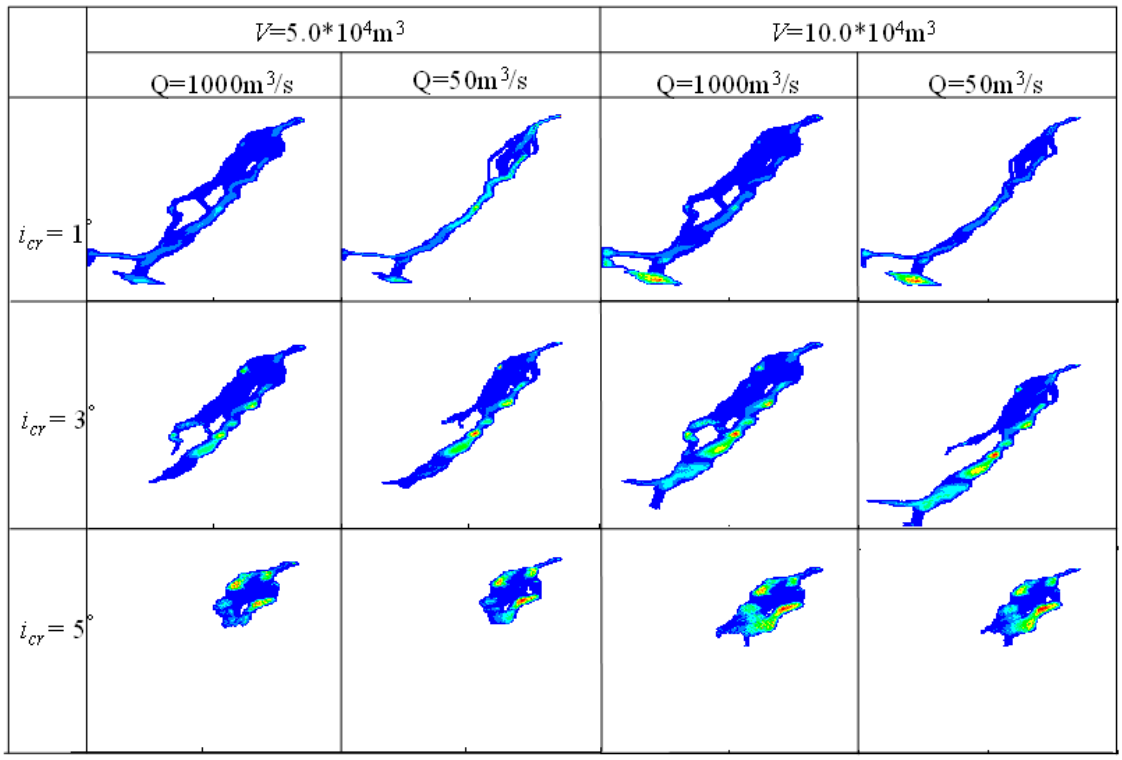

Fig.4.8 Simulation results under different factors

From the above results, it's found that discharge played a critical role in deposition features. All of results are obtained from the SYY area. In order to make the results have enough convince, one more simulation result about the effect of discharge is showed basing on the topography of LJY area (Fig.4.9). In the simulation, 10m mesh size was used and the critical slope was set to 1° as well as the flow volume kept the constant in three cases. It's found that discharge has some influence with the spatial patterns of deposition and extent of deposition. Such influence is smaller than in SYY deposition fan. It's inferred that topographic features governed the deposition features to large extent.

The spatial patterns of debris flow deposition played a critical role in understanding the potential hazards associated with active debris flow processes on fans. Debris flow lateral spread shortly after flowed out of the valley mouth due to the hydraulic pressure between pair-wise particles. Meanwhile, different spatial patterns of deposition were generated on the deposition fan. It's obviously that discharge not only governed the spatial pattern of deposition, and also significantly controlled the extent of deposition, especially in horizontal direction which vertical the flow direction. Both the critical slope of deposition and flow volume strongly influenced the travel distance and extent of deposition. However, there is little difference in spatial patterns of deposition when critical slope of deposition is larger than 3°. The present analysis inferred that flow behavior and topographic features played a critical role in deposition characteristics. The travel distance and extent of deposition varied with the spatial patterns of deposition to large extent. In general, this critical slope

of deposition can be observed in the deposition area of debris flow, which is around 5°. However, this material parameter changes drastically by the water content, it is quite difficult to predict the affected area very accurately.

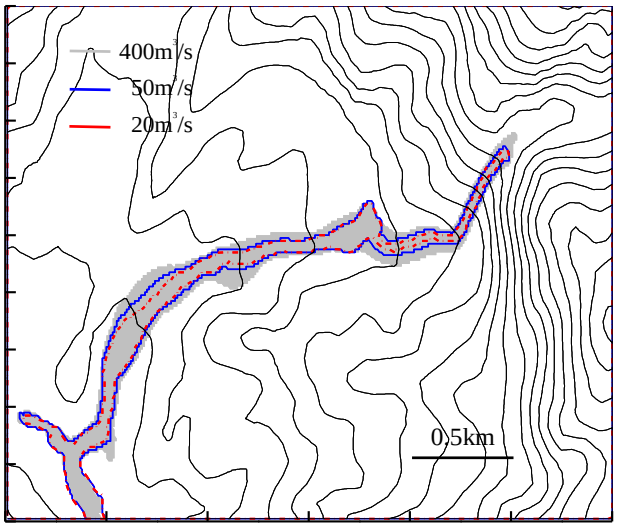

Fig.4.9 The effect of discharge on LJY deposition fan

4.3.2 Step 1: simulation of debris source

Evaluation of debris volume and location of debris sources are very important for the hazard assessment. In particular, loose deposits existing at the bottom of valley may cause the growth of debris flow. Such loose geo-materials are intermittently supplied by the slope failure and lateral erosion, and it is difficult to estimate its volume by 10m digital elevation models directly.

In our simulation scheme, we assume that unstable debris source is generated from relatively steep slopes larger than 60°. First, we determine such unstable slope area from the topographic data, and put debris 'particles' on it. Then, according to the equation of motion, those particles fall down the slope and are heaped up at the bottom of the slope (Fig.4.10). In the present study, the repose angle of loose deposits was set to 26° based on the field observation of slope of loose deposit in valley channels (Fig.4.10), and the Manning coefficient was set to 0.1 based on the literature (Chen & Zhang, 2006). Eventually debris source of $4.296*10^5 m^3$ in volume was generated in both SYY valley and LJY valley if the particle height was set to 1.0m (Fig.4.11). The simulated deposits are shown in black in the figure 4.11.

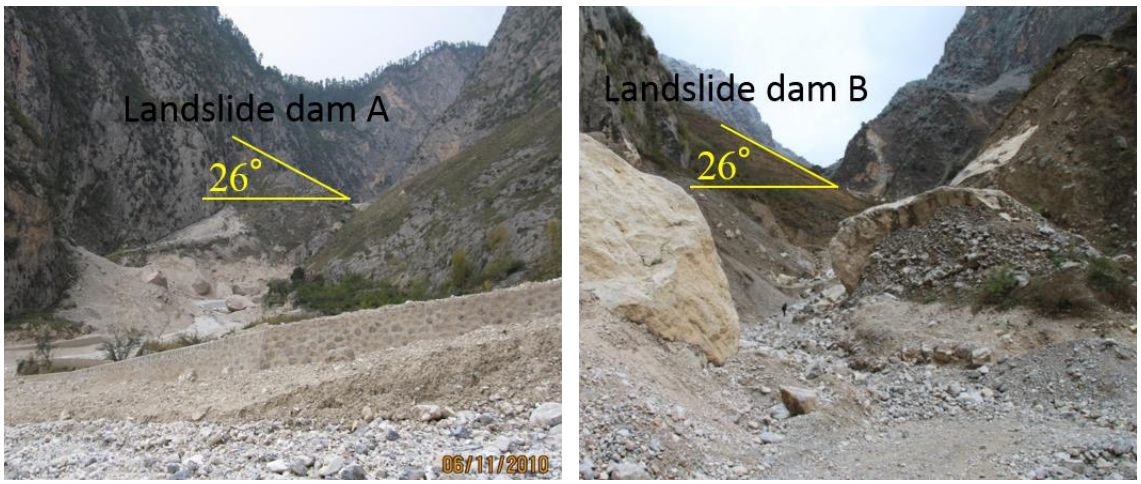

Fig.4.10 The repose angle of large-scale landslide-dams in SYY valley

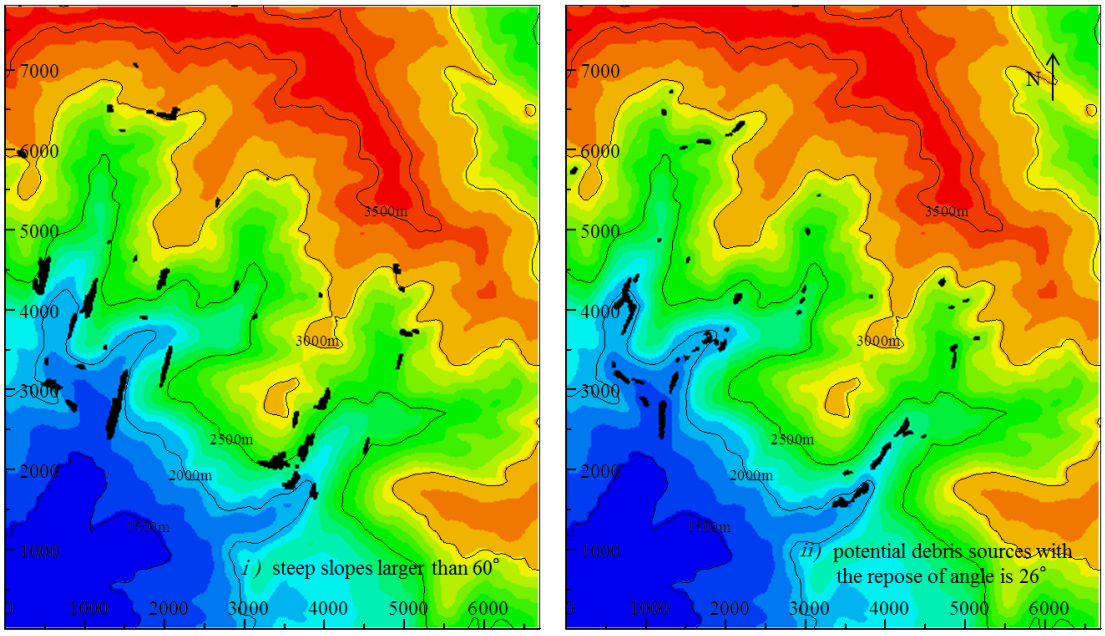

Fig.4.11 Simulation the location and volume of debris sources

Due to the most deposits were derived from the landslide-dams, which generated by the previous earthquake, it's reasonable to check the simulated results of debris source by slope failure larger than 60°. As illustrated in the figure 4.12, the simulated results of debris sources were showed in the red color with overlapping on the pre-event satellite image. It's found that mostly debris sources concentrated on the downstream of valleys and distributed on both sides of valley channels or blocked the valley channel, while there were small particles on the upstream of valleys.

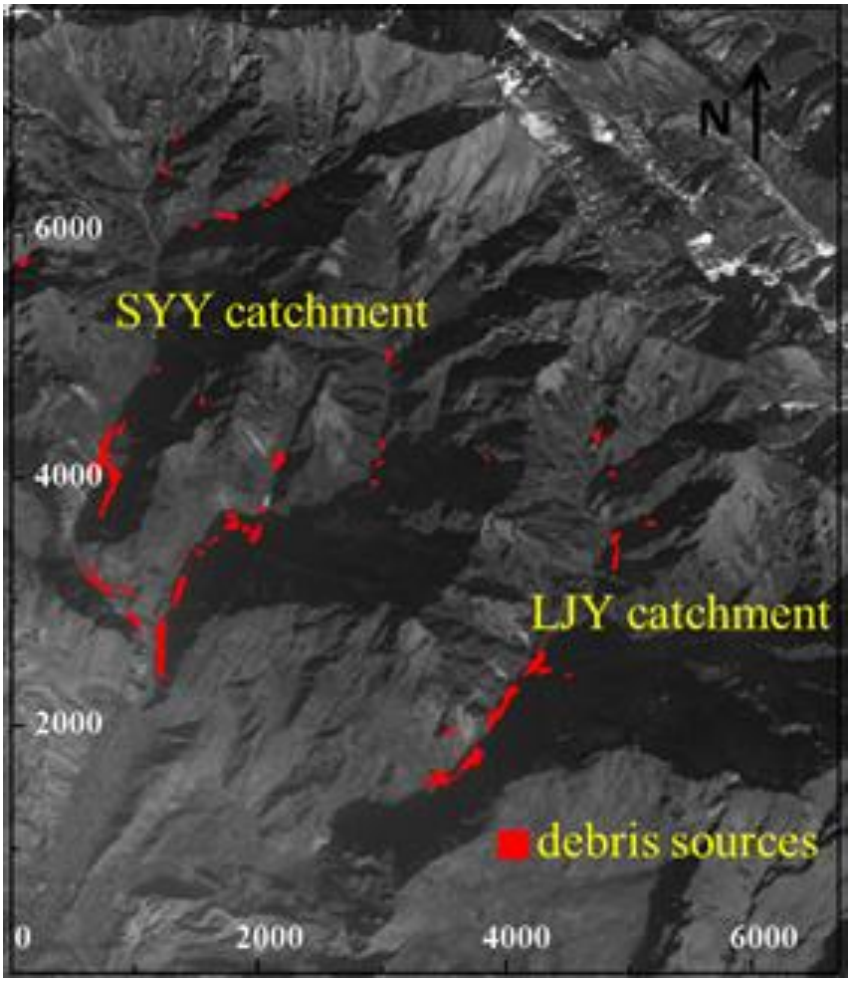

Fig.4.12 Simulation results of debris sources overlapped on the pre-event satellite image

Although it's hard to evaluate the simulation results of debris sources only by pre-event image, we have enough data from field survey. In the figure 4.13, pictures a-e showed the debris sources in the different places of both valleys. It's demonstrated that large-scale landslide-dam and original deposits on the channel bed supplied large amount of debris sources in the last debris flows. The close-up of two landslide dams A and B on the post-event image, it's clearly showed that the margin of landslide-dams were eroded and huge solid materials were entrained into the debris flow. Meanwhile, it showed that there are still enormous amounts of loose solid materials which are still easy to entrain to sequence debris flows. It looks that the agreement of simulation results of debris sources and actual deposits only in term of location of debris sources is good.

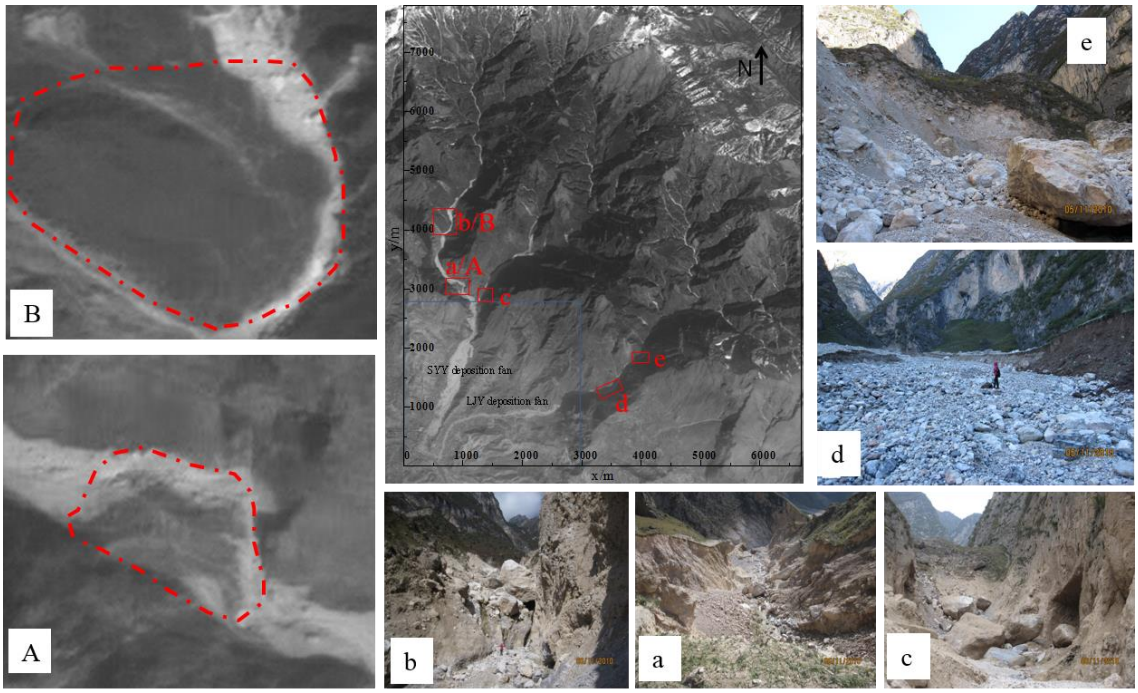

Fig.4.13 Debris sources in the actual events by field investigation

Considering the evaluation of debris source volume,the existing evaluation of voume was $9.29*10^5 m^3$ by Yu et al. (2010), and about 60% of debris sources were derived from landslide-dams that generated from the slope failure and/or collapse due to the preceding earthquake (Ma & Qi, 1997). In addition, rich deposits on channel beds also supplied enough solid materials in this event. By field investigation, the maximum thickness of such deposits on channel beds is higher than 20m. In this event, eroded depth is estimated as 0.5-1.5m and the original truck of 2-4m width was widened up to 5-9m in the upstream rills of the debris flow initiation area at SYY valley (Tang et al., 2011). It is estimated that the erosion depth was up to 1-4m, and the erosion width and length was about 20-40m and 2-3km respectively in LJY valley. Tang et al. (2011) also provided the similar survey report. In the present method, the volume of debris source was determined by the number of unstable particles and the initial particle height.Four small zones were selected to evaluate the thickness of debris sources. The thickness of debris sources is in a realistic value ranging 0-8m in multiple zones (Fig.4.14). In the landslide dam B and LJY valley channels, the thickness of debris sources is larger than the thickness of debris sources near the landslide dam B and the mouth of Xiaoyanyu valley.

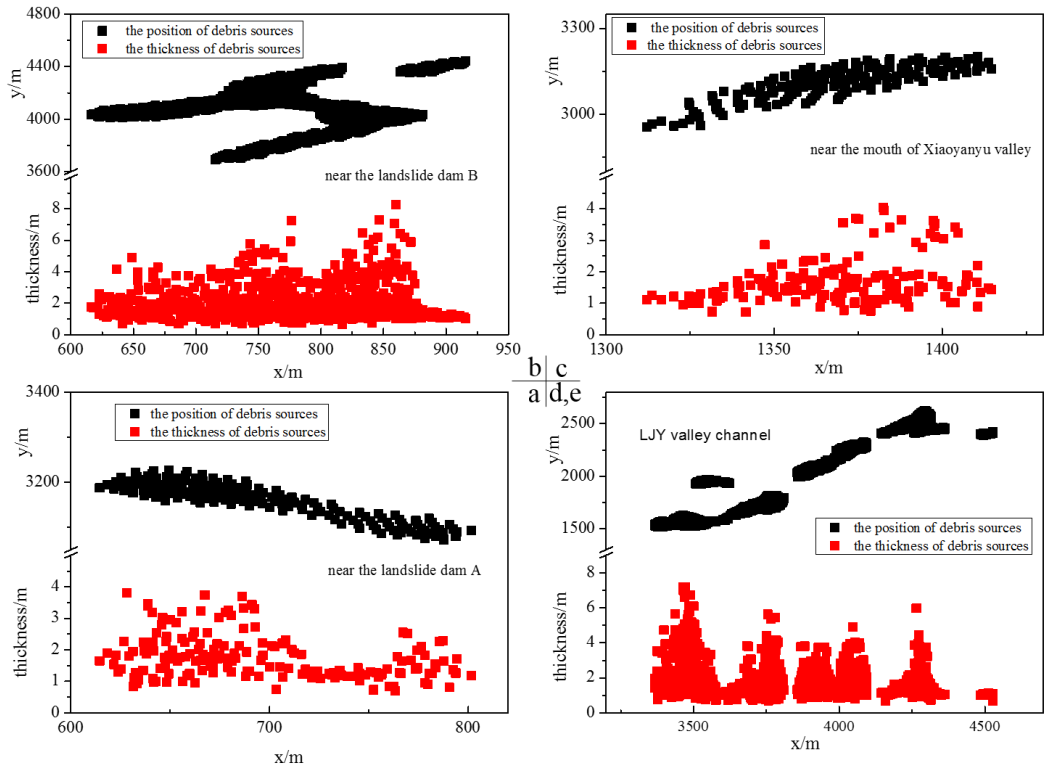

Fig.4.14 The thickness of simulated debris sources

In our preliminary research, the distribution of debris source is in good agreement with the filed observation. Therefore, it's reasonable to evaluate debris flows based on the current information of debris sources.

4.3.3 Step 2: simulation of debris flow

Here, two simple initiation models were used to simulate the initiation, transportation and deposition processes of debris flow. And then the differences between two models were discussed.

(1) Re-initiation model

In the re-initiation model, debris flow was initiated only by changing physical properties of particles that generated in the step 1. Using the debris source particles simulated in the step 1, debris flow simulation was carried out by setting Manning coefficient and critical slope of deposition to 0.1 and 1° respectively. Then debris flows of both valleys flowed further down according to the equation of motion, and reached to the Bailong River after 1330s from initiation. Finally, most of the debris flows were accumulated on the deposition fans and the river.

Detailed transport processes in the entire research area were composed of six stages (Fig.4.15). The SYY debris flow and the LJY debris flow flowed out of the valley mouth around 360s after the initiation. Then both debris flows diverged on the deposition fans following the given topography. After 820s from the initiation, the SYY debris flow was divided into two, and the main flow head

directed to the eastern part of the deposition fan; the LJY debris flow kept the entire and continually flowed along the topographic features. At 1150s later, two branches of SYY flow converged into one near the downstream of deposition fan. Meanwhile, the LJY flow has a clearly turning and the width of cross-section was up to maximum value. The SYY flow divided into two again after 1200s from initiation near the margins of deposition fan, while the eastern main flow still predominant until it flowed into the Bailong River in the front of deposition fan. Both debris flows flowed into the River after 1330s, and deposited in the river. After 30 min from the initiation, most of particles finished the transportation process and deposited on the downstream of deposition fan, while there were small particles deposited in the valley channels. In the whole transport processes, the SYY debris flow had a clearly lateral spread on the deposition fan, while the LJY debris flow always kept as the entire due to topographic feature. The local topographic features, such as bifurcation, depends on the used topographic data to large extent. Such detailed flow processes may help to design countermeasure facilities.

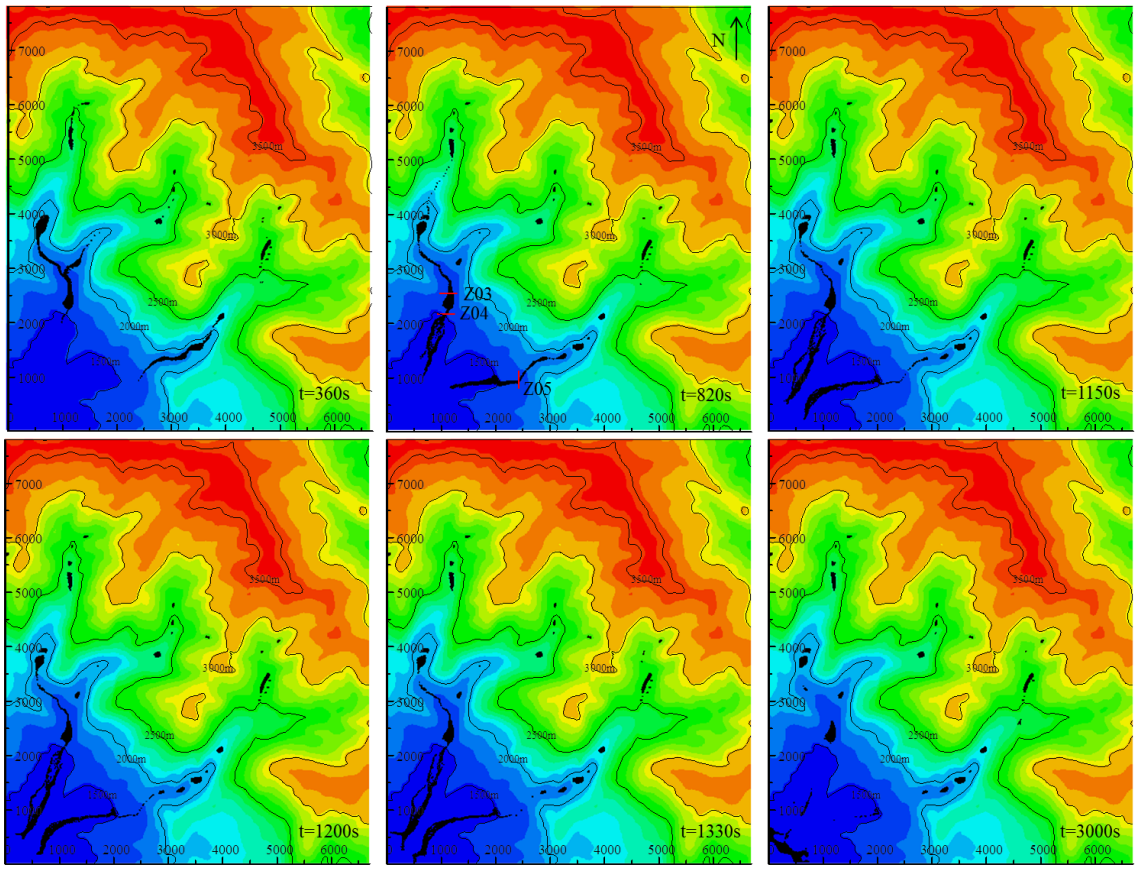

Fig.4.15 Transportation process of both debris flows

Deposition fan is common used for agriculture and/or human habitation because of the scarce low-gradient land in mountainous area. And hence mostly damage occurred on the deposition fan. We focused on the depositional characteristics on deposition fan, such as the spatial patterns of

deposition, the travel distance and the extent of deposition. In the figure 4.16, a-e are the overlapped figures of both simulated affected area and pre-event satellite image under different critical failure slopes i_f. The red lines stand for the maximum depositional boundary in the simulation results, and the smaller enclosed areas by red lines were the unaffected area where the debris flow crossed that zone and did not cause any damage. f is the post-event satellite image, and light gray-white area is actual damaged areas. Three cross-sections of Z03, Z04 and Z05 are selected to count the numbers of crossing particles.

In the present simulation results of five cases, the number of particles is 5847, 4296, 2890, 2371 and 1934 if the critical failure slope i_f is set to 59º, 60º,61º,61.5º, and 62º, respectively. In all of five cases, debris flows of both valleys flowed out the mouth of valleys and travelled different distances on the deposition fans (Fig.4.16). There generated more additional debris sources near the mouth of SYY valley and the affected areas were larger than the actual damage areas if i_f was set to 59º, while there were small particles reached to the deposition fans and the travel distance and affected areas were smaller than actual events if i_f was set to 62º. The agreement between simulation results and actual events is good in terms of spatial patterns of deposition and travel distance, when i_f was set to 60º, 61º and 61.5º. Regarding the affected areas, it's found that the simulation results of affected area was only 3% larger than the actual damaged area in SYY deposition fan, while the simulation results of affected area was 177% larger than the actual damaged area in LJY deposition fan, if the i_f was set to 60º. The affected areas on LJY deposition fan were close to actual damage areas with reducing the number of debris flows, while the affected areas on SYY deposition fan were smaller than the actual damage areas.

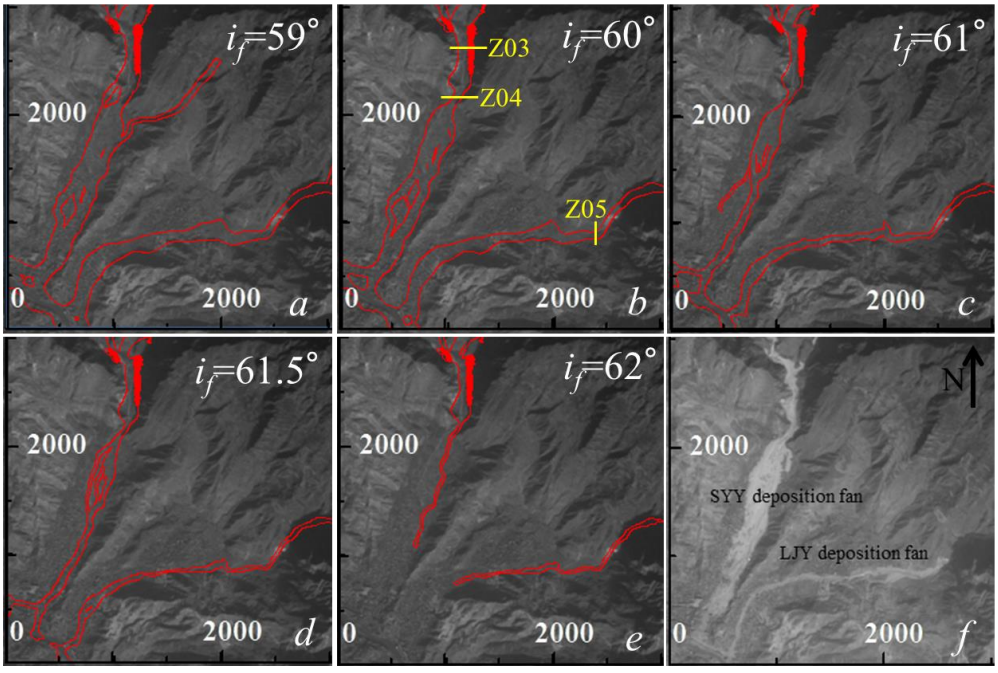

Fig.4.16 Affected areas on deposition fans

Regarding the simulation results of deposition, the discharge played a critical role in influencing the spatial patterns of deposition, affect areas and distance (Zhang et al., 2014b). As illustrated in the figure 4.17, the hydrograph varied with different positions and simulation times. The peak value of particle number is 23, 9 and 14 for Z03, Z04 and Z05 respectively, if the i_f was set to 60º. Due to the special topographic features near the mouth of SYY valley, the discharge clearly reduced in Z04 comparing Z03. When the affected areas of LJY debris flow is close to the actual damage areas, the peak value of particle number is less than 5 at Z05. It inferred that the discharge in SYY debris flow was larger than in the LJY valley.

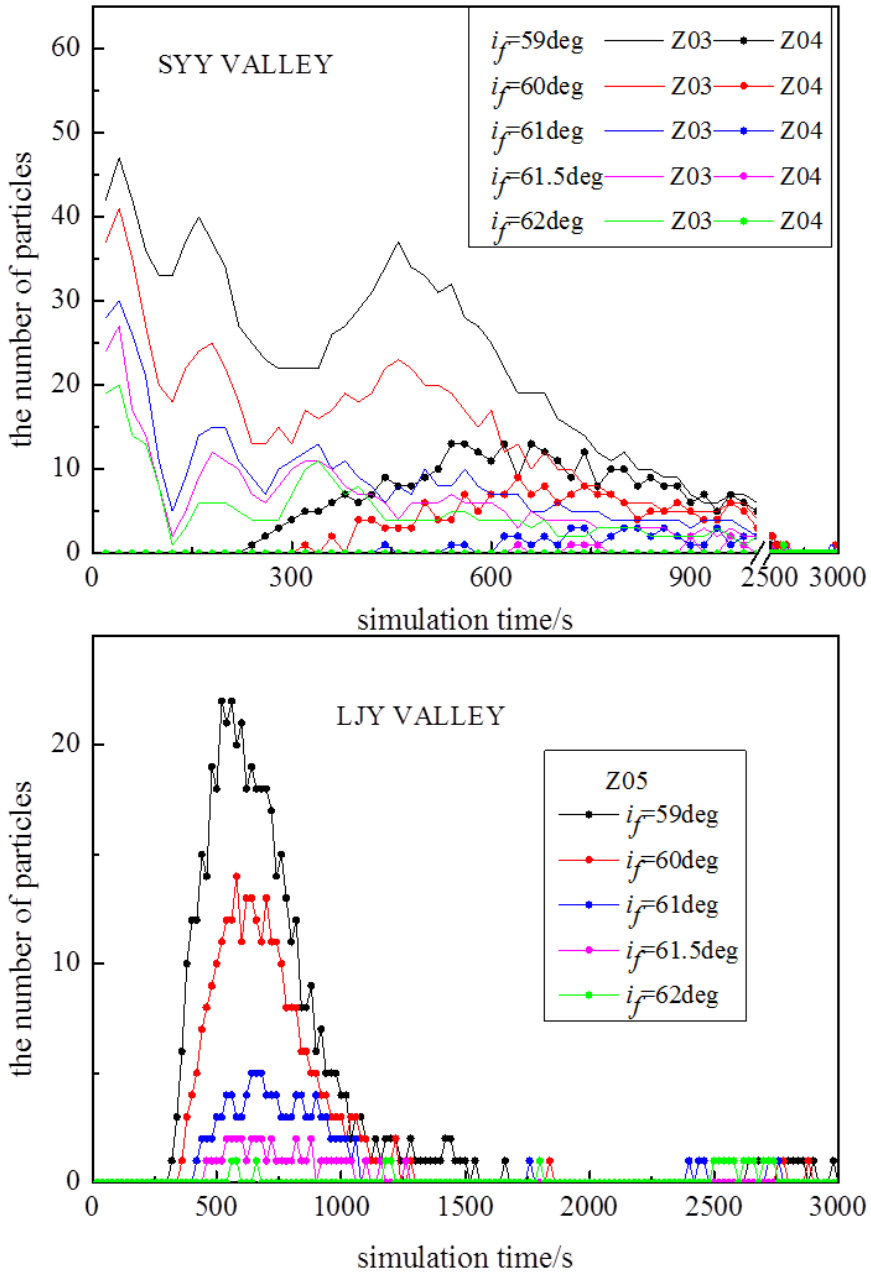

Fig.4.17 Hydrograph of both debris flows near the mouth of valleys using re-initiation model

In order to reproduce the actual debris flow, the discharge was set to different value for both debris flows. To efficient control the discharge of debris flows near the mouth of valley, the debris flow particles were set to generate automatically near both valley mouth. The simulation results showed in the figure 4.18, if the discharge was set to 1000m^3/s and 50m^3/s for SYY and LJY valleys, respectively. It agreed well with the actual damage areas. The discharge of actual events was estimated to 1358m^3/s and 572m^3/s for SYY and LJY valleys respectively (Yu et al., 2010). Therefore, it seems that the flow properties is one of important reasons to cause the whole simulation results had some differences with the actual debris flows.

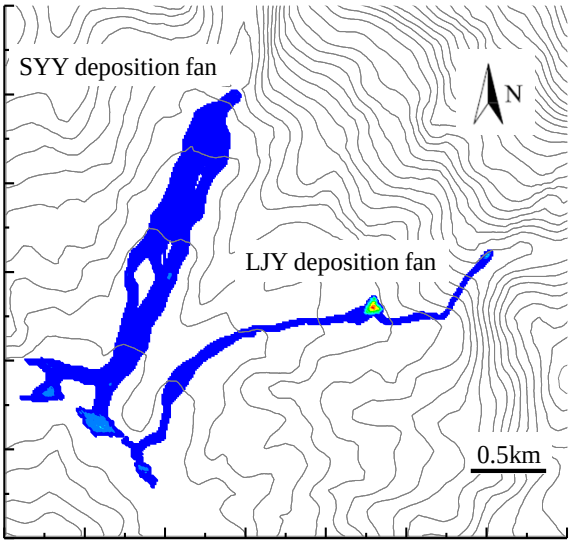

Fig.4.18 Simulation results of affected areas by setting different discharge for both debris flows

In the present model, debris sources were estimated only by the critical failure slope and didn't consider more factors, such as lithology. Therefore, it's hard to generate reasonable debris sources in both valleys by the same critical failure slope. Moreover, all of particles were initiated simultaneously in the step 2. The location of debris sources also influenced the simulation results. The present used mesh size might be larger than some existence elements with characteristic size, which such as buildings, roads and drainage channels etc. Actually, the existing drainage channel of pre-disaster played an important role in transporting debris flow on LJY deposition fan, while the existing channel of SYY deposition fan was too narrow to transport debris flow (Fig.4.19). The width of pre-existing drainage channel on the upstream of SYY deposition fan was only 2.6m. Even though the overflowed debris flows on LJY deposition fan damaged both sides of drainage channel, the damage width was reduced to minimum due to the pre-existing drainage channel.

Fig.4.19 The pre-existing drainage channels on both deposition fans

Since the flow velocity is very sensitive to impact force acting on the structure in the flow, it's very important to accurately evaluate the velocity of debris flow to efficient prevent and mitigate the potential disasters. In the proposed method, the Manning coefficient as one of two important parameters, it not only reflects the roughness of topographic surface, and also influences the velocity of debris flow. Figure 4.20 shows the computed velocity varied with simulation time at three cross-sections. It was found that the velocity of simulated debris flow is within the range of realistic value (0-8m/s) under the Manning coefficient was set to 0.1. Due to the wide and flat topographic features near Z03 cross-section, the velocity ranged 3-4m/s, even if the discharge is rather large. The velocity increased to 6-8m/s when the debris flow flowed out the mouth of SYY valley, while the velocity ranged 3-5m/s near the mouth of LJY valley. This might be one of reasons to cause serious damage on the SYY deposition fan. However, Tang et al. (2011) estimated that the peak velocities were 9.7m/s and 11m/s near Z03 for the SYY and near debris source d and e for LJY valleys respectively according to empirical equations.

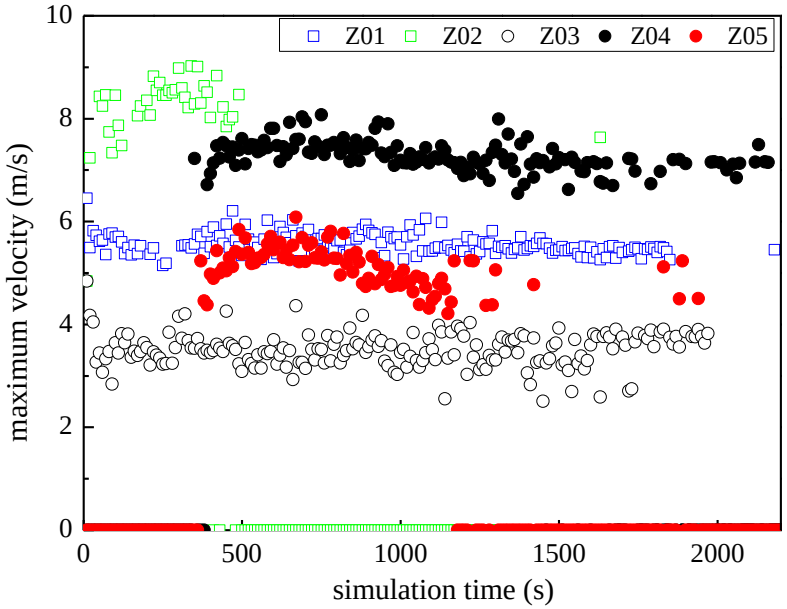

Fig.4.20 The velocity at three cross-sections (i_f is 60º)

(2) Mixing model

In the mixing model, the distribution features of water particles influenced the simulation results of debris flow. First, the rainfall features were analyzed by averagely distributing water particles in the whole research area using 50m mesh. As illustrated in the figure 4.22, above 30s, water particles can flow to the valley channel under Manning coefficient is set to 0.033. It took 500s to transport the water flow from the summit to deposition fan. Noted that more than two flows flowed into the deposition fan around 30s. The water particles from the mountain areas with the elevation ranging 2000m-3000m between SYY catchment and LJY catchment finally formed two water flows and flowed into the SYY and LJY deposition fan after 90s from the initiation. Five cross-sections (Z01-Z05) were selected to analyze the discharge in both valleys (Fig.4.21). Due to the larger catchment area of SYY valley, the peak value of hydrograph at Z03 is clearly larger than Z05. The hydrograph curve at Z04 is always lower than Z03, it inferred that water particles became dense in the range from Z03 to Z04. This special topographic feature can reduce the flow discharge for flowing outside of valley. Even though such special topographic feature near the SYY valley mouth, the peak valley at Z04 is still larger than peak value at Z05.

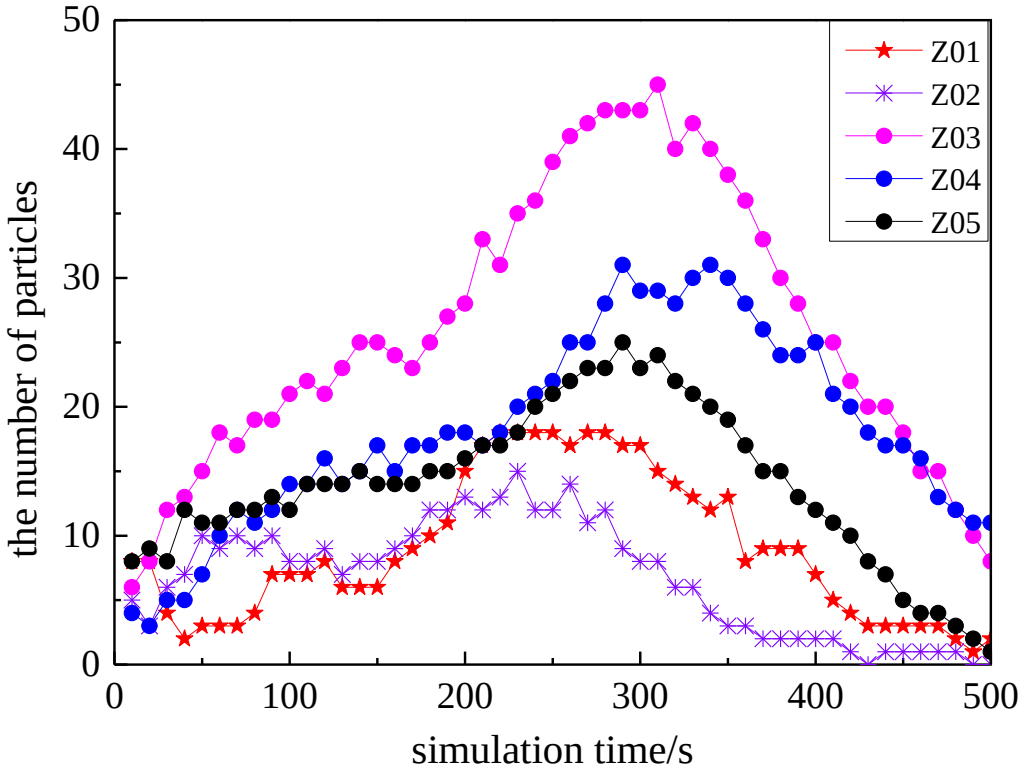

Fig.4.21 Hydrograph of rainfall for both SYY and LJY valleys

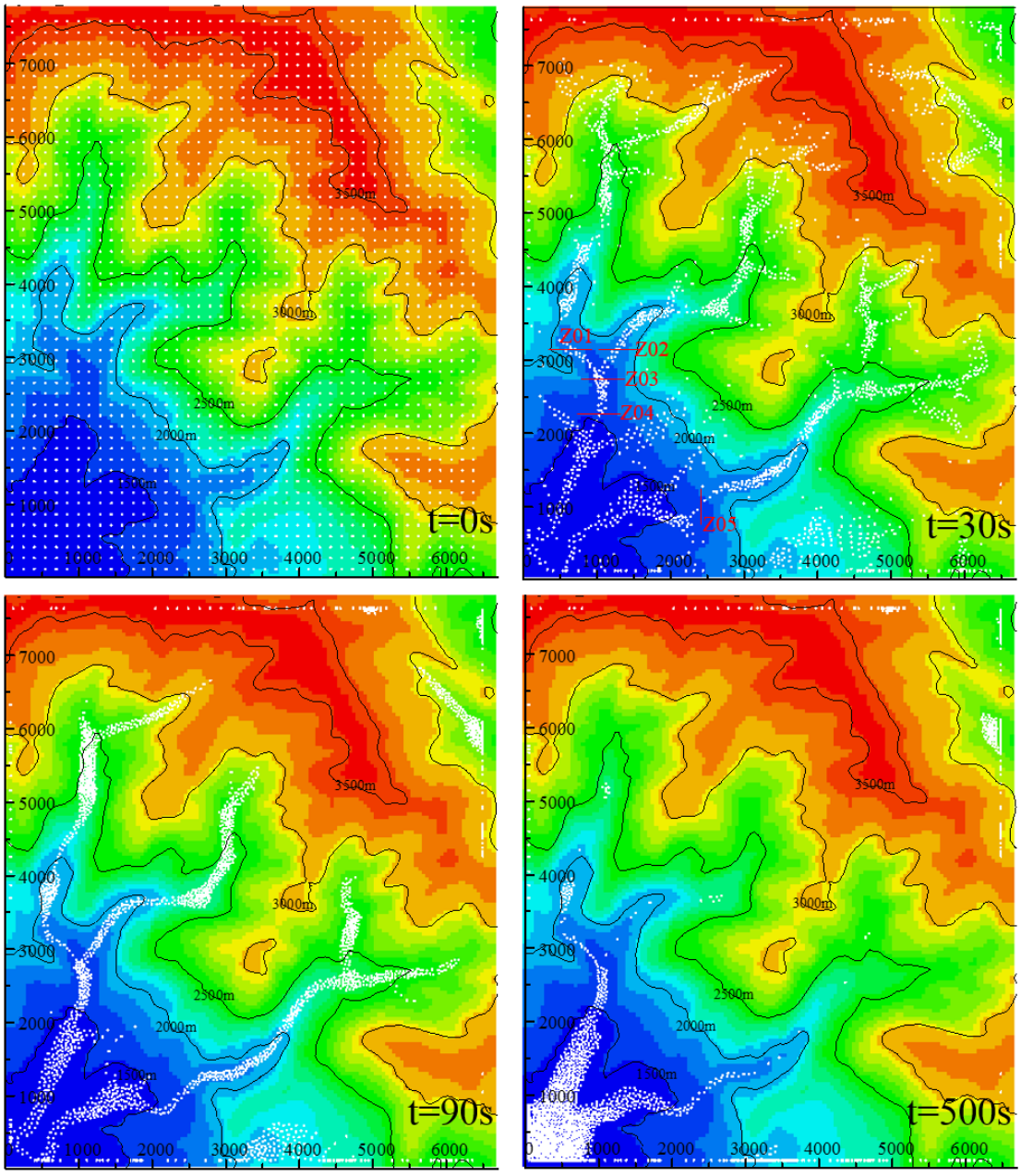

Fig.4.22 Rainfall features in the research area using 50m mesh

As mentioned in the section of rainfall, the records of Zhouqu rain gage station showed it was mild rain from before the debris flow occurred at 23:20 on 7 Aug. 2010 to the next day. There was not any information about flood from the mountain and valley at that period. It inferred that the heavy rainstorm only limited on the high-elevation and upstream of valley. Therefore, to reproduce the actual debris flow, water particles were averagely distributed on the upstream of valley where the elevation is larger than 3000m. The number of water particles is 4679 if the interval distance is set to 50m. It means that the mean rainfall amount is 29.03mm in the rainfall areas.

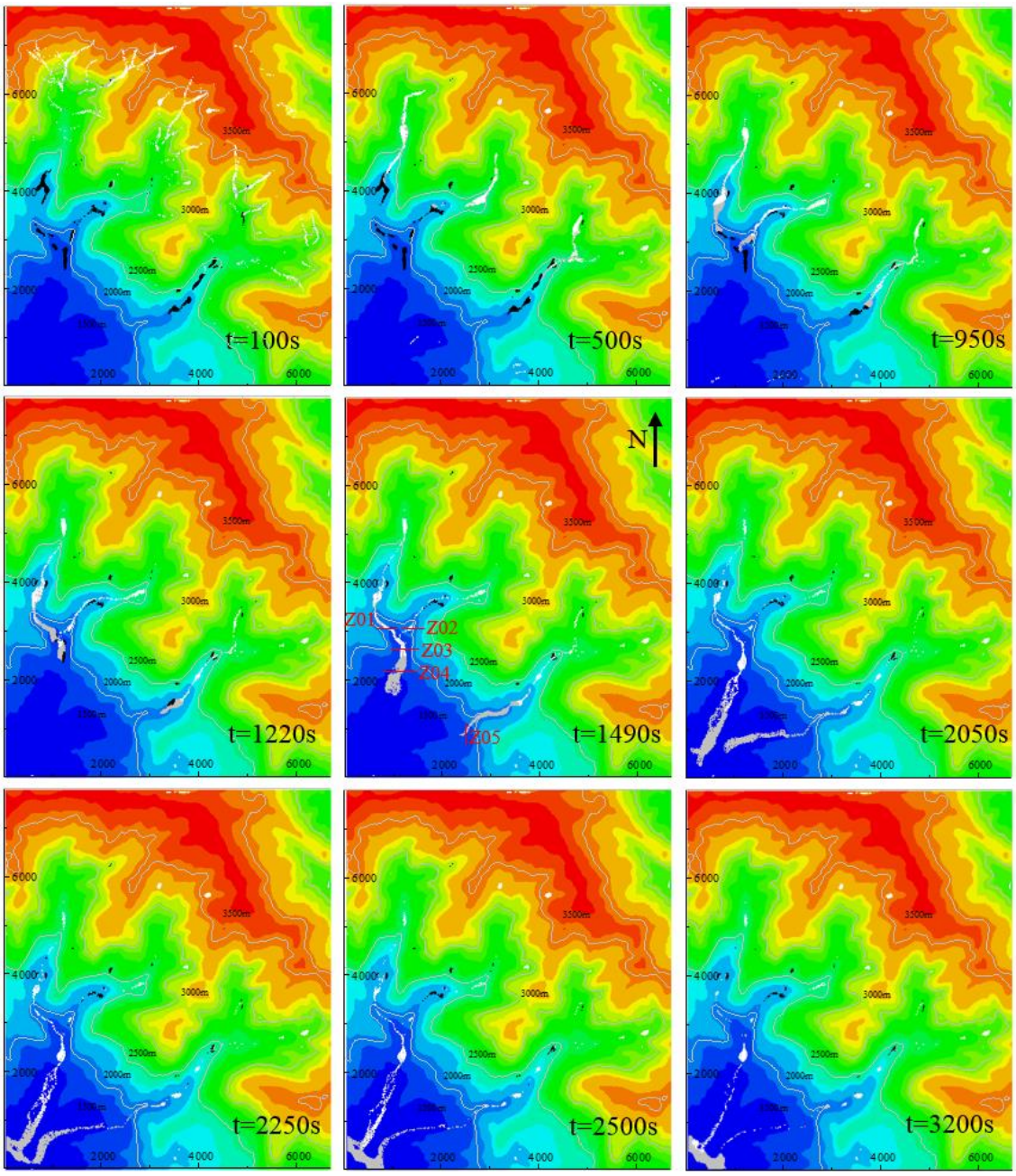

Fig.4.23 Transportation process of debris flow by mixing model

Based on the information of debris source that generated in the step 1 if the critical slope of failure is set to 60º, evaluation of debris flows using mixing model. Manning coefficient, diffusion coefficient and fitting coefficient for critical deposition slope is set to 0.1, 0.1 and 80 respectively. The detailed simulation processes showed in the figure 4.23, it took 100s to reach to the valley channels for water particles if 10m mesh was adopted. After 500s from the initiation, water flow arrived at the zones of main debris sources and mixed with solid particles. Around 950s, one of main braches of SYY valley flowed to the vicinity of the mouth of SYY valley, while the other one

reached to the confluence area 270s later. After small time for initiating debris sources near the SYY valley mouth, the debris flow quickly flowed out the valley mouth. The LJY debris flow flowed out the valley mouth near 1490s. The SYY debris flow reached to the river was 200s earlier than LJY debris flow. After 2250s from the initiation, both debris flows reached to the river and began to deposit on the deposition fans. The debris flows lasted about 250s, and the sequence water flow also reached to the river. After 3200s, most of particles were moved to the deposition fan, while there were small particles on the valley.

As illustrated in the figure 4.24, the debris flow from the left branch played a critical role in increasing the discharge of SYY debris flow. Due to two branches flowed into the main valley channel, the hydrograph at Z03 showed two peak values. But this characteristic didn't behave at Z04. In comparison with the peak valley of Z01 and Z03, the peak value is smaller at Z04 and Z05. Actually, the debris flow disaster was determined by the peak value of Z04 and Z05 to large extent. The peak value at Z04 is larger than at Z05, and the arrived time of peak value at Z04 is also earlier than at Z05. It inferred that the disaster on SYY deposition fan occurred earlier than LJY deposition fan.

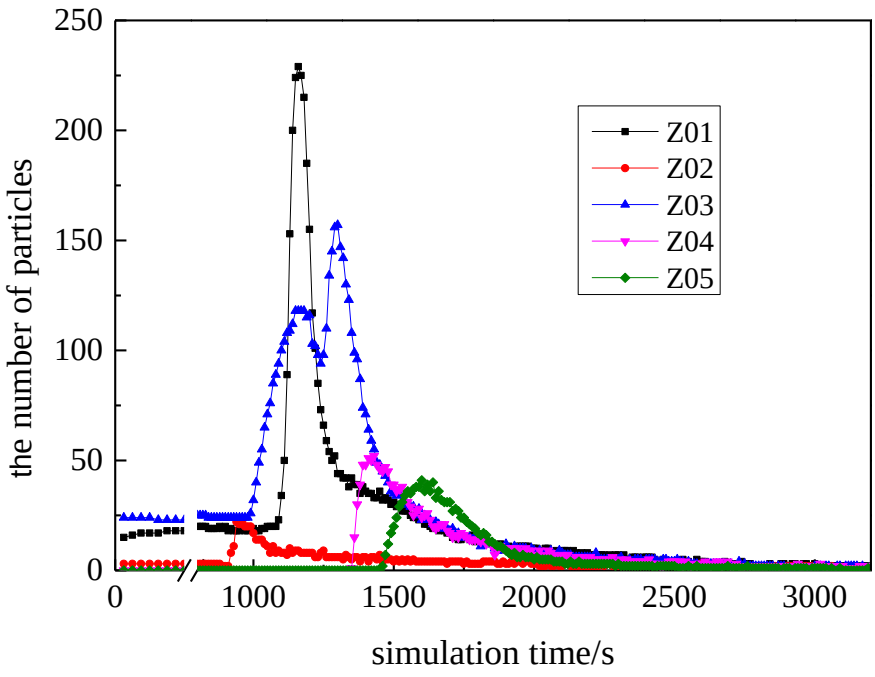

Fig.4.24 Hydrograph of debris flows in Zhouqu using mixing model

From the concentration distribution features varied with simulation time, it's easily observed the initiation features by concentration. Such information contributes to understand the physical properties of debris flow in different stage. The debris flow particles with large concentration in the front were pushed to flow down by the large amount of water flow. The first arrived debris flow behaved high concentration, and the sequence arrived particles behaved low concentration. This

result is very similar with the heavy rainstorm triggered debris flow.

The velocity also varied with simulation time, topographic features, etc. It's found that the velocity near the bend and both valley mouths was large (Fig.4.26). Therefore, whether is it reasonable to build check dams on the bend and valley mouth? This result is very useful to provide adequately protection measures in prevention and mitigation works. The velocity was smaller than 4m/s on the deposition fan.

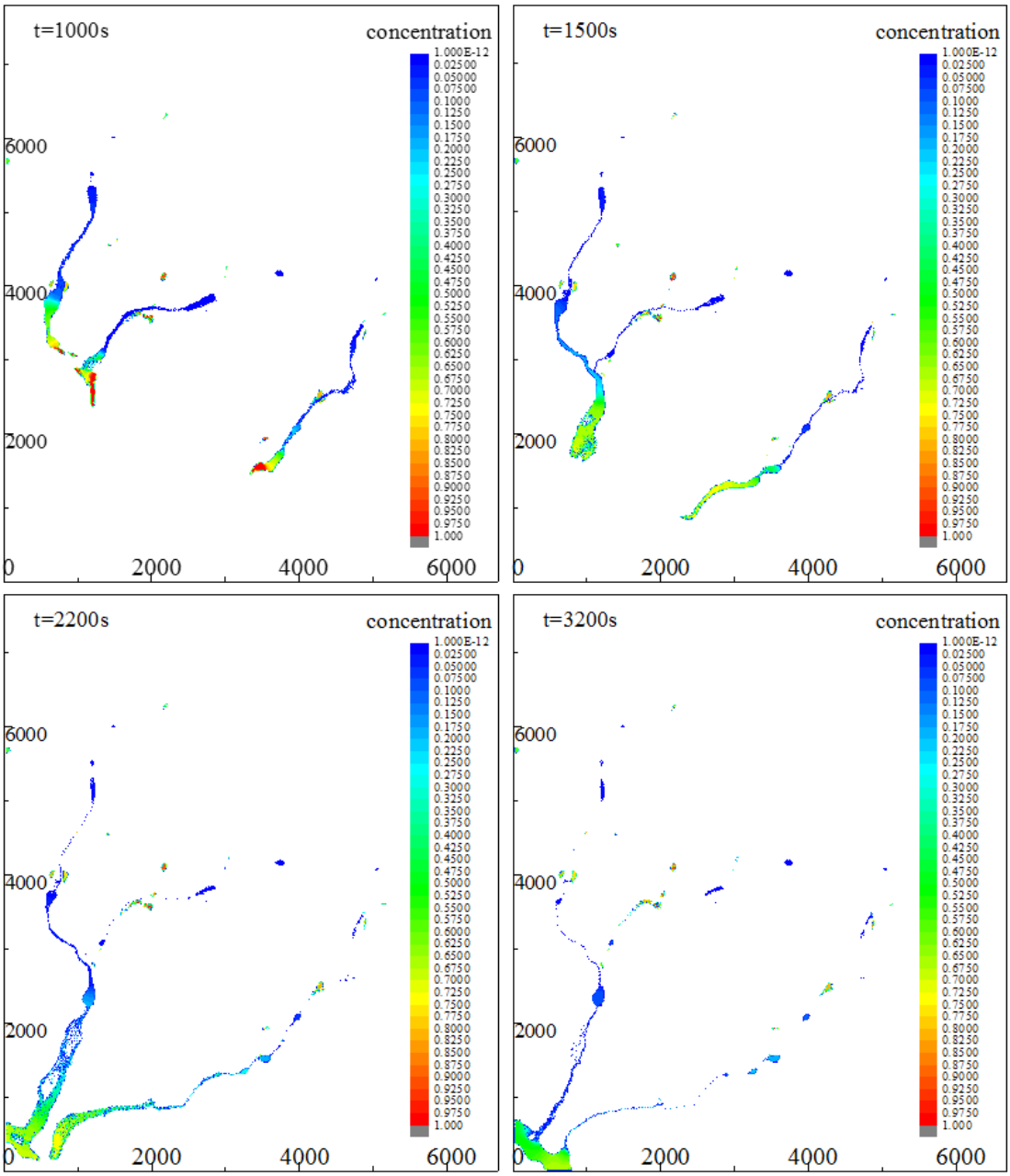

Fig.4.25 1Concentration distribution varied with transportation process

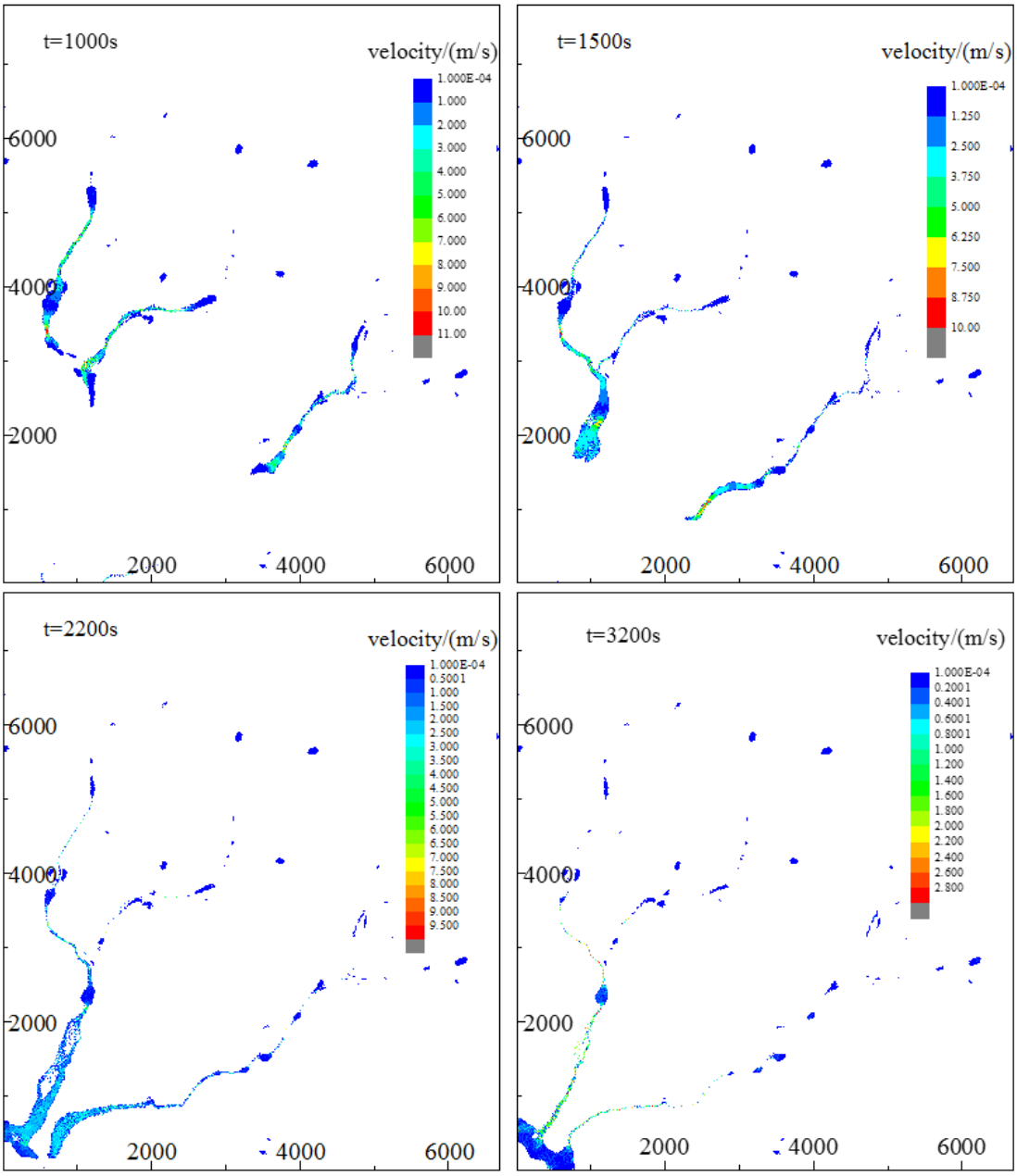

Fig.4.26 Velocity distribution varied with transportation process

After more than 50min, most of particles were transformed into debris flows and were transported on the deposition fan. The deposition thickness on the deposition fan ranged 0-6m at the final state (Fig.4.27). The extent of deposition is clearly larger than actual damage area, due to 10m mesh can't accurately describe the more detailed topographic information, such as buildings. The strong debris flow mostly damaged and buried all of things along the flow path. The deposition thickness varied the previous topographic features. The thinnest thickness was 0.3m and most areas were larger than 1m. It looks that the density of debris flows were large, and belonged to viscous debris flow. Regarding deposits on deposition fan, one of large differences is there were more than

30 boulders on the SYY deposition fan, while no one was found on LJY deposition fan.

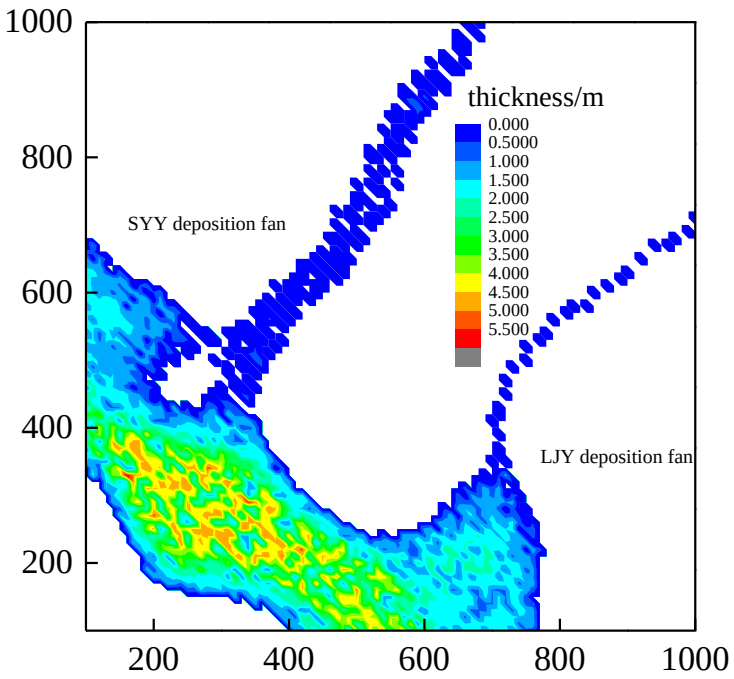

Fig.4.27 Deposition thickness on the deposition fan at t=3200s

Fig.4.28 The damage and deposition on both deposition fans

By simulating a series of cases under different rainfall amount and diffusion coefficient, it's found that rainfall amount and diffusion coefficient clearly influenced the entrainment rate. As shown in the figure 4.29, the entrainment rate up to 0.9 when the mean rainfall and the diffusion coefficient is set to 29mm and 0.1, while the entrainment rate reduced to 0.35 when the mean rainfall and the diffusion coefficient is set to 15mm and 0.001. According to the field observation (Fig.4.30), the entrainment rate was clearly smaller than 0.9, therefore, the diffusion coefficient should be smaller than 0.1 in this case.

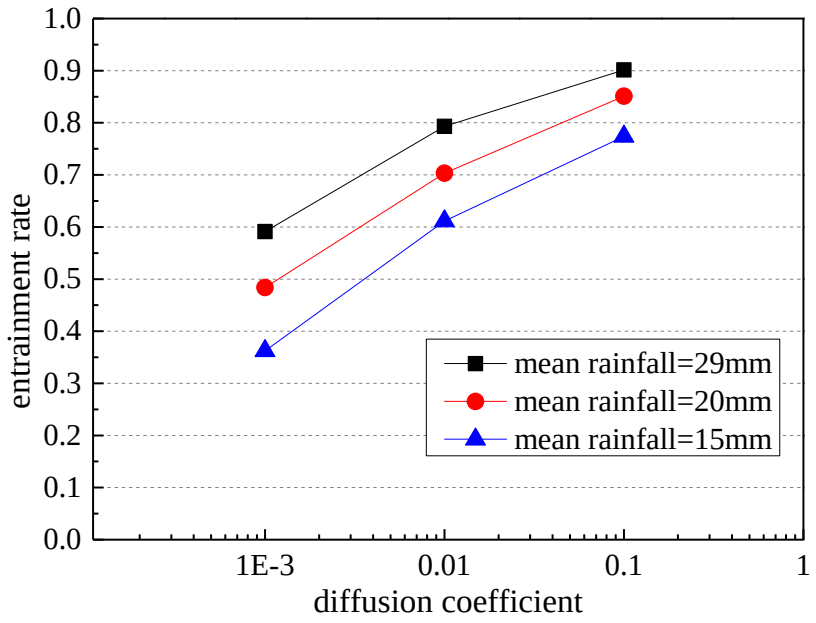

Fig.4.29 The entrainment rate varied with mean rainfall and diffusion coefficient

Fig.4.30 The entrainment rate varied with mean rainfall and diffusion coefficient

In the actual debris flow event, the SYY debris flow occurred lateral spread shortly after flowed out the mouth of valley and the previous artificial drainage channel was buried instantly. The width of pre-existing drainage channel on the upstream of SYY deposition fan was only 2.6m. The LJY debris flow also occurred lateral spread shortly after flowed out the valley because the width of

cross-section is only 7-8m at the mouth of valley. Wide farmlands were buried near the mouth of valley. It's found that the debris flow quickly flowed into the drainage channel before reached the village. Although some debris flows overflowed the channel and caused damage on both sides of the channel, the destructive degree was clearly lower than in SYY deposition fan. It's further demonstrated that the drainage channel played a critical role in transporting debris flow in LJY deposition fan.

Analyzed the detailed depositional process, it found that there were many local and entire deposition characteristics agreed well with field observation and post-debris flow image. It inferred that this method can be used to reproduce the actual debris flow, and further contribute to understand the occurrence of disaster. Moreover, such information can supply advice to build countermeasure structures to prevent and mitigate the damage.

The debris flow hazard was evaluated by re-initiation model and mixing model. It's found that the simulation by re-initiation model is more efficient because of small particles. The mixing model is very time-consuming due to more than 2 or 3 times of particles were increased. The efficient re-initiation model evaluated debris flow only by the information of debris sources, furthermore, all of particles were initiated at the same time. Therefore, the distribution features of debris sources completely determined the debris flow features, particularly for hydrograph. Although the mixing model is not so efficient and two additional parameters (diffusion coefficient and fitting coefficient for the relationship between critical deposition slope and concentration) are taken into account, it seems that more realistic to reproduce the actual debris flow. The debris flow behavior not only determined by the debris source, and rainfall amount and intensity strongly influenced the flow behavior. Moreover, the critical slope of deposition, which value determined by the concentration, is not a constant for all of particles any more. Additionally, more concentration-related phenomenon can be described using the mixing model. Therefore, re-initiation model is suitable to evaluate the extent of deposition and flow path on deposition fan, while the mixing model is more suitable to evaluate the actual debris flows from the initiation, transportation and deposition.

4.4 Analysis on the disaster mechanism

Based on the deposition factors, it's demonstrated that discharge played a critical role in the spatial patterns of deposition and extent of deposition. The simulation results also showed that the difference of extent of deposition on both deposition fans might be derived from the discharge. It's found that the dam breach of check dam played an important role in increasing the discharge at the mouth of SYY valley according to field survey (Fig.4.31). It's not very hard to infer that the check dam didn't failure until the debris flow filled the room of inside of it. Large amount of debris flow rushed out the valley mouth instantly shortly after the dam breach. It's no doubt that the discharge increased rapidly. The special deposition features near the mouth of SYY valley was the product of

large discharge (Zhang et al., 2014). Therefore, the seriously destructive damage on SYY deposition fan largely resulted from the extremely large discharge.

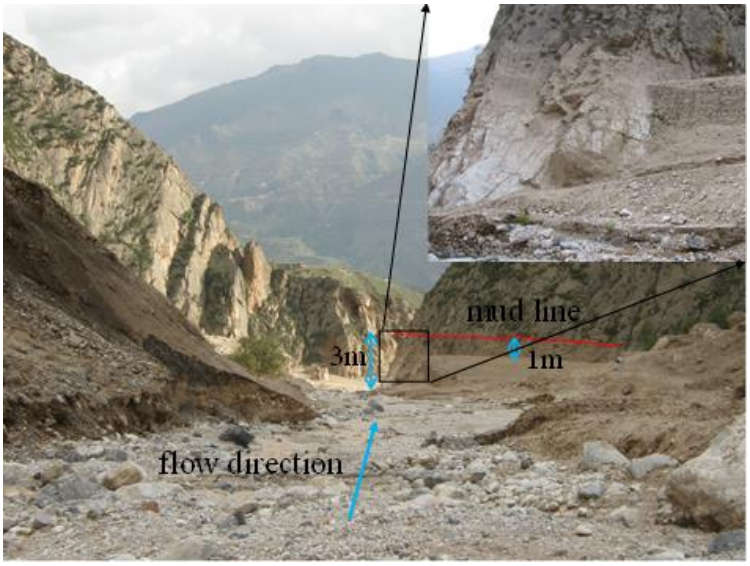

Fig.4.31 The features of post-debris flow near the mouth of SYY valley

As a matter of fact, there built 13 check dams after 1997 on SYY valley before this destructive debris flow, while there was none in LJY valley before 7 Aug. 2010. All of dams were damaged in this disaster. As a consequence, the magnitude of debris flow increased step by step with the dams breaching one by one. Cui (2011) analyzed the mechanism of dam breach and also agreed with the phenomenon increased destructive degree in this event. In addition, the previous drainage channel rarely played a role in transporting debris flow on the SYY deposition fan due to small size. By field observation, it's also found that most debris flows transported along the existing channel on the LJY deposition fan, although some overflowed the channel.

The high population density maybe another reason why there were large causalities. The city population increased to more than 40,000 in 2010 from 21,400 in 1996 (Liu et al. 2011). The city population increased by two times during 15 years. The rapidly increased population must lead to build more houses to use on the limitation room. This is also a basic situation in China. According to the damage rate on both deposition fans (Fig.4.32), it's found that Yueyuan village and the downtown of Zhouqu located on the most seriously damage areas. That's why the entire Yueyuan village was damaged and so many people were killed on the SYY deposition fan.

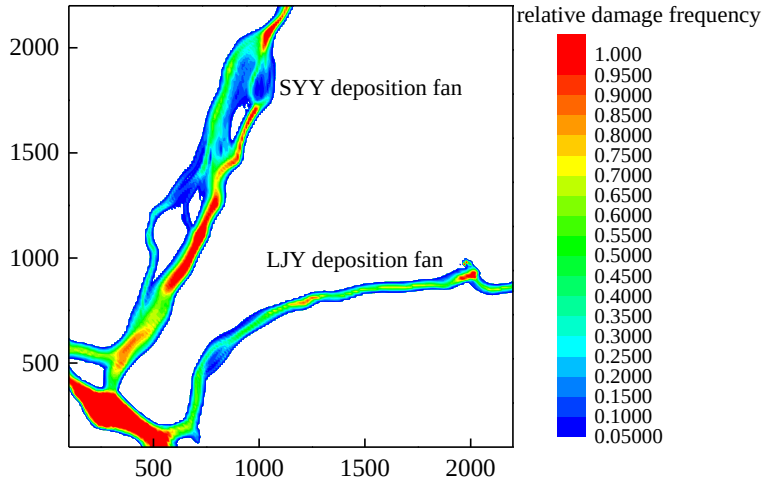

Fig.4.32 Relative damage frequency on both deposition fans

Advantage topographic features, rich debris source and rainstorm together triggered this debris flow event. The failure of some countermeasure structures and high population density enlarged the destructive nature to large extent.

There are still extremely rich debris sources in terms of landslide dams and sediment of previous debris flow on the valley channel in both valleys. Particularly, the landslide dam contained numerous of boulders, and the magnitude of the outflows can be significantly amplified due to the cascading failure effect. Therefore, it's likely to occur debris flow in both valleys in the future. After this disaster, the whole valley channel was seriously disturbed because of building check dams. Many check dams have been built again in the SYY valley and even LJY valley. It's necessary to evaluate the debris flows again in this region to avoid such disaster to occur again.

4.5 Summary

The depth-integrated particle method can be applied to simulate large-scale debris flows based on detailed DEM. By a series of simulations, it's found that accurate topographic data played a critical role in simulating actual debris flow. The critical slope of deposition strongly governed the travel distance, while discharge significantly influenced the spatial patterns of debris flow deposition.

Two-step evaluation scheme can be efficient evaluated debris sources and debris flows. It's available to check the location of debris sources by satellite image, but it's very hard to evaluate the volume of debris source only depending on satellite image. The debris sources in the research area were evaluated in terms of location and thickness combined the post-event satellite image and filed survey. It's reasonable to evaluate debris sources in Zhouqu region by setting critical failure slope and repose of angle is 60º and 26º respectively. By assuming the initial particle height is 1.0m, the thickness of debris sources ranged 0-8m. Two models (re-initiation model and mixing model) were

adopted to evaluate the debris flow hazard. It's found that the re-initiation model is very efficient with small particles (only solid particles), while the mixing model is rather time-consuming because of more than 2 or 3 times of solid particles were increased as water particles to initiate debris flow. However, all of solid particles were initiated simultaneously in the re-initiation model and debris flow behavior completely governed by the information of debris sources. The re-initiation model is suitable to evaluate the extent of deposition area and flow path on the deposition fan with only two parameters (Manning coefficient and critical deposition slope). Although two more additional parameters (diffusion coefficient and fitting coefficient for the relationship between critical deposition slope and concentration) were taken into account in the mixing model, it's reasonable to evaluate debris flow hazard to consider the physical properties of particles. Moreover, concentration-related phenomenon is also described in the mixing model.

Affected area was evaluated using re-initiation model, the agreement is good on SYY and LJY deposition fan if the critical failure slope is set to 60º and 61.5º. The debris sources were initiated when the mean rainfall was 29.03mm at the upstream of valley and the diffusion coefficient was set to 0.1. A series of simulation results showed the difference of discharge on both valleys strongly influenced the debris flow hazard on deposition fan. Advantage topographic features, rich debris sources and rainstorm together triggered this debris flow event. The failure of some countermeasure structures and high population density enlarged the destructive nature to large extent.

It's still hard to forecast the debris flow hazard only by rainfall in rural mountainous zones in China because of wide regions and limited technology. So far, more works should focus on the prevention and mitigation of disasters. The parameters of quantitative evaluation of debris flow in terms of velocity, hydrograph, the extent of deposition and flow path can contribute to provide adequately protective measures to prevent and mitigate the disasters.

CHAPTER 5 REGIONAL DEBRIS FLOWS IN THE WENCHUAN EARTHQUAKE-STRICKEN AREAS

5.1 Introduction

The Wenchuan earthquake occurred on 12 May 2008 in Sichuan province, China, and led to more than 80,000 fatalities and enormous economic losses. The quake originated in the Longmen mountain fault zone at the eastern margin of Tibetan Plateau. Consequently, it triggered more than 60,000 destructive landslides (Table 5.1 and Fig.5.1) over an area of 35,000 km^2 (Gorum et al., 2011), and directly caused $10^9 m^3$ loose materials (Huang, 2010). By the survey results (Yin et al., 2009), more than one-third of the total number of fatalities was directly killed by secondary geo-hazards of the earthquake (Table 5.1). Furthermore, debris flows quickly instead of landslide and rockfall in the earthquake-stricken areas and continually threat the safety of more than 566595 population(Lin et al., 2008) because of huge amounts of loose debris materials.

Table 5.1 The list of main disastrous landslides

landslide/ rockfall	location	volume /10^4 m^3	fatalities	landslide/ rockfall	location	volume /10^4 m^3	fatalities
Wangjiayan	Beichuan	1000	1600	Maanshi	Pingwu	400	34
Yingtaogou	Beichuan	188	906	Zhengjiashan	Pingwu	1250	60
Jingjiashan	Beichuan	1000	700	Mayuanzi	Pingwu	800	23
Chenjiaba	Beichuan	1200	400	Zhaojiafen	Pingwu	1250	17
Hongyancun	Beichuan	480	141	Yaogoushen	Pingwu	720	11
Taihongcun	Beichuan	500	150	Wenjiaba	Pingwu	300	10
Hanjiashan	Beichuan	30	50	Linjiaba	Pingwu	200	60
Shaba	Wenchuan	6.51	10	Beichuan middle school	Beichuan	240	500
Zhoujiaping	Dujiangyan	120	62	Yanmengou	Wenchuan	10	10
Guihuashu	Dujiangyan	11	11	Sanjiangcaoping	Wenchuan	100	10
Shazipo	Dujiangyan	11	10	Niushidun	Wenchuan	8	10
Taian	Dujiangyan	120	62	Niujuangou	Wenchuan	100	18
G213	Dujiangyan		1000	Niumiangou	Wenchuan	750	
Limingcun	Dujiangyan	20	120	Maerping	Qingchuan	40	19
Liangaiping	Pengzhou	40	30	Dayanke	Qingchuan	70	41
Tonglonggou	Pengzhou	100	20	Donghekou	Qingchuan	1000	260
Xiejiadianzi	Pengzhou	40	30	Jiulongou	Chongzhou	0.5	13
Xiaolongtan	Pengzhou	5.4	100	Guantan	An county	144	100
Dalongtan	Pengzhou	10	100	Daguangbao	An county	742000	38
Xiejiadian	Pengzhou	400	100	Yibadao-xiaoguanjian	Mianzhu		50

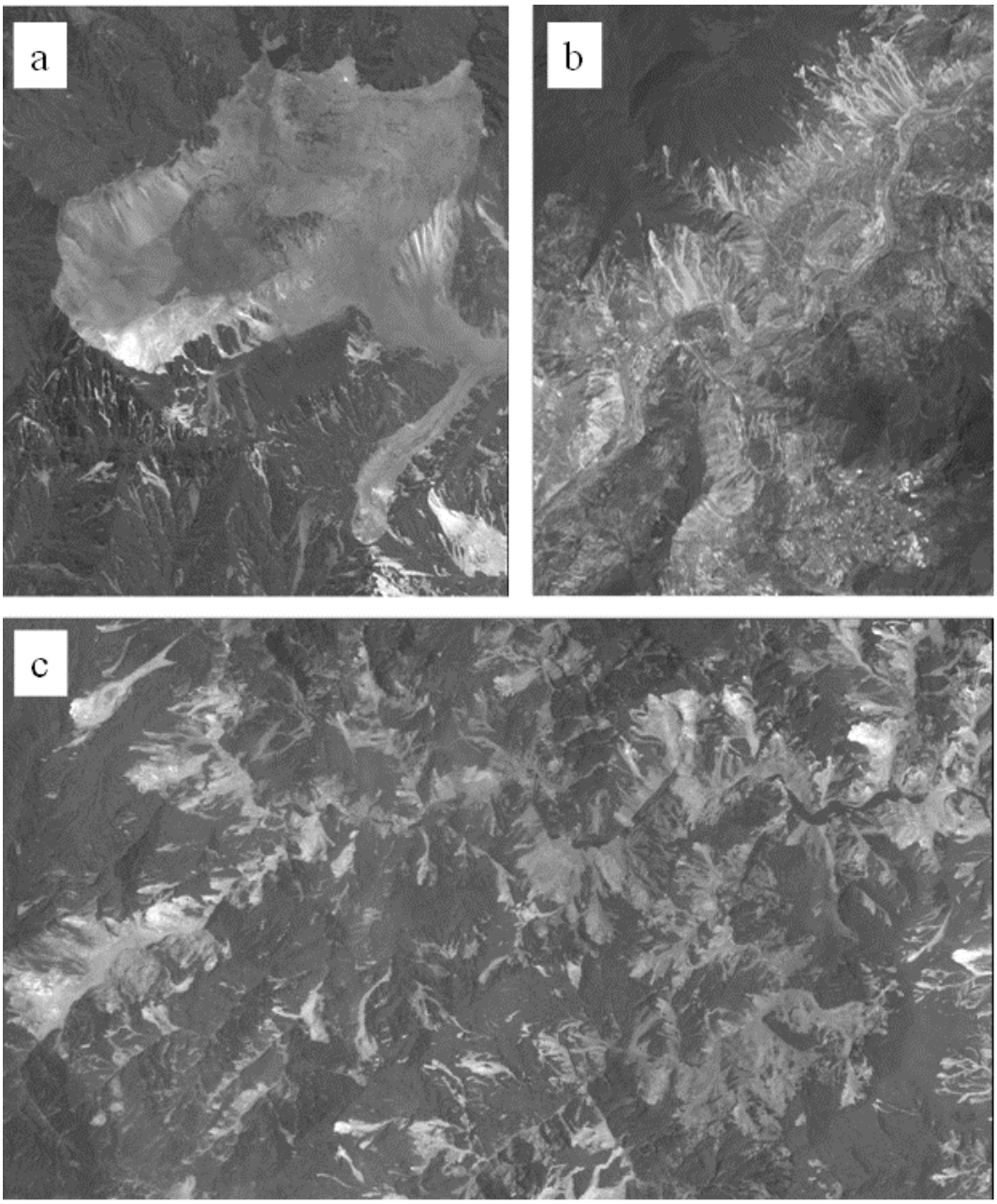

Fig.5.1 Landslides were triggered by the Wenchuan earthquake

(Note: a, b and c are all derived from the post-earthquake image which observed on 4 June 2008. a is the Daguangbao landslide. This was the largest landslide that occurred in the 2008 Wenchuan earthquake; b showed the landslides near Wenchuan along Min river; c showed the large-scale landslides in Mianzhu region)

Due to the damaged area is very wide and such post-earthquake effect will last several years or even hundreds of years, it's very essential to evaluate debris flow hazard in the earthquake-stricken areas. Furthermore, it's important to predict their flow path, velocity and affect area in order to provide adequate prevention and mitigation measures in the post-earthquake reconstruction and

planning. Therefore, it will be more significance to assess regional debris flows in the earthquake-stricken areas.

In this chapter, firstly, surface damage features are analyzed using high-resolution post-earthquake satellite image. Secondly, several post-earthquake debris flow events are shown and debris flow characteristics are summarized. Then, two regions are selected to evaluate regional debris flow hazards in the earthquake-stricken areas. Finally, a series of simple simulations for countermeasure structures are carried out and simple prevention and mitigation advice is proposed.

5.2 Evaluation of earthquake-induced surface damage using satellite image

The existing filed investigation and research showed the most serious damaged area by geo-hazards in Pingwu, Qingchuan, Beichuan, Anxian, Maoxian, Mianzhu, Lixian, Shifang, Pengzhou, Wenchuan, Dujiangyan, etc (Fig.5.2). Several satellite images in different regions were chosen to evaluate the surface damage features by the earthquake.

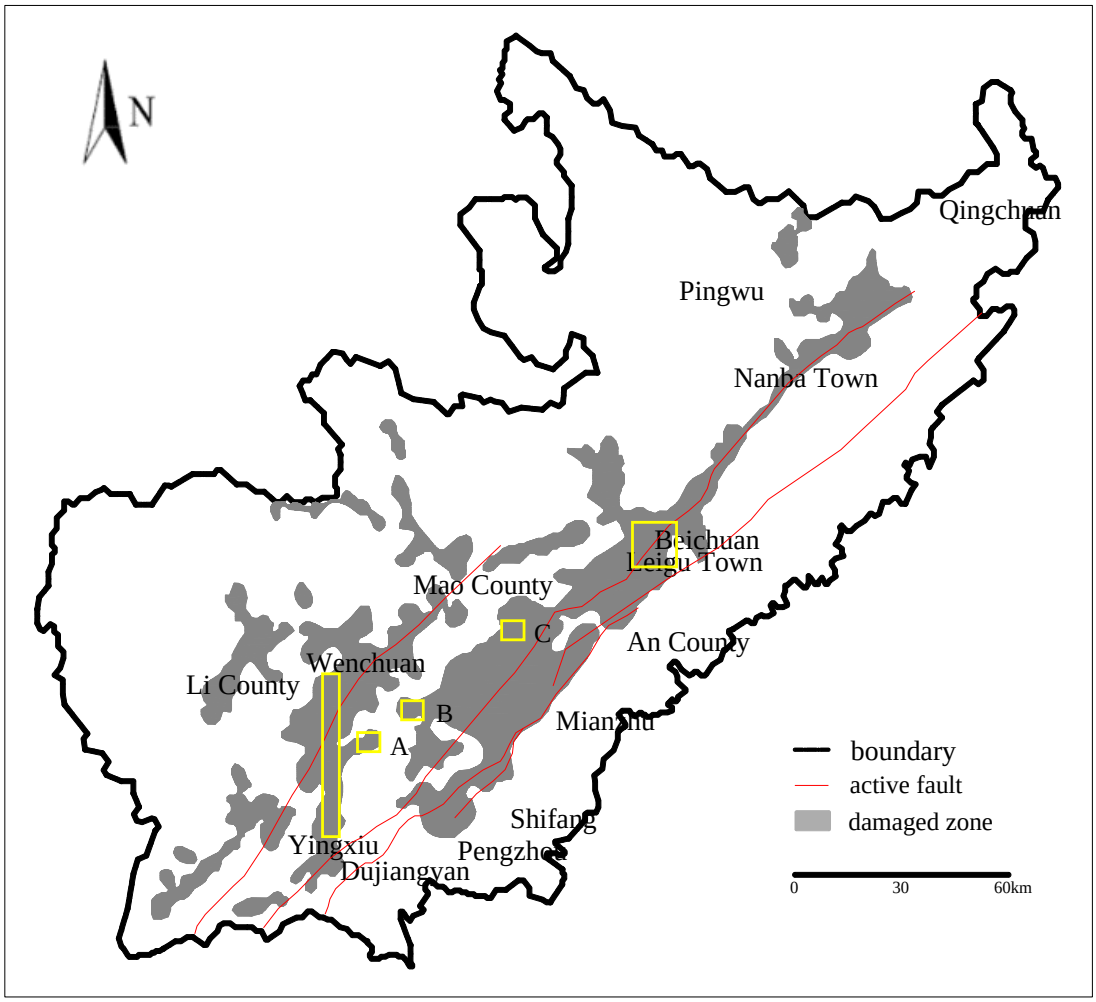

Fig.5.2 The distribution map of damaged area by geo-hazards in Sichuan earthquake zone (modified after Han et al., 2009)

Due to the spatial resolution of images is 2.5m at Nadir, it's very clearly to recognize the detailed damage information. By analysis on several post-earthquake images that observed shortly after the earthquake, it's found that the surface damage in the earthquake zone had several following features.

(1) Distribution along the fault and focus on the hanging wall

Figure 5.3 illustrated the surface damage information in Beichuan region by post-earthquake images (ALPSMW123272960). It's very clearly that the landslides and rockfalls mainly distributed along the fault, and particularly behaved seriously in the valley and river. The width of affected zone in the center of fault is about 5km, and there were rarely damage beyond this range. Huang & Li (2009) agreed that 76% landslides distributed within 5km range from the earthquake fault. It's interesting that most disasters distributed on the northwest side of fault (hanging wall) while that opposite zones (footwall) showed less disasters. Xu & Li (2010) argued that more than 70% damages occurred on the hanging wall, which was called the hanging-wall effect (Huang, 2010). It means that the hanging-wall of reverse fault led to more serious disasters in the earthquake. It also clearly showed several barrier lakes near Beichuan City in the figure 5.3. The most disastrous barrier lake was formed in this region. Such information contributed to take rescue measures in time.

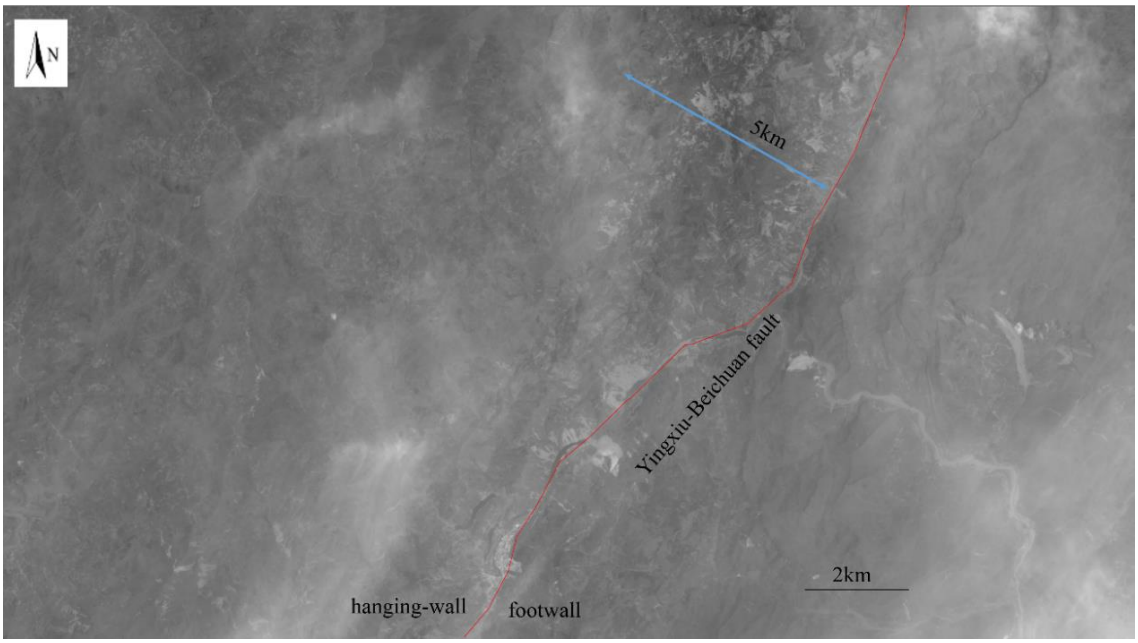

Fig.5.3 Surface damage information in Beichuan region

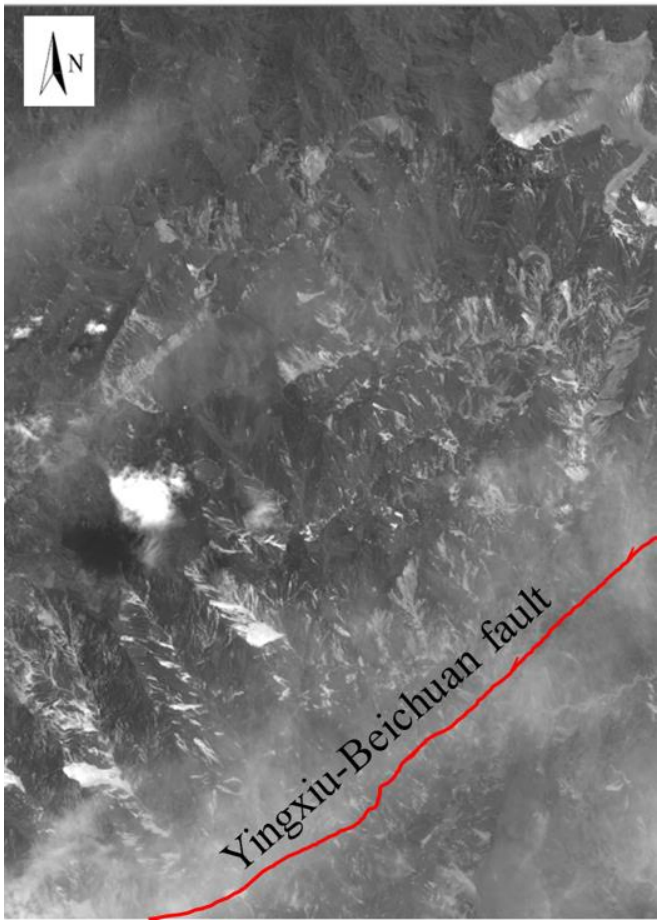

Fig.5.4 Surface damage information in An County

The surface damage features in local region of An County (Fig.5.4) also behaved serious damage in the hanging wall by image of ALPSMB125753020. As illustrated in the figure 5.4, the largest landslide was clear identified on the upper right of image. It's available to evaluate its size by clear boundary.

(2) High density

In order to evaluate the surface damage rate in different regions, the A, B and C three regions were selected from three images of ALPSMB125753030, ALPSMB125753025 and ALPSMB125753020 respectively. As illustrated in the figure 5.5, figure 5.6 and figure 5.7, the scars of landslides and rockfall are very clear recognized in these three regions. It seems that the damage was rather serious, even the whole mountain was damaged. In the region C, it mainly showed both sides of a river were damaged in the earthquake. Moreover, the river was blocked at many sites. By rough statistics, the surface damage rate is 37%, 20% and 36% in the region A, B and C respectively.

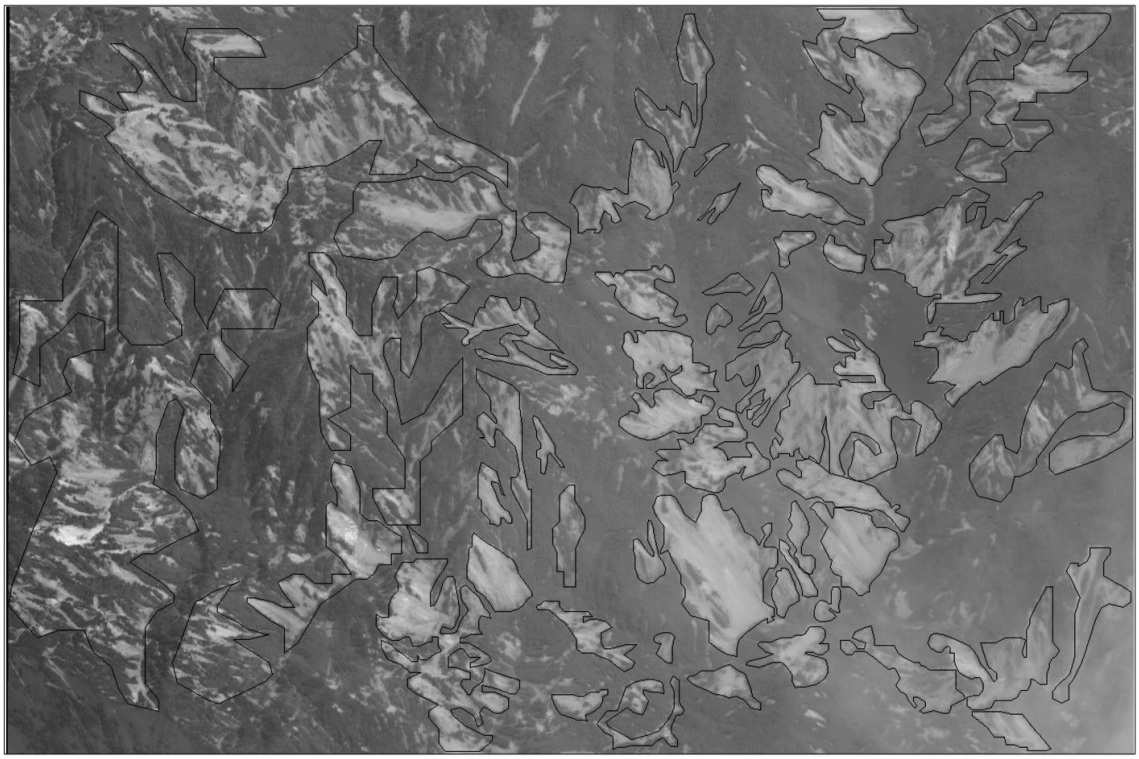

Fig.5.5 The high density of geo-hazards in the region A

Fig.5.6 The high density of geo-hazards in the region C

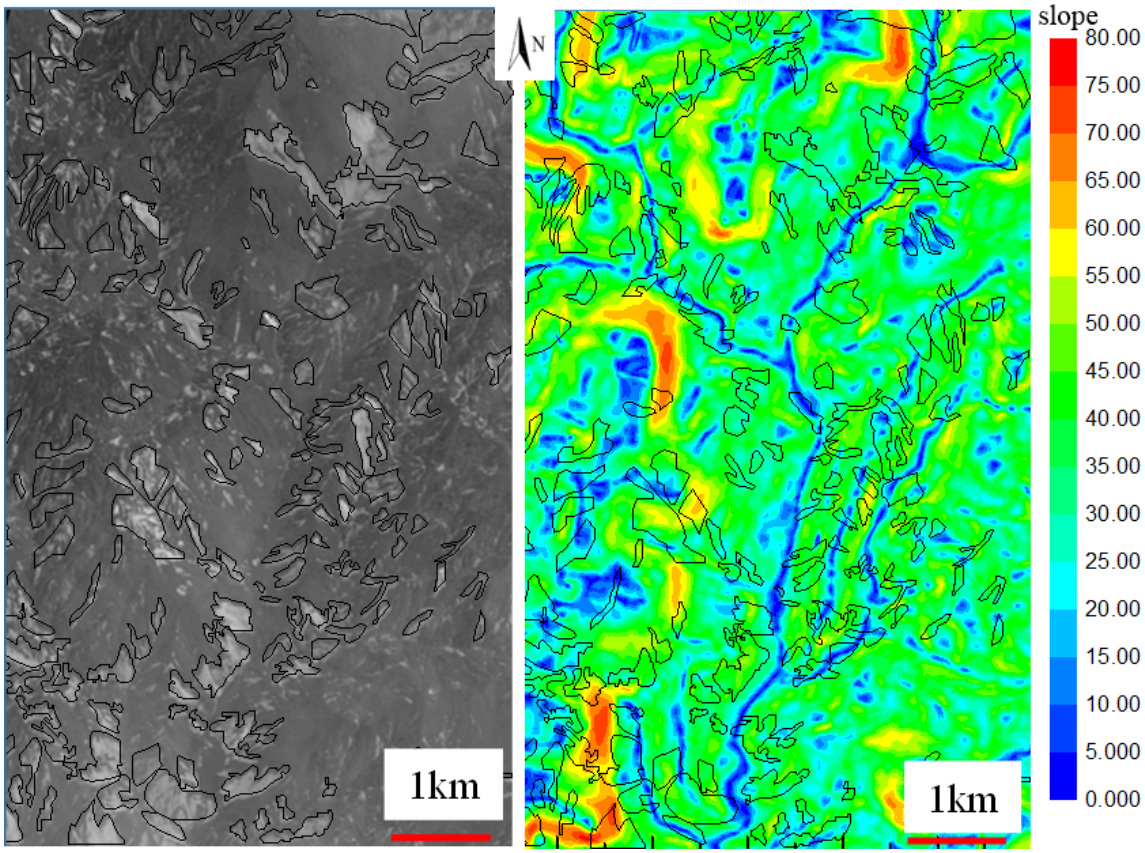

Fig.5.7 The relationship between damaged area and the slope angle in the region B

According to the overlapped areas of both damaged areas and slope distribution map, it's revealed that not all of steeper slope were very sensitive to the earthquake. Certainly, it has a large relation with lithology that is not taken into account in this study. As illustrated in the figure 5.7, the damaged areas distributed so complex that not a clear relationship between damaged area and the slope angle. The main reason is the damaged area coving failure zone and deposition zone. More than 80% damaged zones concentrated on the areas where slope angle ranges from 20° to 50° (Huang, 2009). Although mostly slope failure hadn't reached to the bottom of valley, it's noted that where damaged zones covered the valley channel (e.g. the upper right zones of region B) is very dangerous. Such phenomenon called landslide dam, which can enlarge the magnitude of debris flow once it failure.

(3) Various damage patterns

The earthquake seriously damaged more than 10,000km^2 in terms of various damage patterns. Regarding different damaged objects and features, several damage patterns in the Sichuan earthquake-stricken areas were showed in the figure 5.8, in which image a and f are derived from ALPSMB125753025; image d is from ALPSMB125753020; image c, e and f are originated from ALPSMW123272960; image b and d are from ALPSMB125753030.

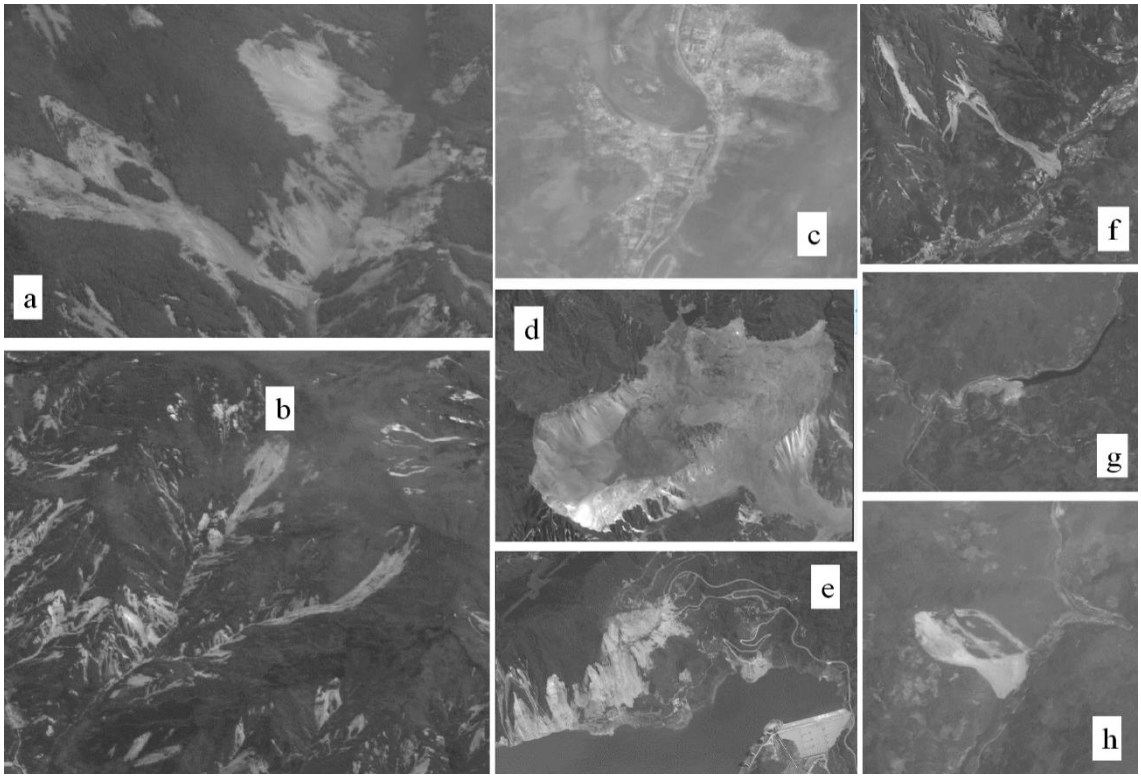

Fig.5.8 Various damage patterns by post-earthquake images

Image a showed multiple landslides on both sides of valley together deposited on the valley channel and formed large-scale landslide dam. Multiple small landslides occurred in the same catchment (image b). The size of every damage zone is so small that it would be ignored in the sequence evaluation works. Actually, on Aug. 2010, the Zoumaling valley where the damaged features are similar with the image b occurred debris flow and caused damage. It's inferred that such valley is the potential high-risk zone in the sequence rainy season to trigger debris flow. The Wanjiayan landslide and Beichuan new middle-school rockfall showed in the image c. Both are regarded as the most destructive landslides in the earthquake because they occurred in a high population density zone. The entire mountain collapsed and generated numerous debris materials. Such as Daguangbao landslide in image d. A large amount of solid materials filled into the reservoir would reduce the effective capacity of reservoir. Image e showed a series of collapse in the bank of reservoir near Dujiangyan. Image f also showed another type of landslide, its slide distance was rather long and finally buried road, buildings and river. Image g and h showed two single landslide, which located 10km away from the main active fault, buried village and blocked a river even formed a barrier lake. All of such disasters can be quantitative evaluated in term of size.

The satellite image of ALOS is characterized by wide coverage area and high resolution. It clearly supplied damage information in the earthquake-stricken areas. If such images were used to evaluate the distribution features of damage, it would efficiently provide a guideline for disaster rescue operations and emergency response shortly after the earthquake. Furthermore, it is very

precious data for evaluation of geological disasters in an extremely wide area. It also can be used to determine the locations of landslides and landslide dams that are potential debris sources for the sequence debris flows. In this study, such images are used to analyze the features of the debris flow source areas and thus evaluate debris flows in the earthquake-stricken areas.

5.3 Post-earthquake debris flow events in the earthquake-stricken areas

Extremely rich loose solid materials, which are easy to trigger debris flow in rain-days, bring enormous threat to resident and properties in the earthquake-stricken areas. Debris flows will become the most significant geo-hazard type instead of landslide and rockfall after earthquake in the earthquake zone. It's no doubt that there must be a debris flow frequent occurrence place in the near future after the earthquake because of advantage topography, enormous loose debris materials and rich rainfall. Therefore, it's an urgent work to evaluate the potential high-risk debris flow hazards in earthquake zone.

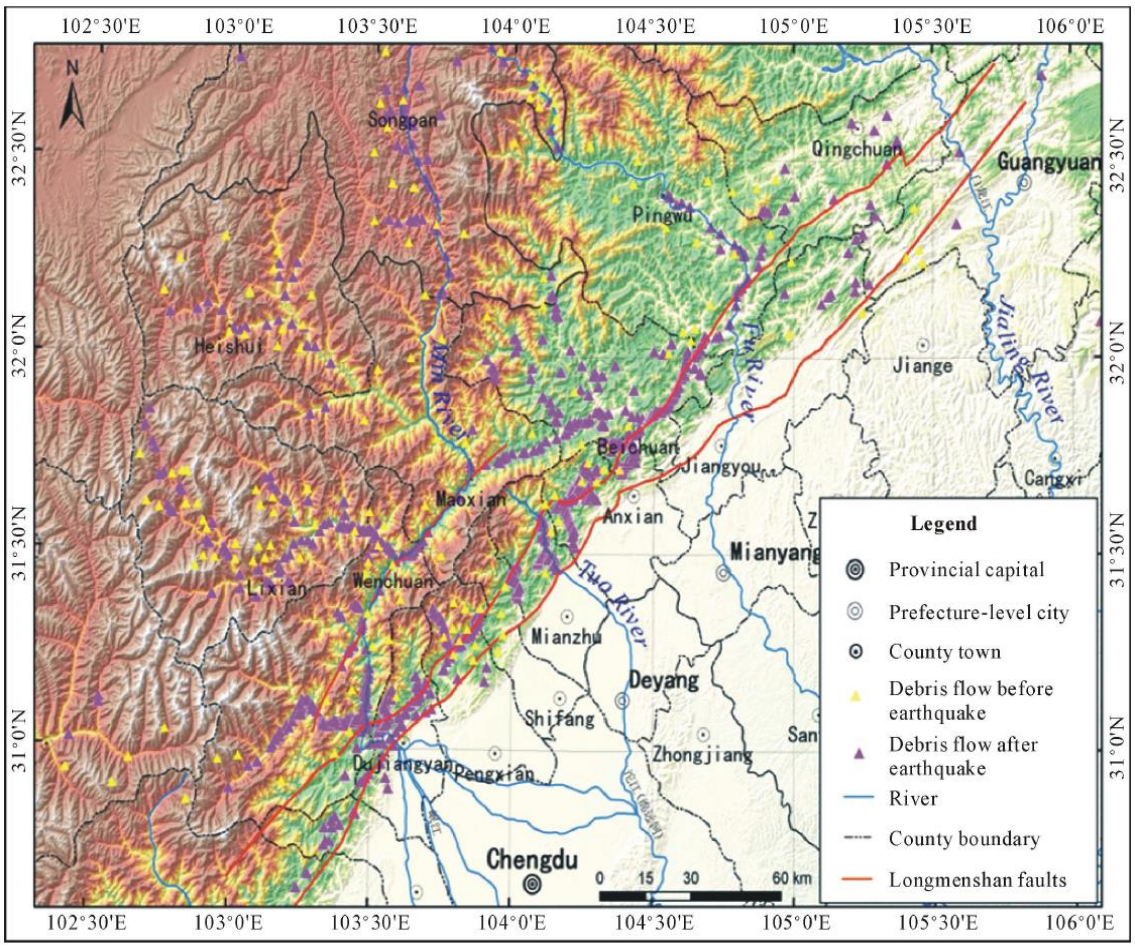

Fig.5.9 The distribution of debris flows in the earthquake-stricken areas (Ge et al., 2014)

Although debris flows didn't directly cause large damage during the earthquake, the sequence

debris flows had caused many causalities and properties losses since 12 May 2008 (Zou et al., 2014; Guo et al., 2014). There were more than 450 fatalities killed by debris flows for only six months in 2008 after the Wenchuan earthquake (Xie et al., 2009). Review on the literatures of debris flows in Wenchuan earthquake zone (Zhang et al., 2013; Xu, 2010; Zou et al., 2014; Gan et al., 2010; Liu et al., 2012), it's found that many debris flows occurred every year in last five years (Fig.5.9 and Table 5.2). Due to more than 70% of the earthquake-induced landslides occurred in the areas between Yingxiu and Beichuan (Gorum et al., 2011), mostly debris flow disasters also concentrated on these regions. The occurrence frequency of debris flows is very high even in the same valley, such as Wenjia valley (Table 5.3), it occurred at least five times after the earthquake. The largest one almost damaged the whole of Qingping Town in 2010 (Fig.5.10). There are many debris flow valleys, which are similar with the Wenjia valley and characterized by high frequency and seriously destructive of debris flows.

Table 5.2 The list of main post-earthquake debris flows in the earthquake-stricken areas

Time	place	losses
Jul. and Aug. 2008	Mozi valley, Wenchuan	G213 highway was destroyed
24 Sep. 2008	Gan valley, An County and 72 debris flows in Beichuan County	42 fatalities, 16 debris-flows occurred
27 Jun. and 17 Jul. 2009	Niumian valley, Yinxiu town	destroyed G213 highway
13-14 Aug.2010	21 valleys near Yinxiu town	31 fatalities, blocked Min River, destroyed G213 highway
12-13 Aug.2010	Wenjia valley and Zoumaling valley, Qingping town	12 fatalities, blocked Mianyuan River, destroyed large-scale regions
13 and 18 Aug.2010	More than 50 valleys in Longchi Town, Dujiangyan city	Road and houses were destroyed
13-19 Aug.2010	Hongkong town, Dujiangyan city	4 casualties
18-19 Aug.2010	Qingchuan county	G212 and S105 highway were destroyed
1-4 Jul.2011	Gaojia valley, Yinxingping valley and Chediguan valley	G213 highway was destroyed
9 Jul.2013	Daguangbao-Huangdongzi valley	
10 Jul.2013	Many valleys in the upstream of Min river	G213、G317、S9，and dozens of bridges were damaged

Table 5.3 Typical debris flows developed in the Wenjia valley after the 2008 Wenchuan earthquake

time	rainfall/ day(mm)	rainfall/h (mm)	discharge ($*10^4 m^3/s$) (Xu)	volume ($*10^3 m^3$) (Tang)	affect area ($*10^4 m^2$) (Xu)
24 Sep.2008	88	11.5mm/10min (Tang)	90	500	12.5
31 Jul.2010	60.2 (Xu) 92.6 (Tang)	51.7(Xu) 35.5(Tang)	30	100	
13 Aug.2010	>200(Xu) 82.6(Tang)	70(Xu) 37.4(Tang)	450	3500	63.5
19 Aug.2010	145.9(Xu) 127.9(Tang)	- 31.9(Tang)	30	300	12
18 Sep.2010	52.0(Xu) 51.9(Tang)	- 16.5mm/30min (Tang)	17.6	170	8.5

Fig.5.10 Debris flow in Wenjia valley on 13 Aug.2010 (Xu et al., 2012)

Summarized the characteristics of those post-earthquake debris flow events, it's found that the debris flows are characterized by high occurrence frequency, multiple valleys occurred simultaneously (coupling effect), unpredictability (Xu et al., 2012). However, more works concentrated on the prediction of debris flow by monitoring the rainfall in the earthquake-stricken areas.

Due to extremely rich loose solid materials distributed in the valley, it becomes much easier to initiate debris flows in theoretically under smaller critical rainfall and early cumulative rainfall compared pre-earthquake. By studying the Beichuan debris flows of 24 September 2008 (Tang and Liang, 2008), the early cumulative rainfall threshold for debris flows in the Beichuan was reduced by approximately 14.8%-22.1%, while the hourly rainfall intensity was reduced by 25.4%-31.6%.

The post-seismic critical hourly rainfall of the Beichuan debris flows recorded by rainfall observation stations was 37.4 mm (Cui et al. 2010). However, on 14 June 2008, it only triggered small debris flows in the northwestern of Beichuan city with the cumulative rainfall was 133mm (Tang, 2010). The cumulative rainfall with 192mm triggered large-scale debris flows in wide areas on 23 September 2008, while the cumulative rainfall with 182mm didn't trigger any debris flows in Beichuan region on 17 July 2009. The rainfall intensity of 37.4 mm/h and 16.4 mm/h and antecedent rainfall of 82.6 mm and 162 mm were recorded in Qingping area and in the Yingxiu respectively between Aug. 12 and Aug. 14, 2010 (Tang, 2009).

Regarding the rainfall features, the existing data showed complexity and behaved that: (1) not every rain event would trigger debris flow; (2) not potential high-risk large valley was easier than small valley to occur debris flow; (3) not all of valleys occur debris flow in the same region under the same rain event. Xu et al. (2012) argued that the variability in both rainfall duration and threshold for debris flow after the earthquake contributed to the unpredictability of debris flow.

The rainfall is a very variable, uncertainty and heterogeneity factor in a wide region. No one realized that the limited rain gauge station can't supply enough much and accurate rainfall information for predicting debris flows in the mountain areas. Another reason is researchers adopted the rainfall data might be from different rain gauge stations (Table 5.3). It led to there is not a unified conclusion. The occurrence of debris flow is an extreme complex process that has a close relation with many factors, such as the volume and location of debris source, early cumulative rainfall and rainfall intensity, lithology, physical properties of solid material, topography, etc. Therefore, it's rarely likely to predict debris flow by a single factor, particularly in such wide earthquake-stricken areas. More quantitative evaluation works should be done to provide adequate prevention measures.

Facing so large threat of debris flows, there still encountered the damage of debris flow. Why? Several reasons are summarized as followings. Firstly, the destructive of potential high-risk debris flow were underestimated (Huang & Fan, 2013). Secondly, there is not a completely correct recognize to post-earthquake debris flow. Many new debris flow valleys were generated and some small valleys became destructive debris flow valleys. Multiple valleys often occurred debris flows at the same time, however, the existing prevention measurements only focus on an individual valley according to traditional methods. As a consequence, unexpected disasters occurred, such as '8.13' Qingping debris flows (Xu et al., 2012) and '7.10' debris flows along G213 highway (Zou et al., 2014). Then, reconstruction works were not hesitate to be carried out shortly after the earthquake before get a reasonable and available assessment. Finally, there is not a good prevention work. The failure of new built check dams were regarded to enlarge the magnitude of debris flow in Wenjia valley and Hongchun valley.

Therefore, two regions (Beichuan city and areas from Yingxiu to Wenchuan along Min River) are selected to quantitative evaluate the regional debris flow hazards in terms of affect areas, flow path,

velocity, hydrography, concentration, deposition thickness, etc. to provide adequate mitigation and protection measures using mixing model based on the high-resolution satellite images. The study will focus on the evaluation of earthquake-induced debris sources and deposition features in the Beichuan region and the phenomenon of blocking river in the area from Yingxiu to Wenchuan along Min River. Furthermore, coupling effects by multiple debris flows and the effect of building countermeasure structures are also evaluated in the earthquake-stricken areas.

5.4 Debris flows in Beichuan region

The Beichuan city is about 125km away from the epicenter Yingxiu. It is situated in the transitional belt between the Sichuan Basin and the Western Sichuan Plateau, and is mainly composed of mountainous areas. The Yingxiu-Beichuan fault crosses the Beichuan city (Fig.5.11). In this region, the topography is characterized by medium elevations mountain ranging 600-2000m, and the slope concentrated on 10°-50° (Fig.5.12). The Jian River crosses the city, and local resident mainly lived on a narrow valley terrace of the Jian River, with an area less than 2km^2. The research area has a sub-tropical humid monsoon climate with an annual mean precipitation is 1400 mm; the highest annual precipitation of 2340 mm was recorded in 1967. As seen in Table 5.4, the rainfall is mostly concentrated on the four months (June to September), which are about 83% of the annual precipitation.

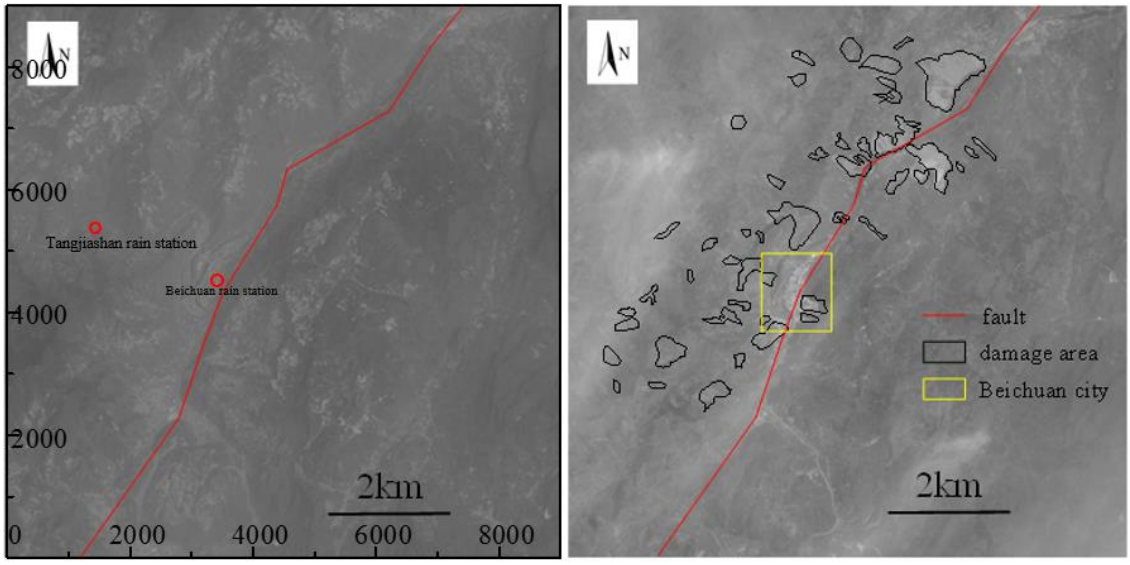

Fig.5.11 The pre- and post-earthquake images in the Beichuan region

Table 5.4 Mean precipitation in the Beichuan County from 1971 to 2000

Month	Jan.	Feb.	Mar.	Apr.	May	Jun.	Jul.	Aug.	Sep.	Oct.	Nov.	Dec.
Precipitation/mm	5.9	11.4	22.8	52.6	97.3	135.3	370.8	350.4	206.6	64.4	18.6	4.1

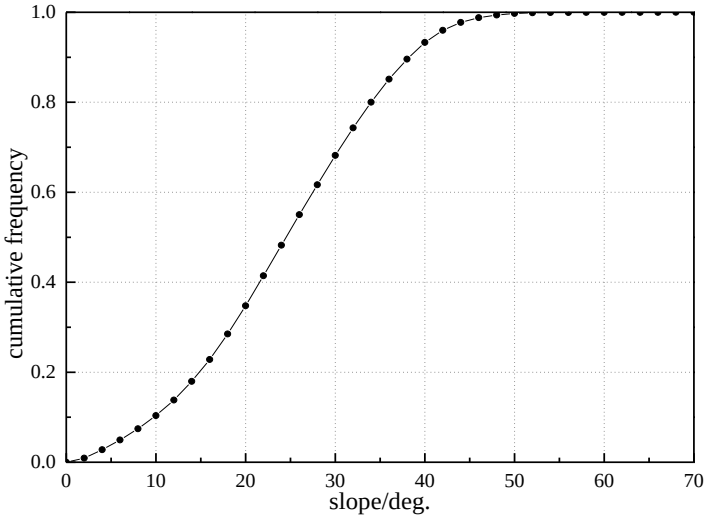

Fig.5.12 The slope distribution features in Beichuan region

In the earthquake, more than 50% people (about 20,000) (Wang, 2009; Yin et al., 2009) died in the Beichuan city because of high-density landslide and collapse around the city (Fig.5.11 and Fig.5.22). The Wanjiayan landslide and Xinbei mid-school landslide are two of the most destructive landslides in the earthquake (Yin et al., 2009). Such landslides and collapse not only killed many people and also destroyed large infrastructures as well as generated several large barrier lakes in the vicinity of Beichuan city. The barrier lake of Tangjiashan landslide located on the upstream of Beichuan city. It led to local resident can't keep normal daily life more than one month.

The damage of the earthquake, slope failure and barrier lakes strongly hit the local resident. However, a rainfall caused more damage again in the September only four months after the earthquake. That rainfall triggered more than 70 debris flows in the Beichuan region (Tang et al., 2010). Consequently, more than 40 people were killed again and three houses as well as one temporary settlement were destroyed. So far, three large-scale debris flows occurred on 24 September 2008, 17 July and 10 September 2009 in the Beichuan region. These disasters have seriously endangered the lives and livelihood of local residents. More than 20,000 m^2 farmland were buried and the majority of which rarely be recovered. Additionally, a considerable amount of debris flow was transported into river, resulting in the main channel being pushed to the other side (You et al., 2011). All of such disaster will influence the security of local resident and properties for a long period in the future. Therefore, it's necessary to evaluate the debris flow hazard in Beichuan region.

5.4.1 Evaluation of potential debris source

The loose solid materials generating in the earthquake are potential debris sources for the sequence debris flows to large extent. As illustrated in the figure 5.11, geo-hazards not only generated along the active main fault, and also distributed along valley and river in comparison with the

pre-earthquake image. It's easy to identify the damaged area by the high-resolution image. Due to the hanging-wall effect (Huang & Li, 2009), mostly damaged areas distributed in the northeastern and southwestern of Beichuan city while there were small damages in southeastern direction. To check the relationship of damaged areas with slope features, the main damage areas were traced and then overlapped it with the slope distribution map of the same region (Fig.5.13). There is not a clear relation between damaged area and slope. One of reasons is the surface of damage zone contained the failure zone and deposition zone. Another reason is the slope failure strongly governed by earthquake acceleration velocity as well as lithology, strata features, the distance from fault, etc. This is a very complex process. Meanwhile, it's a rather difficult problem to judge the potential failure zone in both the simulation and practical engineering.

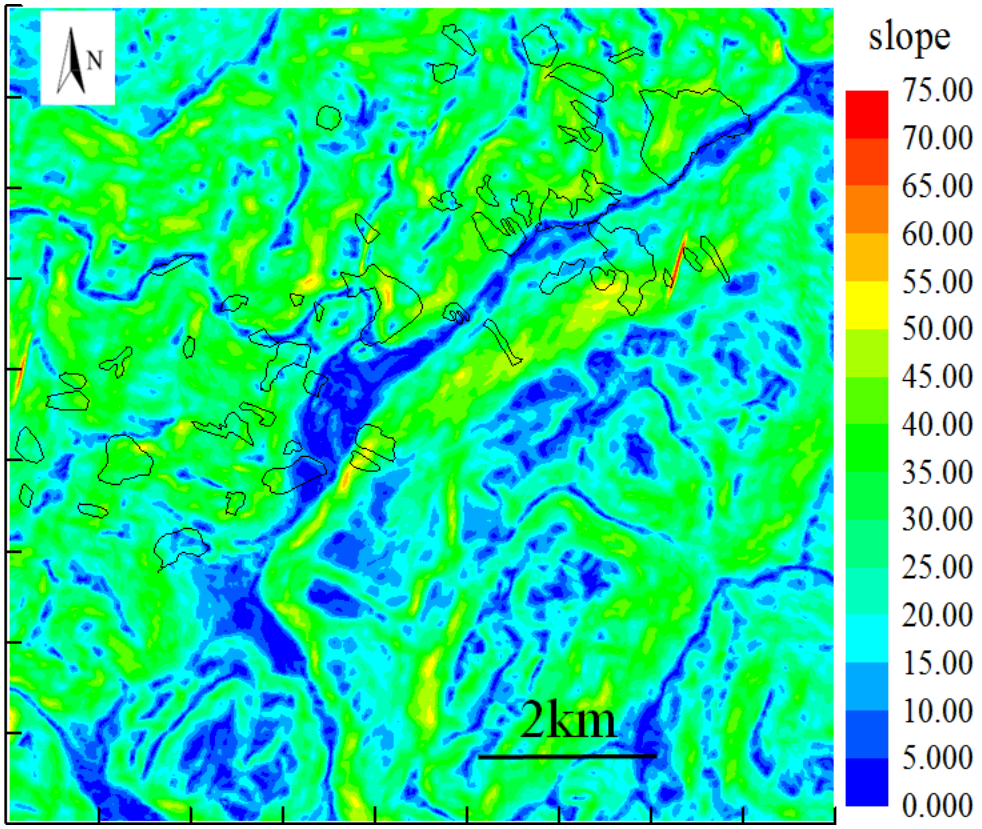

Fig.5.13 The distribution features of earthquake-induced landslides based on the slope distribution map in Beichuan region

It's very essential to make sure the distribution information of debris source in the evaluation of debris flow hazard in a region. The distribution features of potential debris flow hazard in a wide region rely largely on the distribution features of debris source that significantly influence the flow behavior, discharge and affected area. Based on the current information, one of advantages is the location of exact damaged zones can be correctly determined. It might not suitable to define the critical slope of failure to a constant in a wide region of earthquake-stricken areas, particularly the

research area contained both hanging-wall and footwall zones. Due to the earthquake-induced landslides are mainly depended on the distance to the active faults and slope gradient (Qi et al., 2010), it's reasonable to evaluate the debris sources by the two step scheme in the depth-integrated particle method. The slope distribution characteristics were analyzed by roughly dividing the research area into three parts by the river and fault, which are western, northern and eastern part in the center of Beichuan city, respectively. It's very clearly that the damaged slopes of western part are smaller than the other two parts. Hence, the information of debris sources can be generated by roughly setting different critical slope of failure in three different parts to ensure the relative accurate location information.

Considering the relation between the location of damage area by the earthquake and the topographic characteristics, the critical failure slope was set to 38°, 42° and 46° for western, northern and eastern part respectively, basing on the pre-earthquake topography. The failure areas in western and northern zone are clearly more than in eastern zone. It also inferred that the critical failure slope is smaller in hanging wall than in footwall. Then, such slope failure particles moved down according to the equation of motion with the repose angle is 30°. The actual damaged area had a strong relation with earthquake acceleration velocity, lithology, strata features and the distance from fault, etc. About 64% of debris sources located in the Silurian slates and phyllites and small debris sources located in the sandstones, limestones, etc. in the Beichuan region (Tang et al., 2009). As illustrated in the figure 5.14, there are 47 debris sources in red in the whole research area. The largest enclosed area by a single curve in red is the whole affected areas by the simulation results, while the dense areas by red color are the final deposition areas of steep slopes with the repose of angle is 30º. The number of entire or partial overlap areas is 35, and the overlap areas are 70% of actual damaged areas. Mostly failure zones matched well with the actual damage zone in terms of location and coverage area by separately setting critical slope of failure in three zones, while there is a large failure zone in eastern part where didn't be damaged in the earthquake.

Noted that the loose solid materials that generated in the earthquake are not all of debris sources in sequence debris flows. The sequence rainstorm also triggered the slope failure and generated new deposits in the valley. Tang et al. (2011) agreed that the damaged areas increased by more than 24% in terms of landslide by rainstorm on 24 Sep. 2008 in the southern of Beichuan city.

Assumed the initial height of failure particles is 1.0m, the thickness of debris sources ranged 0-3m (Fig.5.15).

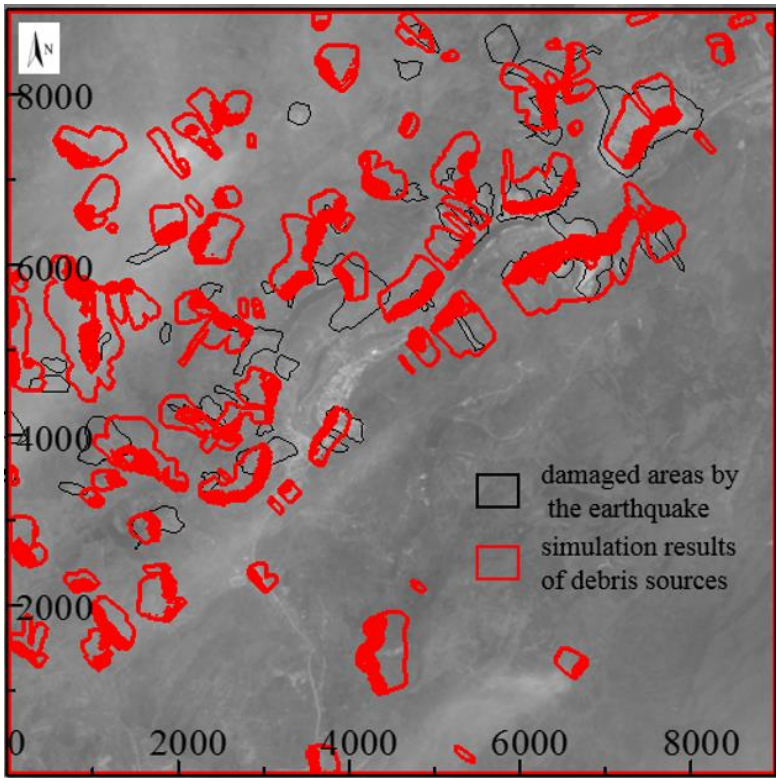

Fig.5.14 Simulation results of failure zones in Beichuan region

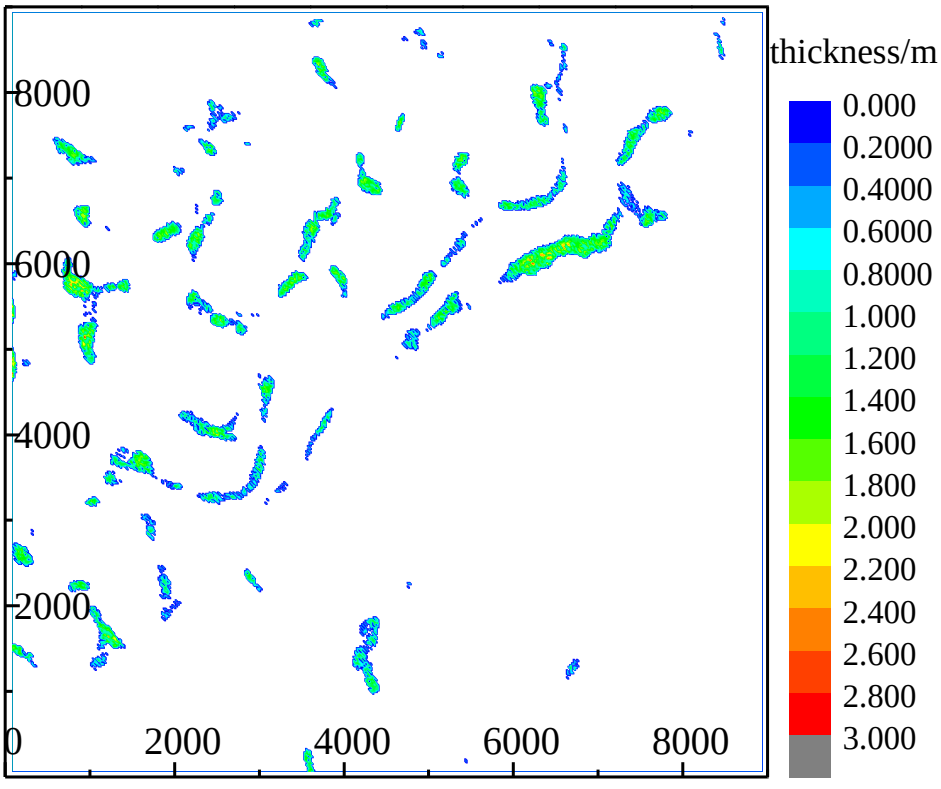

Fig.5.15 The thickness of debris sources

5.4.2 Rainfall

Rainfall is the most important factor to trigger debris flows in the earthquake-stricken zones. So far, NASA and JAXA can supply database of the rain radar satellite, called TRMM (Tropical Rainfall Measuring Mission) in real-time. Although the monitoring cell is 0.1×0.1 degrees in JAXA smaller than 0.25×0.25 degrees in NASA, the accuracy is very low in real-time in JAXA TRMM and the data hasn't been dealt with in the present research area. Fukuoka et al. (2008) provided the rainfall data by the NASA TRMM in the Beichuan region (Fig.5.16). It showed extra-ordinary intense rainstorm was recorded from September 22 until 24 and largest daily precipitation was 198 mm of September 23. They also verified this rainstorm was not localized but widely distributed intense rainstorm by analysis of adjacent cells from September 22-24. The records of rainfall by Tangjiashan station showed there was a heavy rain from the Sep.23-24 (Fig.5.17). However, the cumulative precipitation was 234mm for August 2008 from Beichuan station (Tang et al., 2009). It's larger than the cumulative precipitation (120mm for August respectively) by the NASA TRMM in the figure 5.16. It's still hard to obtain the accurate rainfall recordings in the rural mountainous areas.

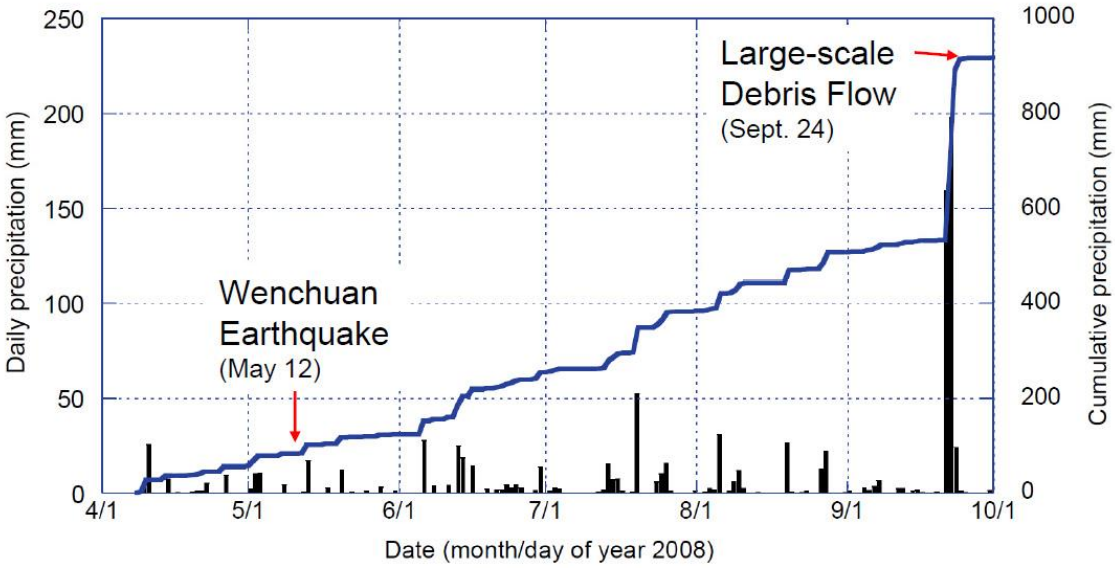

Fig.5.16 Daily and cumulative precipitation for the cell covering the Beichuan city obtained by TRMM satellite rainfall monitoring system (Fukuoka et al., 2008)

The eyewitness verified the debris flow occurred around 06:00 on 24 Sep.2008. Therefore, the antecedent cumulated rainfall and critical rainfall intensity were estimated to 272mm and 41mm by recordings of Tangjiashan station (Tang et al., 2009).The pre-earthquake critical cumulative rainfall and critical rainfall intensity were 320-350mm and 55-60mm/h respectively in Beichuan County (Tang et al., 2008).

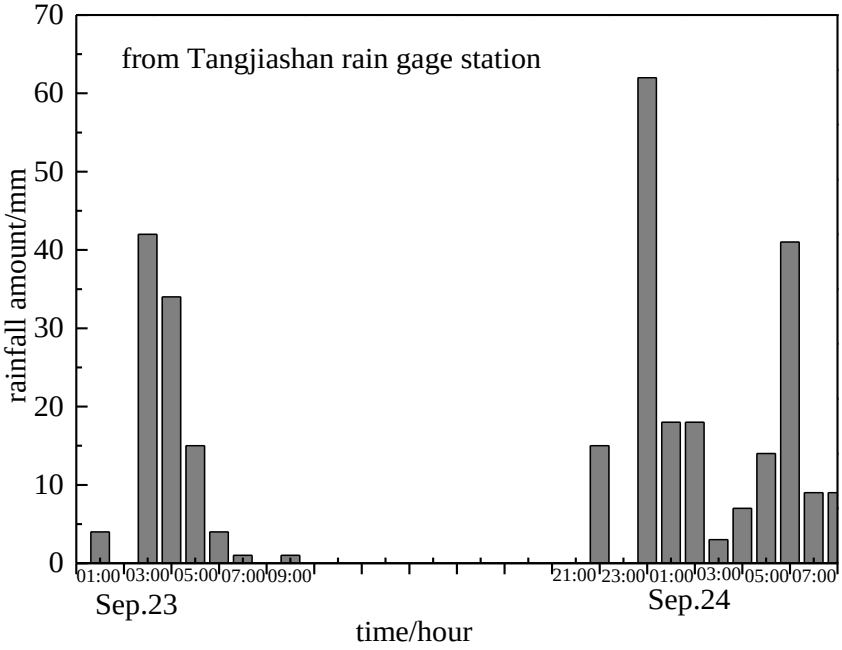

Fig.5.17 The rainfall features in Beichuan region from 23-24 Sep. 2008

5.4.3 Evaluation of the debris flow hazards in Beichuan region

Based on the information of debris sources in section of 5.4.1, debris flow will be simulated from initiation, transportation and deposition using the mixing model. In order to efficient simulate regional debris flows, 20m by 20m mesh was adopted, and water particles were averagely distributed by 100m interval distance. Therefore, the number of water particles is 7921. It means that the mean rainfall amount is 39.12mm in the whole research areas. The Manning coefficient, diffusion coefficient and β are set to 0.1, 0.05 and 80 respectively.

As illustrated in the figure 5.18, the 6 (D01-D06), 6 (D07-D12) and 3 (D13-D15) debris flows were generated in the western, northern and eastern part respectively. The four debris flows (D01-D03) in the western part finally reached to the city, while D04 flowed to the Leigu town and D05-D06 moved to Jian river. The 6 (D07-D12) debris flows in the northern of Beichuan city finally reached to the river. The D13 in the eastern part washed away the solid particles blocking the valley channel and finally flowed to river and deposited with D11 in the river. It's very dangerous in this case. It's very likely to completely block river and form barrier lake. Furthermore, the backwater will drainage the upstream and threat the safety of downstream. In the earthquake, the damage of D13 valley had ever blocked river and formed barrier lake (Fig.5.11). Small solid particles were initiated by water particles in the D14 and D15. The filed survey (Tang et al., 2012) demonstrated that mostly valleys in this region occurred debris flows on 24 Sep. 2008, except D14 and D15. The main reason originated from the generating process of debris source. Where the debris source of triggering the D14 and D15 debris flows didn't be damaged at all in the earthquake.

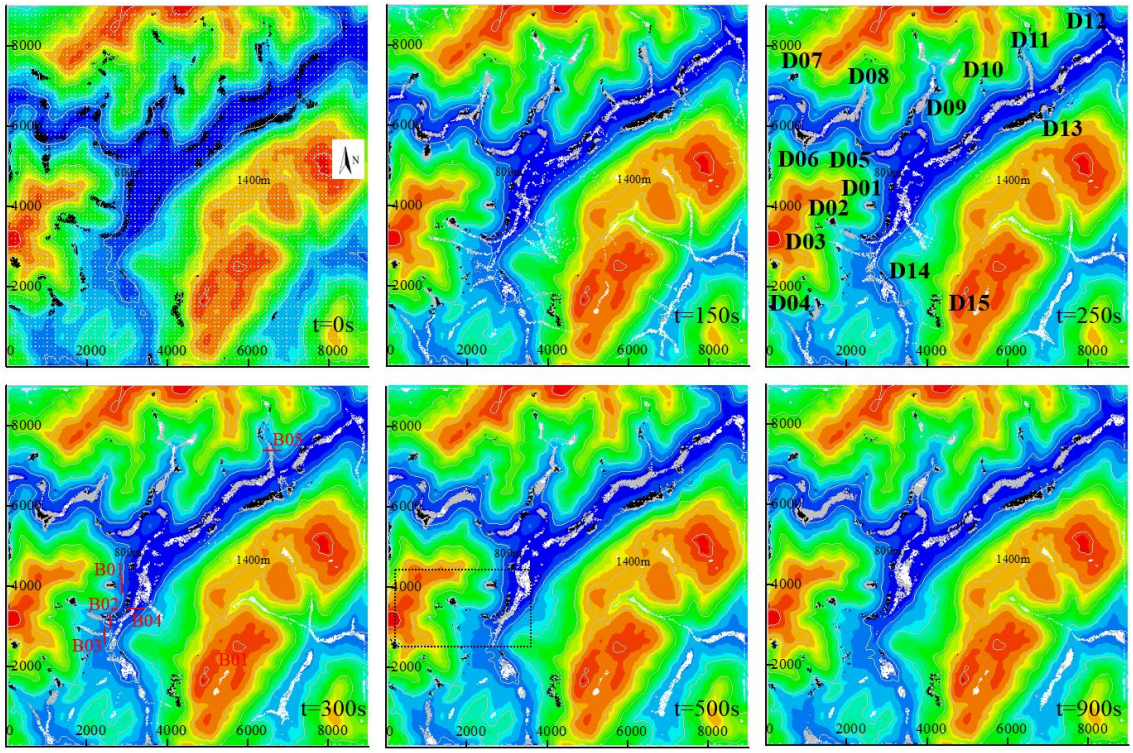

Fig.5.18 The simulation processes of debris flows in Beichuan region

Due to large amount of solid materials blocked on the valley channels, one of typical features in the debris flows of earthquake stricken areas is water flow from the upstream of valley washed out the landslide dam and formed debris flow. Such effect was simulated well in the D13 debris flow (Fig.5.19). With the increasing of water particles from the upstream of valley, the concentration reduced gradually (Fig.5.20). After 300s from the initiation, the landslide dam was washed out and the debris flow flowed into river finally.

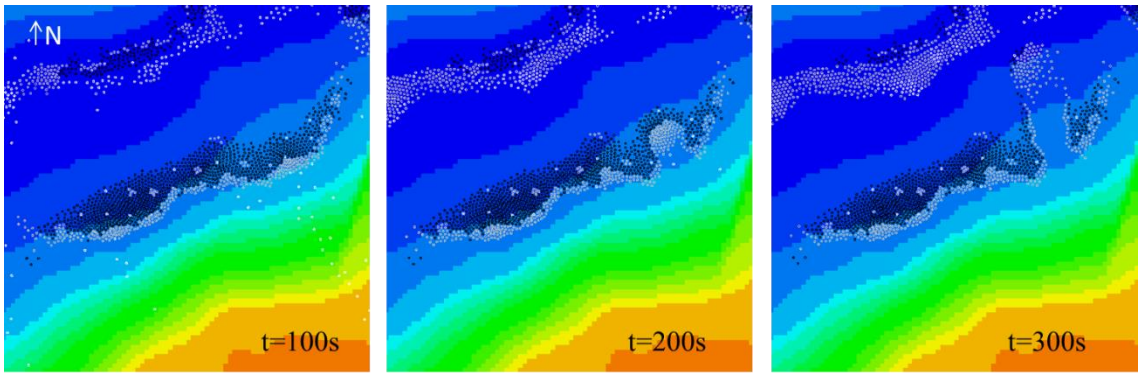

Fig.5.19 The transportation processes of D13 debris flow

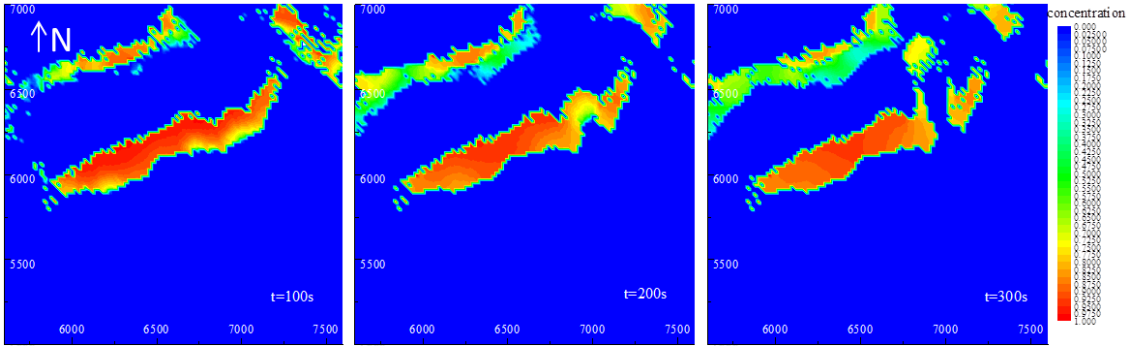

Fig.5.20 The concentration varied with simulation time for D13 debris flow

Three debris flows (D01-D03) flowed to Beichuan city and resulted in disasters on 24 Sep.2008. The hydrograph in five flow cross-sections were obtained in the figure 5.21. The hydrograph of B01-B04 can well explain the hazard in the southern of Beichuan city. In this case, there only small solid particles in D01 were mixed with water particles and were transported on the deposition fan, while there were large particles in D02 and D03 were transported to the resident zone of southern of Beichuan city. Specially, the D02 and D03 together flowed to Beichuan city by confluence at the downstream of valley. The discharge would reach the maximum around 600s from the initiation (Fig.5.21). By the analysis of hydrograph features, it can be used to evaluate the damage time.

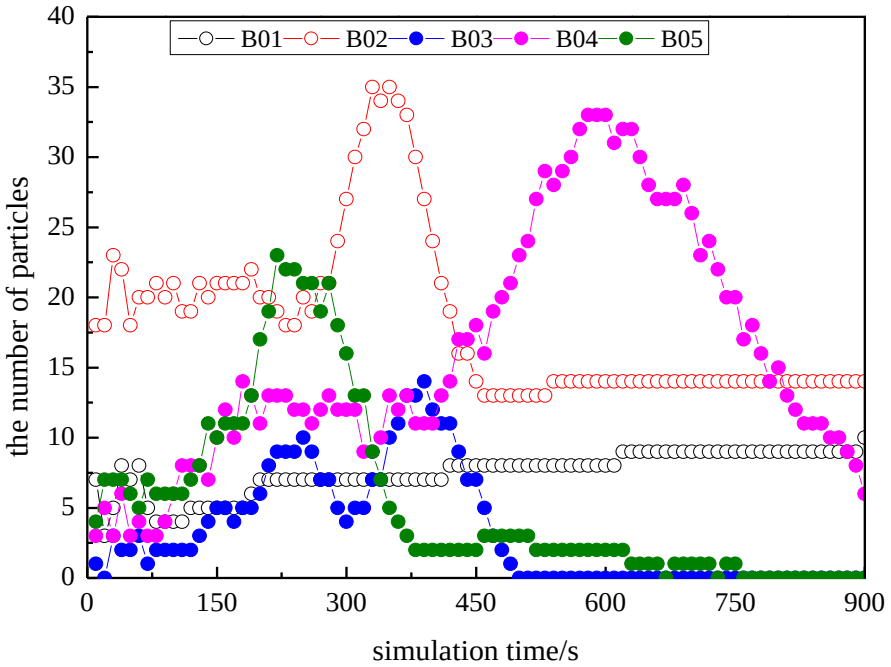

Fig.5.21 The hydrograph of five flow cross-sections in Beichuan region using 20m mesh size

As illustrated in the figure 5.22, the southern of Beichuan city was damaged seriously by debris flows from the D01, D02 and D03 by the images of three different periods. It means that the rainfall intensity of 39mm in this region didn't supply sufficient water to trigger large-scale debris flows.

Therefore, one more case with large amount of water particles were concentrated on the analysis of debris flows (D01-D03) in the southern of Beichuan city.

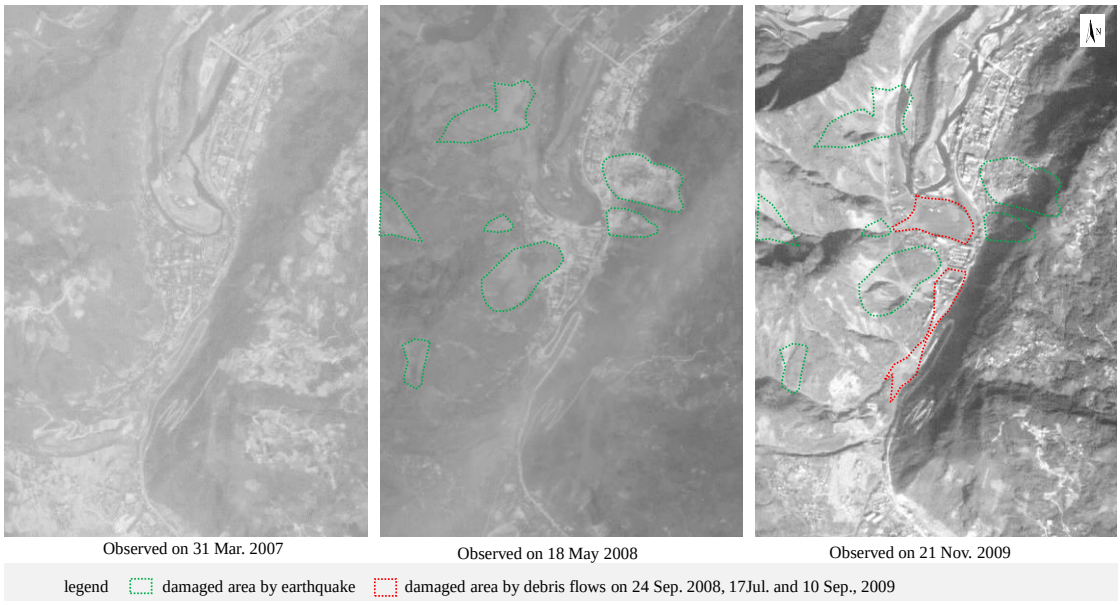

Fig.5.22 The images of southern of Beichuan city in three different periods

In the figure 5.23, 10m mesh size was adopted to evaluate the deposition features on the southern of Beichuan city. The number of water particles were averagely distributed by the 50m interval distance, and the mean rainfall amount is 60.14mm. Diffusion coefficient and fitting coefficient were set to 0.02 and 10 respectively. All of three debris flows were initiated around 100s, and mostly debris flows deposited on the Beichuan city after 1200s. The discharge of D01 and D02 reached to the peak value around 170s and 400s, while there were two peak values for D03 around 280s and 400s. In this case, the discharge is completely different from the small rainfall case for D01, while the hydrograph curves are similar in both cases for B02, B03 and B04. It demonstrated that both D02 and D03 debris flows watershed features significantly influenced the hydrograph of debris flows.

After 1200s, some solid particles remained on the valleys because of large concentrations, although they were mixed with water particles. The concentration of deposits from D01 ranged 0.4-0.8, and the concentration increased from the front marginal to the apex of deposition fan. The thickness of deposits on the deposition zones of D01 ranged 0-2m. The thickness increased from the marginal to the center of deposition fan in the lateral direction and increased from the front marginal to the apex of deposition fan in the longitude direction. Most of deposits from D02 and D03 flowed into river while almost deposits of the actual debris flows deposited on the old Beichuan city. It's obviously that the thickness of deposits ranging 0-0.7m from D02 and D03 is smaller than the actual thickness of deposits with 7-12m (Konagai et al., 2008).

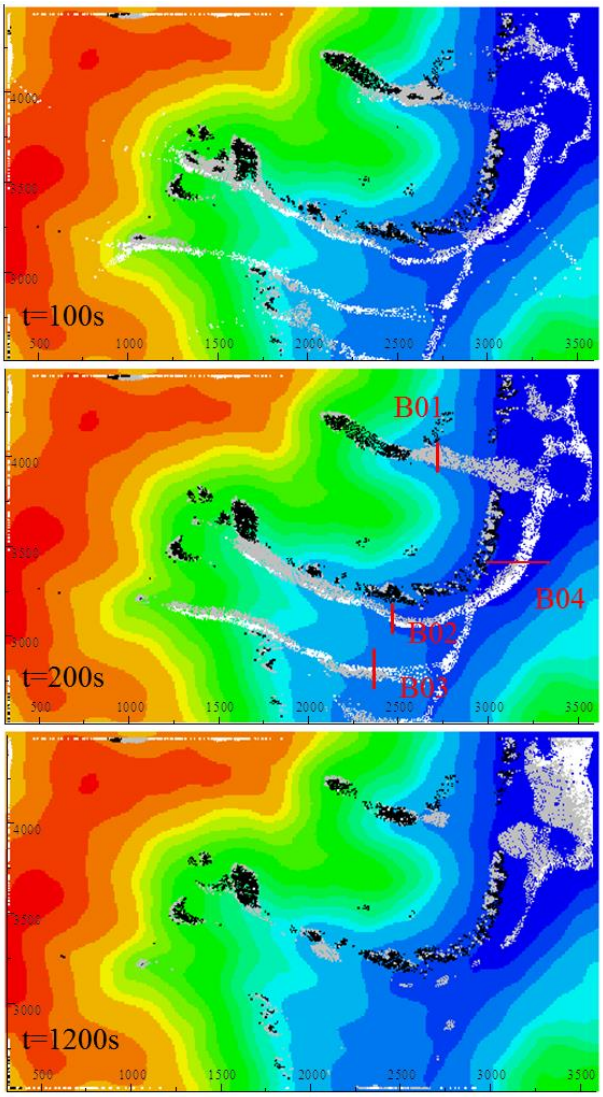

Fig.5.23 The transportation processes focus on the southern of Beichuan city

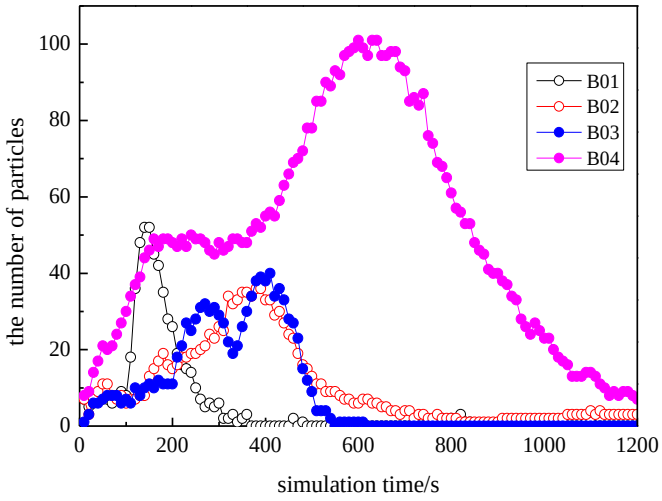

Fig.5.24 The hydrograph for the debris flows in the southern of Beichuan city using 10m mesh size

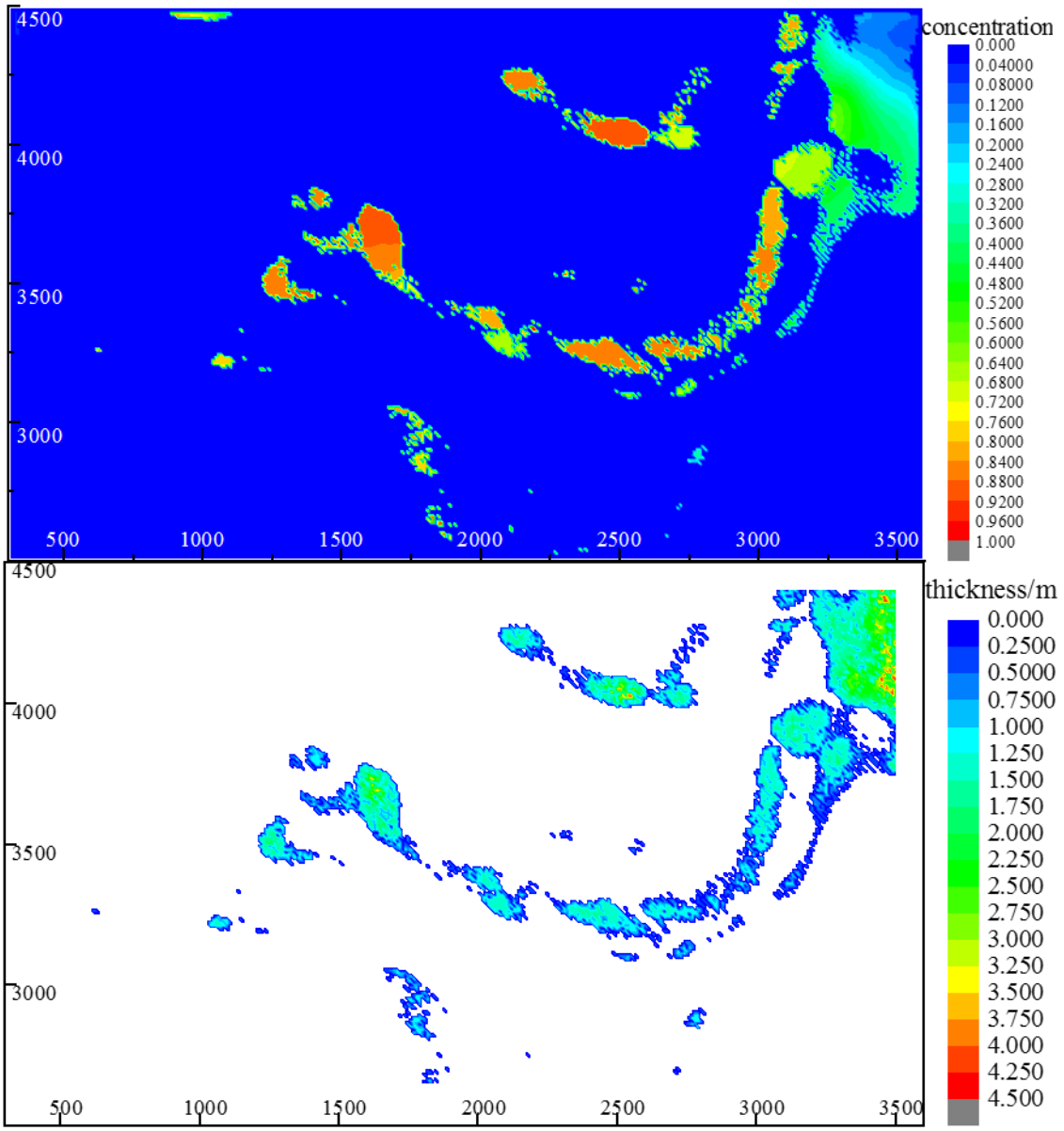

Fig.5.25 The concentration and thickness of debris flow in the southern of Beichuan city using 10m mesh size at t=1200s

It's always hard to know the velocity distribution features in the actual debris flow events. And the estimated velocity always obtained from the empirical equations by measuring discharge and flow depth. In the present method, the velocity distribution features are easy to obtain. As illustrated in the figure 5.26, the velocity distribution features varied with the topographic features, discharge, time, concentration, etc. The velocity ranged 0-11m/s at t=100s, and the velocity of particles that located the upstream of valley is larger due to the large gradient of valley channel. The velocity reduced with simulation time. The velocity in the valley is larger than on the deposition zones. The detailed velocity distribution features contribute to provide adequately protective measures in a

reasonable site.

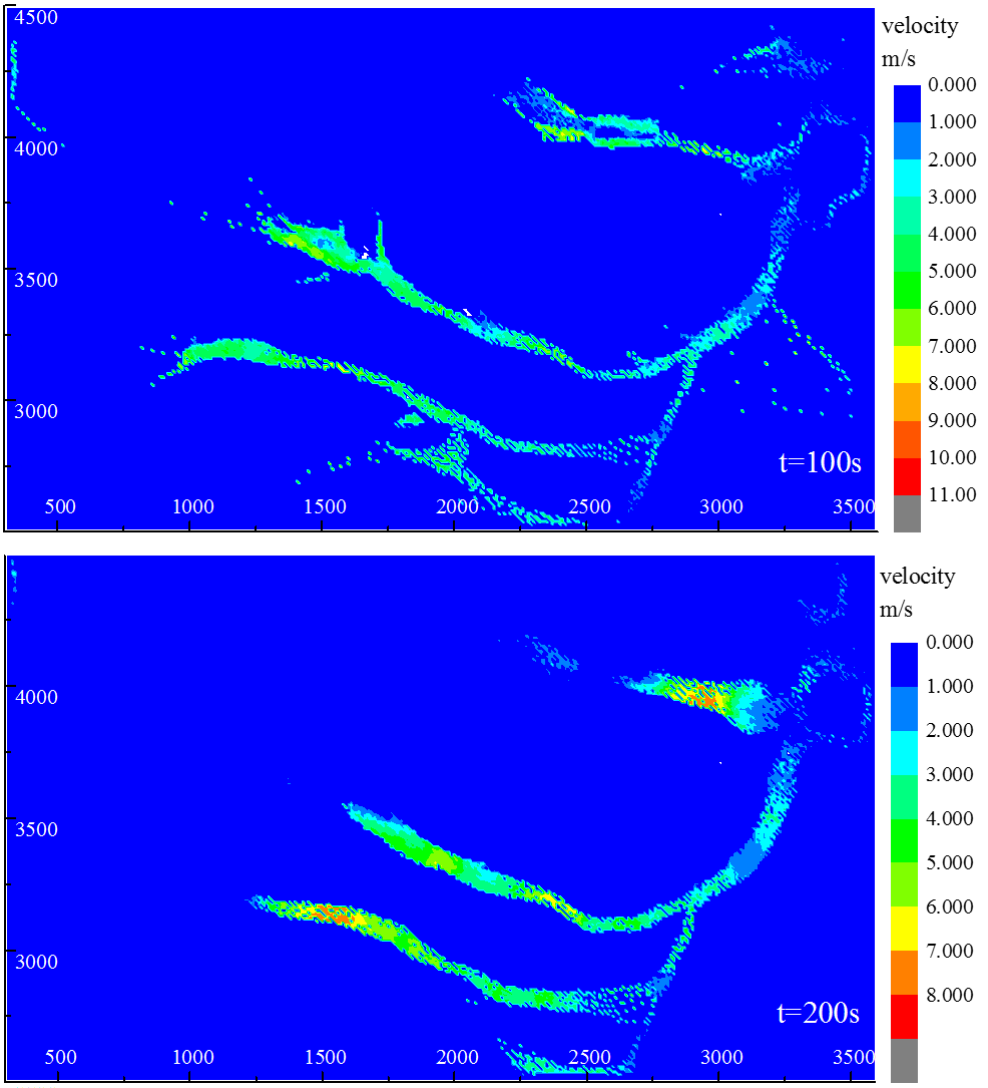

Fig.5.26 The velocity distribution features at 100s and 200s in the southern of Beichuan city

5.4.4 Discussion

The distribution features of debris sources strongly influenced the distribution of debris flow in a wide region. The debris sources were evaluated by dividing the research area into three parts and setting different critical failure slope, according to the distribution features of earthquake-induced landslides. The active fault and river system strongly influenced the critical failure slope in the earthquake. Critical failure slope was set to 38°, 42° and 46° for three parts and the repose angle was set to 30° to generate debris sources. The overlapped area is 70% of actual damage area. It's hard to obtain the prefect agreement between simulation results and actual damage area, because the earthquake acceleration velocity, lithology and the distance from the fault strongly governed the damage zones. All of such information can't be taken into account in the present model. The thickness of deposits ranged 0-3m if the initial particle height is set to 1.0m.

Based on the simulation information of debris sources, the regional debris flow hazards were evaluated using 20m mesh DEM. The 16 debris flows were initiated when the mean rainfall intensity and diffusion coefficient was set to 39mm and 0.1. The agreement is good between the number of actual debris flow and simulation results except two more debris flows that originated debris sources didn't be generate in the earthquake. Therefore, the evaluation results of debris sources strongly influenced the evaluation of regional debris flows. Although many debris flows were initiated under mean rainfall amount was 39mm, the magnitude of debris flow in the southern of Beichuan city is smaller than the actual debris flow in term of damage area on 24 Sep. 2008. The large rainfall intensity with 60.14mm were used to evaluate the debris flow hazard in the southern of Beichuan city. The affect area of D01 had a good agreement with actual deposition zone. However, the affect areas of both D02 and D03 are clearly larger than the actual damage areas, due to smaller critical deposition slope or large mesh was adopted. The thickness of deposits on deposition fan is less than 1m. It's clearly smaller than the actual deposition thickness ranging 7-12m.

The simulation results showed the southern of Beichuan city is the most dangerous zone under the threat of debris flow. The hydrograph and velocity distribution features are favor to analyze the damage. Although the catchment area of valleys is not large, heavy rainstorm can trigger large magnitude debris flow. It demonstrated such small valleys where were damaged seriously can't be ignored in the evaluation of sequence debris flows in Beichuan region. Particularly, the coupling effect of multiple debris flows should be evaluated in detailed.

5.5 Debris flows in the region from Yingxiu to Wenchuan along the Min River

Yingxiu is the epicenter of the 2008 Wenchuan earthquake, it's 10km away from the Dujiangyan and 70km away from the Chengdu, where is the capital of Sichuan province. G213 and S9 highways were built as one of important roads to go to the most regions of northwestern of Sichuan Province crossing the Yingxiu along the Min River. Therefore, it brought huge challenge to enter the epicenter to rescue and survey shortly after the earthquake, because the highways were serious damaged as well as the Min River was blocked at many sites resulting from the earthquake and secondary geo-hazards. This area was not only the most seriously damaged area during the earthquake, and also is the potential high-risk zone of debris flow in the long period after the earthquake because extremely rich loose solid materials were generated by the earthquake.

492km^2 (13km by 44km) area (Fig.5.27) is selected to evaluate regional debris flows in the area from Yingxiu to Wenchuan along the Min River. As illustrated in the figure 5.27, two main faults (Yingxiu-Beichuan and Wenchuan-Maowen) cross this area and the Wenchuan-Maowen fault is nearly parallel with the Min River from Caopo to Wenchuan.

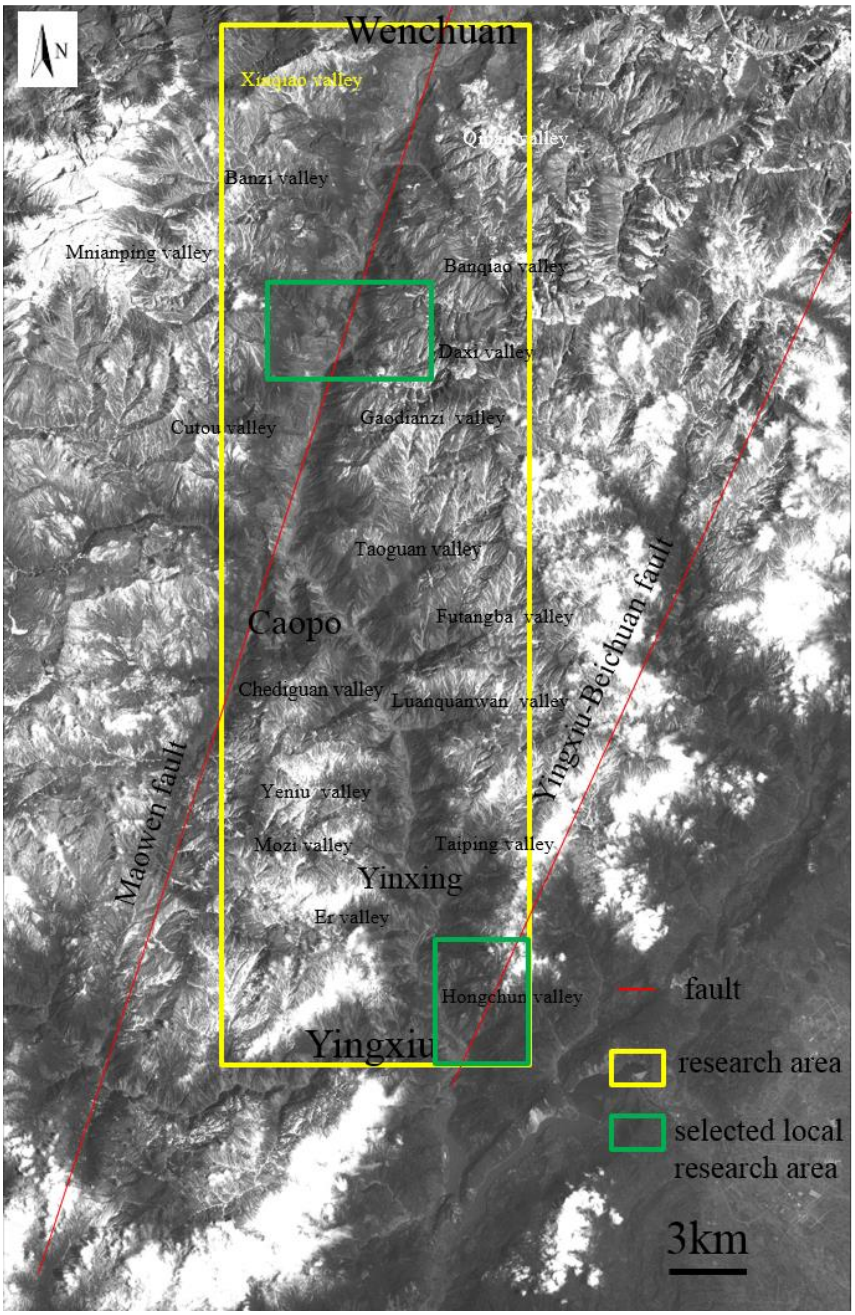

Fig.5.27 The post-earthquake image in the areas from Yingxiu to Wenchuan along the Min River

The main lithology of this region is Granitic rocks, Sinian pyroclastic rocks, Carboniferous limestone and Triassic sandstones. The loose Quaternary deposits distributing in the form of terraces and alluvial fans. All bedrocks is deeply fractured and heavily weathered, covering with a layer of weathered material (Gan et al., 2010; Ge et al., 2014a). The vertical meteorology is clearly, the study area was divided into two different meteorology zones by the boundary of Yinxing. The annual precipitation is 1285mm in the southern of Yinxing, while the annual precipitation is only 526mm in

the northern of Yinxing. The rainstorm concentrates from June to September and account for 70-80% of the total. The annual mean discharge of the Min River is 168-268m^3.

The region from Yingxiu to Chediguan is a low-frequency zone of debris flow in last 100 years before the earthquake. The number of major debris flow valleys is only 8, and the previous debris flows often belonged to dilute debris flow due to scarcity of debris source. In addition, only several debris flows events (such as debris flows in Taiping valley and Luoquanwan valley) had ever blocked the Min River (Tu et al., 2013). In 1978, Banzi valley occurred debris flow and blocked Min river (Liu et al., 2004). However, 56 new geo-hazards were increased as well as 28 sites were activated during the earthquake in comparison with the geo-hazards situation in 2005. More than 0.2 billion m^3 deposits were generated along Min River in this region(Zhuang, et al. 2009).This region instantly became to a high-frequency and high-risk zone of debris flow shortly after the earthquake. The intermittently damages of debris flow were developed and damaged in this region (Fig.5.28). After 12 May 2008, four times catastrophic debris flows events were occurred in this region, on 17 Jul. 2009, 14 Aug. 2010, 3 Jul. 2011 and 10 Jul. 2013. The 21 debris flows occurred on 14 Aug. 2010 (Fig.5.28A) and more than 30 debris flows occurred on 10 Jul. 2013 (Fig.5.28 B and C). These debris flows led to many casualties and destruction among highways, bridges, villages and reconstructions as well as barrier lakes. It's interesting found that most valleys with smaller catchment area occurred debris flow before 2013, while larger valleys occurred debris flow in 2013, such as Taoguan valley, Qipan valley, etc (Ge et al., 2014a).

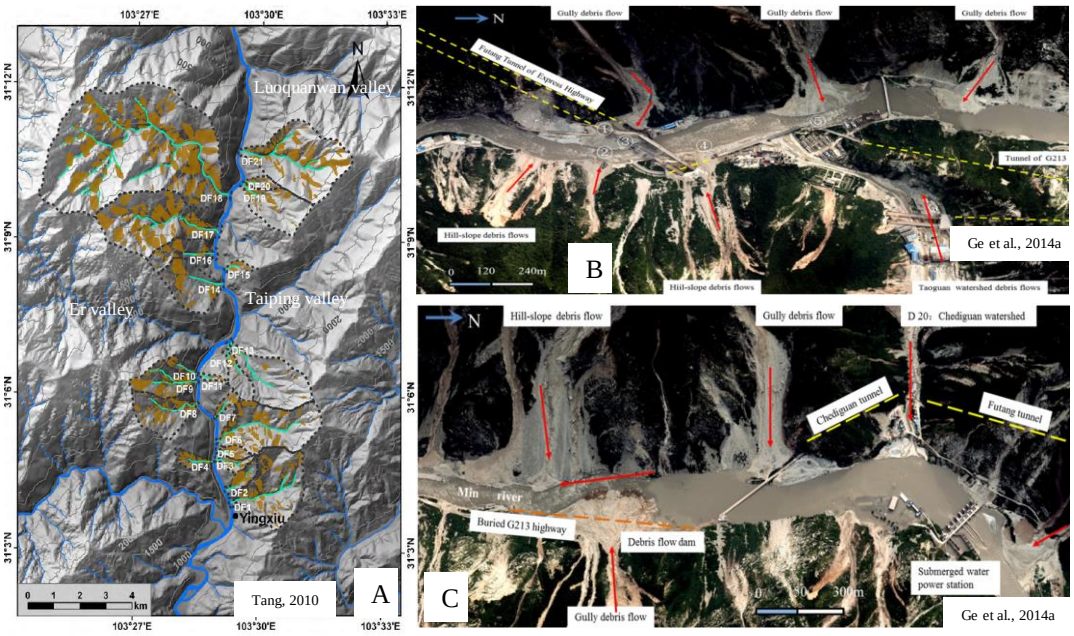

Fig.5.28 Post-earthquake debris flows in the region from Yingxiu to Wenchuan along Min River

According to the existing reports and scientific papers, almost every valley in this region had occurred debris flow after the earthquake (Zhuang et al., 2009). Almost all of debris flows in this

region are characterized by large-discharge, large magnitude and high occurrence frequency. So far, dozens of valleys occurred debris flows more than 2 times and some valleys occurred up to 12 times after the earthquake. Meanwhile the Min River had been blocked and bridges, tunnels as well as roads had been damaged for many times (Tu et al., 2013). Therefore, it's very essential to evaluate the debris flow in this region to provide an adequate prevention and reconstruction planning.

5.5.1 Topographic features

The topography is characterized by rugged mountain and incised valley in the region. And the elevation ranges 880-4500m. The valley density is so large that there are more than 70 valleys with the catchment area ranging 0.25-55km^2 from the Yingxiu to Wenchuan along the Min River (Fig.5.27). From the satellite image, it's easy to identify large valleys and measure theirs' catchment area. By statistic 42 valleys (Table 5.5), it's found that there are 16 valleys which catchment areas are larger than 10km^2. Noted that the other valleys that weren't be measured are less than 3km^2 in catchment area. Therefore, Mostly valleys concentrate on small catchment areas within 3km^2. Such valleys are characterized by short valley channel and large slope gradient. There is not enough buffer zone between the mouth of valley and river for debris flow deposition. It's very likely to flow into the river if large-scale debris flow was generated. Due to the effect of the Wenchuan-Maowen fault, there are at least four pairs of opposite valleys, in which the distance both mouth of valleys is very near, from the Caopo to Wenchuan. There also exist such phenomenon from Yingxiu to Caopo range because many valleys developed on both sides of river.

Table 5.5 The relationship between catchment area and the number of valleys

catchment area/ km^2	<3	3-5	5-10	10-20	20-30	30-40	>40
the number of valleys	14	6	6	4	5	3	4

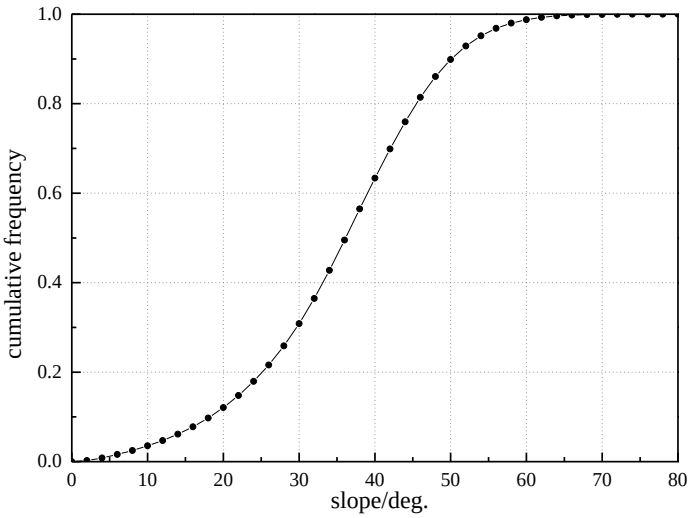

Fig.5.29 The slope frequency in the region from Yingxiu to Wenchuan along Min River

10m mesh size was used to calculate the slope of this area. The slope ranged 0° to 70°, and more than 80% slopes range from 20° to 50° (Fig.5.29). The existing survey showed that the 87.7% landslides distributed on 20°-50° zones (Huang, 2008). It's inferred that mostly areas should have been damaged in this region.

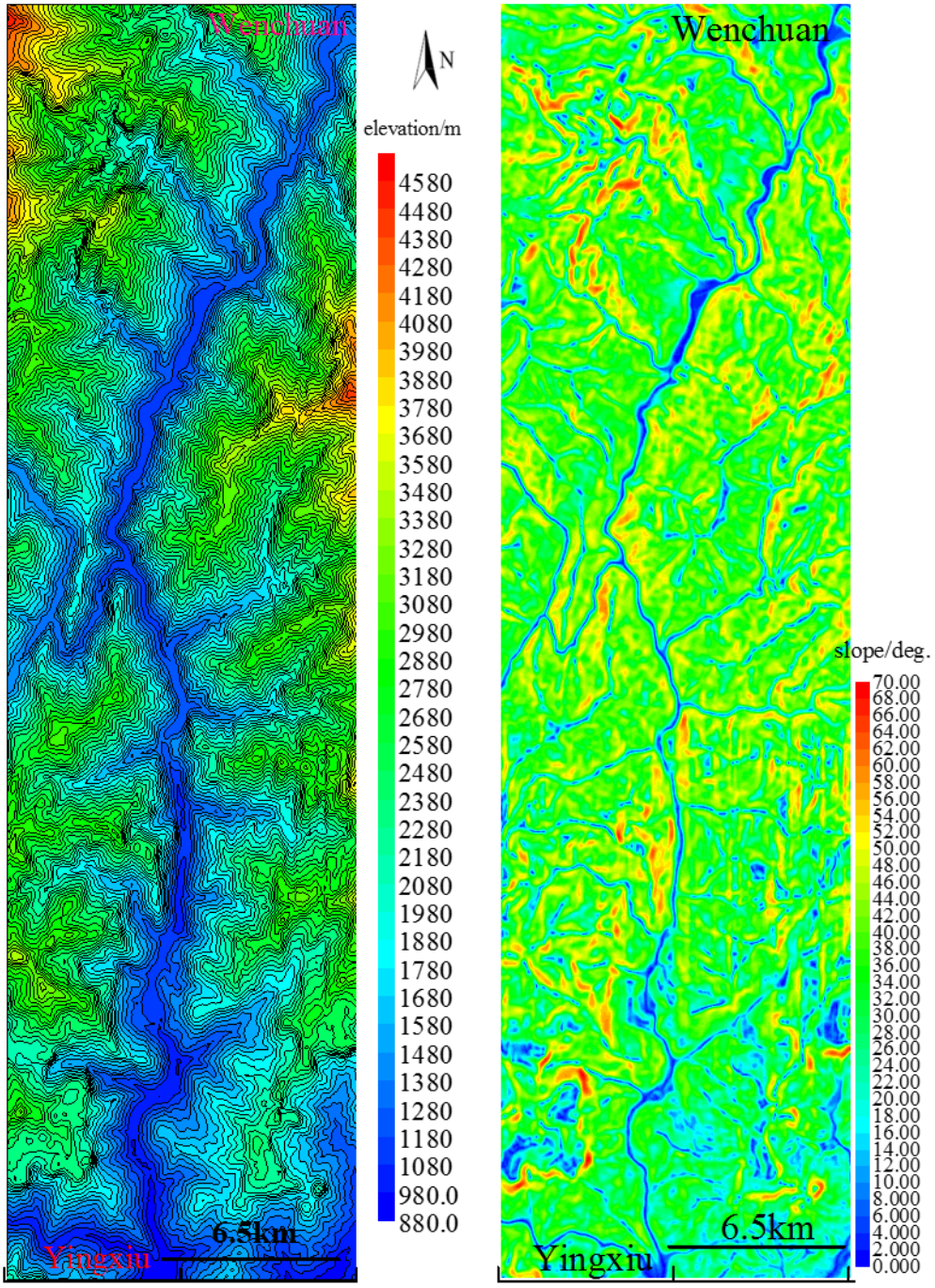

Fig.5.30 The topographic features in the region from Yingxiu to Wenchuan along the Min River

5.5.2 Debris sources

There generated numerous of landslides and rock-falls during the earthquake because of special

topography and near the epicenter. The existing research and field survey demonstrated that the coverage of damaged area varied with different valleys (Zhuang et al., 2009). By statistically analysis of 20 valleys that are primary larger catchment areas, the damage rate ranged 5%-50%. The damage rate of partial small valleys is nearly 100%. The downloaded post-earthquake images in this region were observed on 31 March 2011. Although high-elevation areas were covered by snow and cloud, and it's not easy to recognize the damaged area. From the downstream of valleys and lower places of both sides of river (Fig.5.31), it's still found that the damage was rather serious and rich loosely deposits located on the slope surface and at the bottom of valley. It's noted that such lower-elevation damages are very sensitive to debris flows. The site survey showed 80% and 63% of highways were damaged from Yingxiu to Caopo for old and new G213 highway during the earthquake (Tang, 2008). Huang also argued that the damaged features were significant influenced by the fault, and which led to large differences for damage in different places (Fig.5.32). The mentioned destroyed ration in the figure 5.32 means the percentage of the length of the road blocked by landslides to the total length of the road.

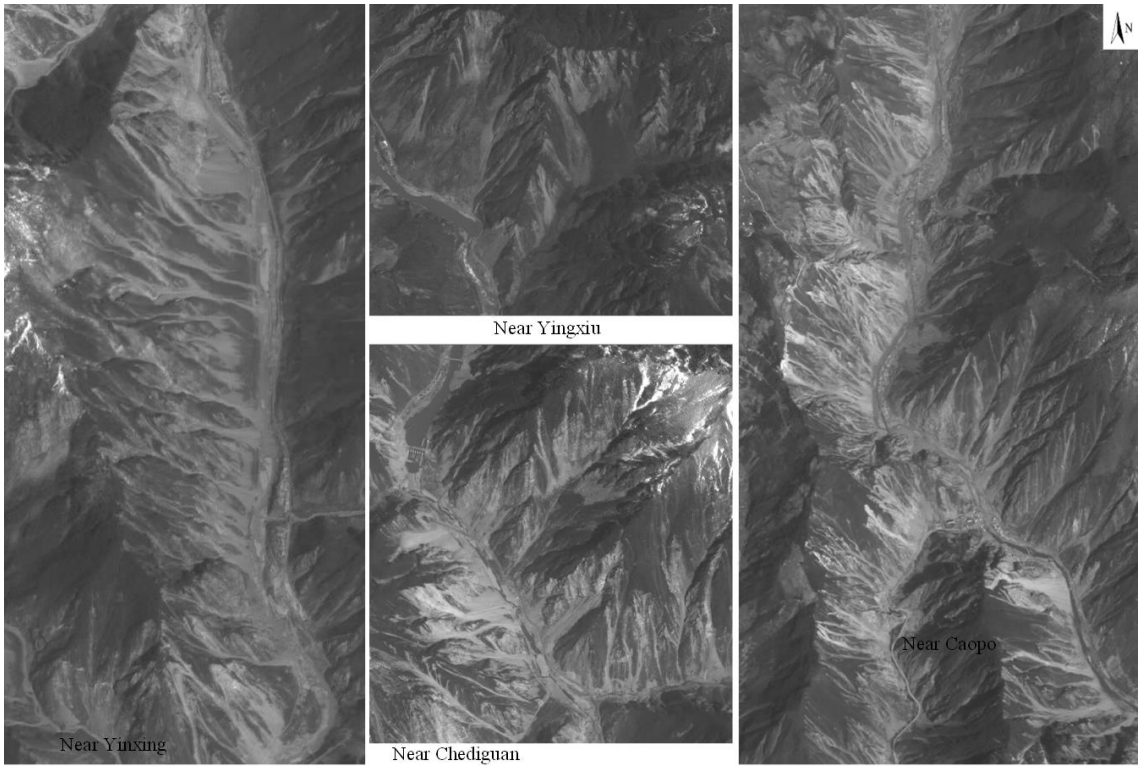

Fig.5.31 Damage in the lower-elevation valleys along the Min River by post-earthquake image

More than 0.2 billion-m^3 deposits were evaluated along the Min River in this region shortly after the earthquake (Zhuang et al., 2009). As illustrated in the figure 5.31, there still distribute large amount of loose solid materials overall region after three rainy-seasons. Moreover, such remained rich debris source must be entrained to debris flow if it rains in the near future. It's an urgent work to evaluate the potential debris flow disaster to reduce the disaster in the earthquake zone.

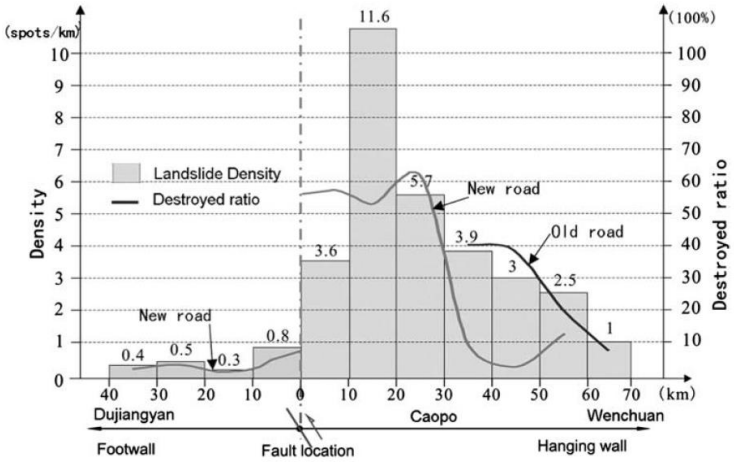

Fig.5.32 Difference of the geo-hazards development in the hanging wall and the footwall along the G213 highway in Dujiangyan-Wenchuan section

5.5.3 Evaluation of debris flow hazards

It's no doubt that every valley has a potential high-risk to occur debris flow in this region with advantage topography, extremely rich debris sources and rainstorm. Rainfall is a very various factor, it can't be simply used to predict the debris flow, particularly in a wide earthquake-stricken region. But we can evaluate debris flow hazards in this region from watershed view by simulating rainfall.

(1) Evaluation of watershed features

In order to evaluate watershed features, rainfall simulation in the whole region was carried out. Due to the research area is very wide, it was divided into two parts to efficient simulate. Water particles were averagely distributed by the interval distance is 300m in the study area and then flowed down based on the given topography (Fig.5.33). It's found that water flow rarely lateral spread after flowed out the mouth of valley and before flowing into river. This phenomenon demonstrated that there are not enough buffer zone for debris flows and the slope of deposition zone is rather large. It means that such topographic features are favor to debris flows flowing into river. Consequently, the riverbed will be increased and the efficient reservoir room will be reduced for the downstream reservoir with large solid materials entering the river. It's also likely to block river by forming temporary dam instantly, if velocity, discharge and density of viscous debris flow is large enough in comparison with river's. Furthermore, the backwater will inundate farmland, highway and railway, even as residence zone. The dam failure also threat the downstream resident and properties (Zhang et al., 2013). Except physical property parameters of debris flow and river, cross-angle is always proposed to evaluate its possibility of blocking river. Cross-angle is defined as the upstream angle of two intersecting flow lines between the debris flow and river flow. The angle is more closed to 90°, it's much easier to block river (Guo, 2004). Xu et al. (2012) also found that the direction of debris flow valleys was more or less perpendicular to the direction of the main river and large amounts of source materials must be available to block the river by analyzing the existing debris flow events in the

earthquake-stricken region.

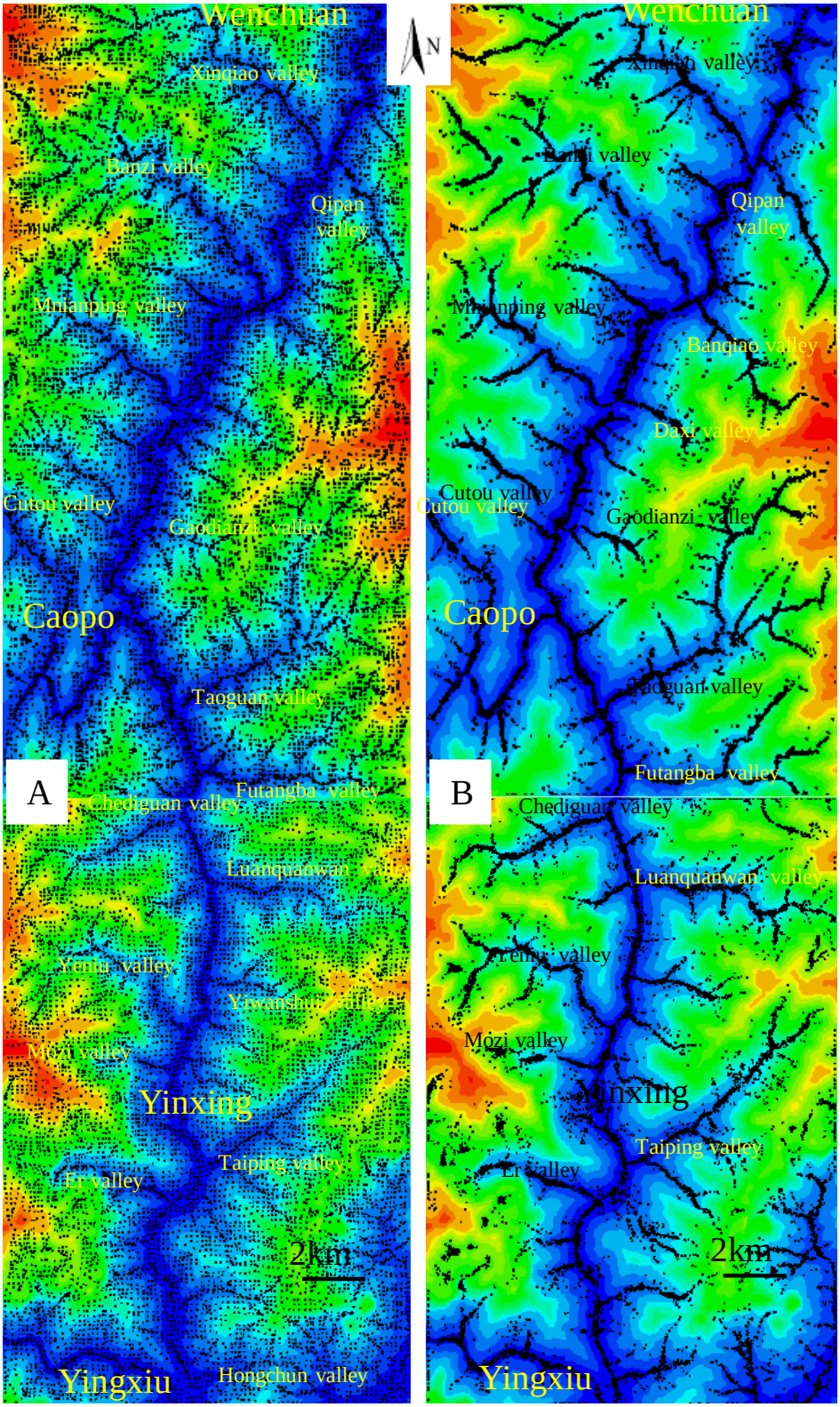

Fig.5.33 The watershed features by simulation rainfall

The cross-angles of 78 flows, which directly flow into the Min River in the region (Fig.5.33 B),

are measured. When the cross-angle is larger than 90°, it's demonstrated that the debris flow direction will be against the river flow direction. In such case, it will be much easier to block river in theoretically. The statistically results (Fig.5.34) showed that 48 cross-angles concentrated on 80°-90° and more than 80% of cross-angles are larger than 50°. Therefore, the potential debris flows in this region are very likely to block the Min River.

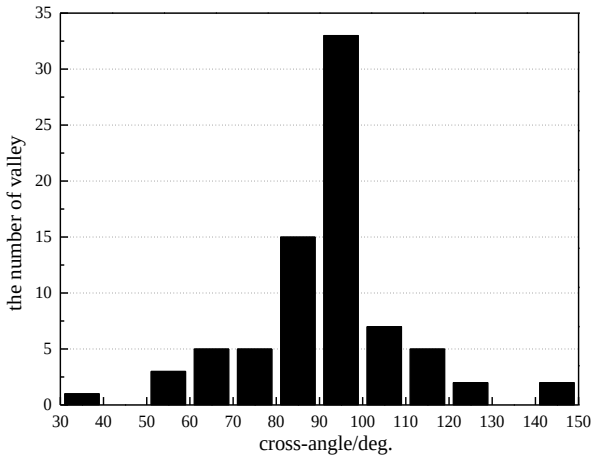

Fig.5.34 The cross-angles in the region from Yingxiu to Wenchuan along the Min River

Actually, more than 20 debris flows had blocked the river since 12 May 2008 in this region (Fig.5.35). On 13 August 2010, all of five debris flows blocked the river on the upstream of Yingxiu town. Resulting in more than half of riverbed was blocked and the river was pushed to the opposite side, and furthermore the new Yingxiu town was flooded. Large-scale debris flows occurred on 10 July 2013 also formed many dammed lakes in the Min River and certainly led to more seriously damage.

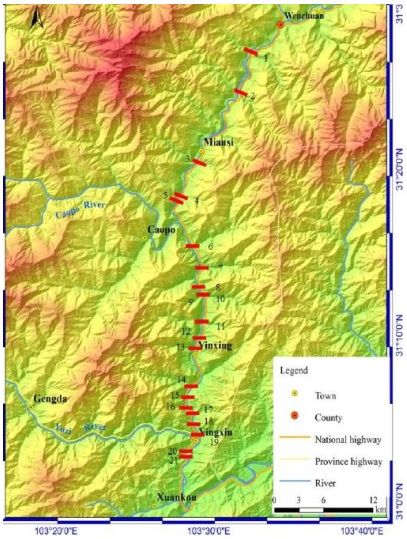

Fig.5.35 Dams of debris flow in the region from Yingxiu to Wenchuan since 12 May 2008 (Ge et al., 2014b)

In addition, the elevation is relatively lower at the valley mouth as well as the width of valley mouth is small and not enough buffer zone for debris flow deposition in this region. As illustrated in the figure 5.36, where the transportation infrastructures cross were often destroyed by debris flows in terms of scouring bridge, burying and washing out roads, blocking and destroying tunnel entrance (Zou et al., 2014). It is extremely important to make sure the safety of lifelines projects during kinds of disasters. Noted that many small valleys where the road crosses from the downstream are becoming new debris flow valleys. It will increase new disasters along the road if none of measures were taken.

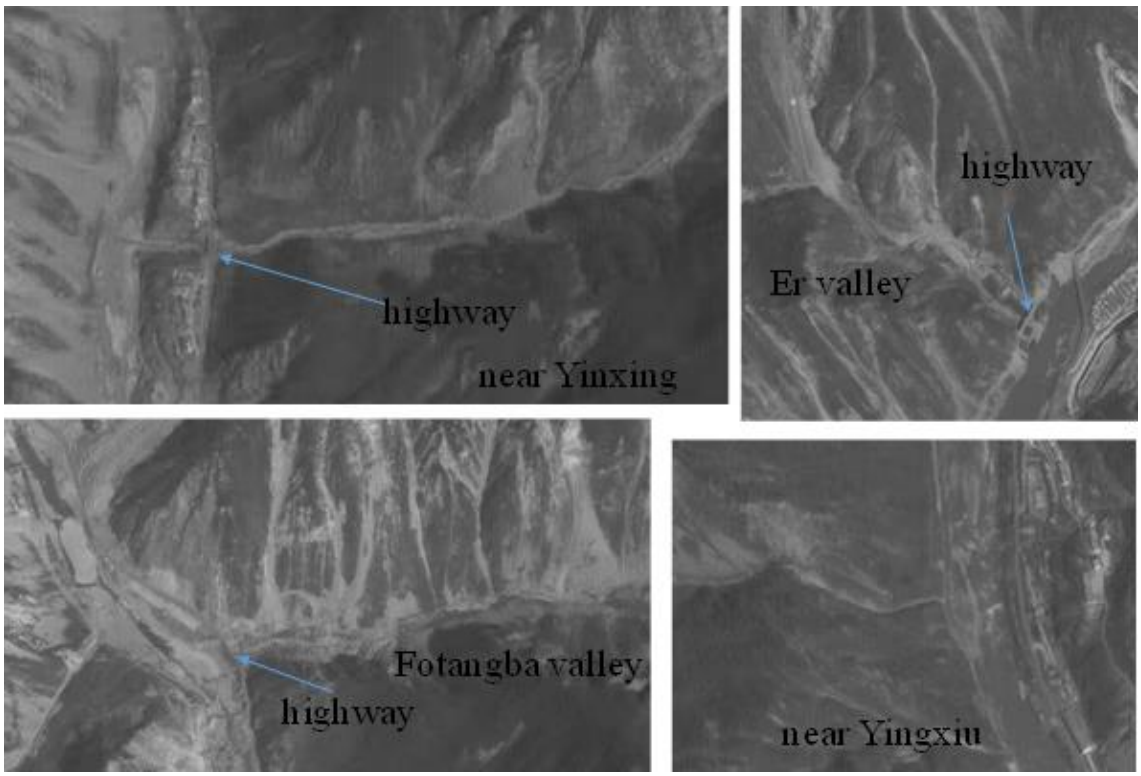

Fig.5.36 The transportation infrastructures cross the mouth of debris flow valley

(2) Simulation of multiple debris flows occur simultaneously

Multiple valleys simultaneously occurred debris flows is a typical characteristic of post-earthquake debris flows in the earthquake-stricken areas. It always caused more seriously damage because of coupling effect by multiple debris flows. On 13 August 2010, a rainstorm triggered more than 20 valleys to occur debris flows from Yingxiu to Chediguan range (Xu et al., 2012). The destructive debris flows blocked the Min River and further damaged the Yingxiu new town (Fig.5.37). It's a tragedy that the epicenter was hit again in 2 years. Here, small region (3.25*4km^2) near Yingxiu was selected to analyze the coupling effect of multiple debris flows.

The basic parameters of five valleys in this zone (Liu et al., 2012) showed in the table 5.6. The catchment area is only 0.5km^2 or even less than 0.5km^2 except 2 larger ones with 5km^2. Although the catchment area is small, debris sources are extremely rich because of a little distance from the

epicenter. The area of deposition fan is also rather small. It's rarely inevitable to flow into river if larger debris flow was triggered. The cross-angles of five flows equal to 90° or close to 90°. It means that these debris flows are very easy to block river once they flow into river.

Fig.5.37 Multiple debris flows blocked the Min River in 2010 (Xu et al., 2012)

Table 5.6 The basic parameters of five valleys near Yingxiu

valley	catchment area	deposition fan area	cross-angle
Hongchun	5.2 km^2	0.064 km^2	90°
Shaofang	0.53 km^2	0.018 km^2	101°
Xiaojia	0.45 km^2	0.012 km^2	99°
Wangyimiao	0.4 km^2	0.013 km^2	90°
Mozi	5.08 km^2	0.01 km^2	90°

In order to generate debris sources, the critical slope of failure and the repose of angle were set to 38° and 30° respectively in the whole research area. As illustrated in the figure 5.38, several large damaged areas agreed well with the actual damage areas in the Hongchun valley. The Mozi valley was damaged seriously in the earthquake. The simulation results only generated large amount of debris source in the upstream of valley, while the large debris sources in the downstream were neglected in the simulation. There also generated some debris sources among three small valleys. Finally, 17% of catchment area was damaged by simulation results in the whole research areas.

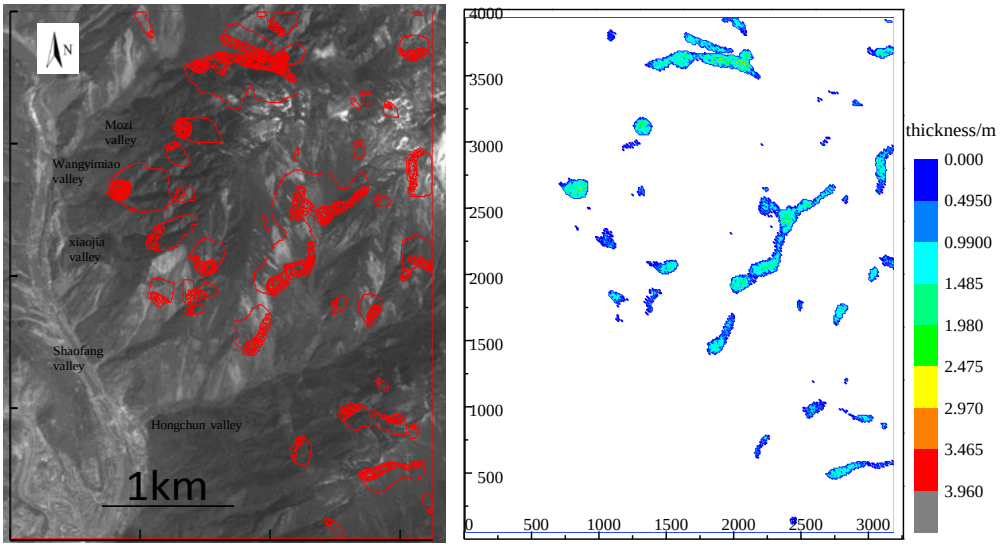

Fig.5.38 The simulation results of debris source

Based on the simulation results of debris source, the water particles were average distributed by 50m interval distance. Then the simulation of debris flows were carried out in this zone. The Main parameters for multiple valleys near Yingxiu showed in the table 5.7.

Table 5.7 Main parameters for multiple valleys near Yingxiu

parameters	value
critical failure slope	38°
repose of angle for solid material	30°
Manning coefficient	0.1
diffusion coefficient	0.05
Mean rainfall amount	38.5mm

The detailed simulation processes showed in the figure 5.39. After 50s from simulation start, the water particles mainly flowed to the valley channel and mixed with solid particles. Around 150s, the three small debris flows were originated and flowed to river, while two large debris flows hadn't been originated yet. After 250s, two of three small debris flows had finished the transportation processes and the other one significantly reached to the river. At the same time, debris flows from small braches flowed to the main valley channel in Hongchun valley, while large amount of solid particles that blocked the valley channel were initiated by the water particles from the upstream of Mozi valley. Aound 500s, three small debris flows completely deposited on the riverbed, while the Hongchun debris flow was flowing into river and debris flows in Mozi valley had finished all of initiation processes. After 15min from the initiation, all of debris flows primary flowed into river and formed five deposition fans on the riverbed.

As the simulation results showed, five debris flows were generated and further five dams of debris flow were formed in the river. It's observed that five dams of debris flows pushed the water to the opposite sides of river and didn't completely block the riverbed with small water particles crossing the marginal of dams of debris flow and flowing down. According to the entire deposition features, the agreement is fairly well between simulation results and actual disasters.

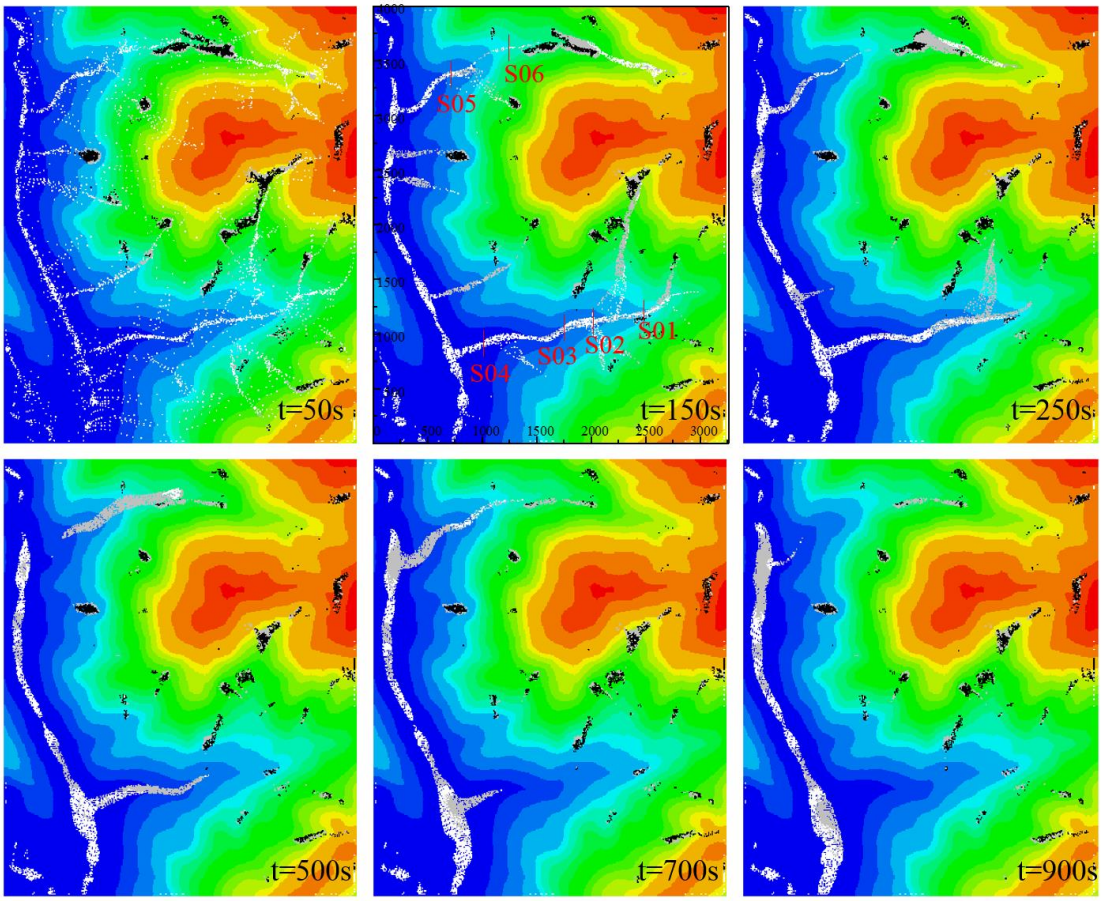

Fig.5.39 Simulation processes of multiple debris flows

The concentration distribution features varied with the distribution features of debris sources and the catchment characteristics. Therefore, the concentration behaved differently in the different stage in the different valleys with the increasing of debris flow volume in the main channel from different branches. Due to the travel distance of three small valleys is short, the debris flows with the extremely heterogeneity concentration already flowed into the river before sufficiently mixed with the water. At the initial deposition time, the concentration on the deposition formed like a series of ring, particularly on both larger deposition fan. However, such phenomenon gradually disappeared with the concentration of debris flows in the river trends to homogeneous because the diffusion effects between the previous reached water and debris flows.

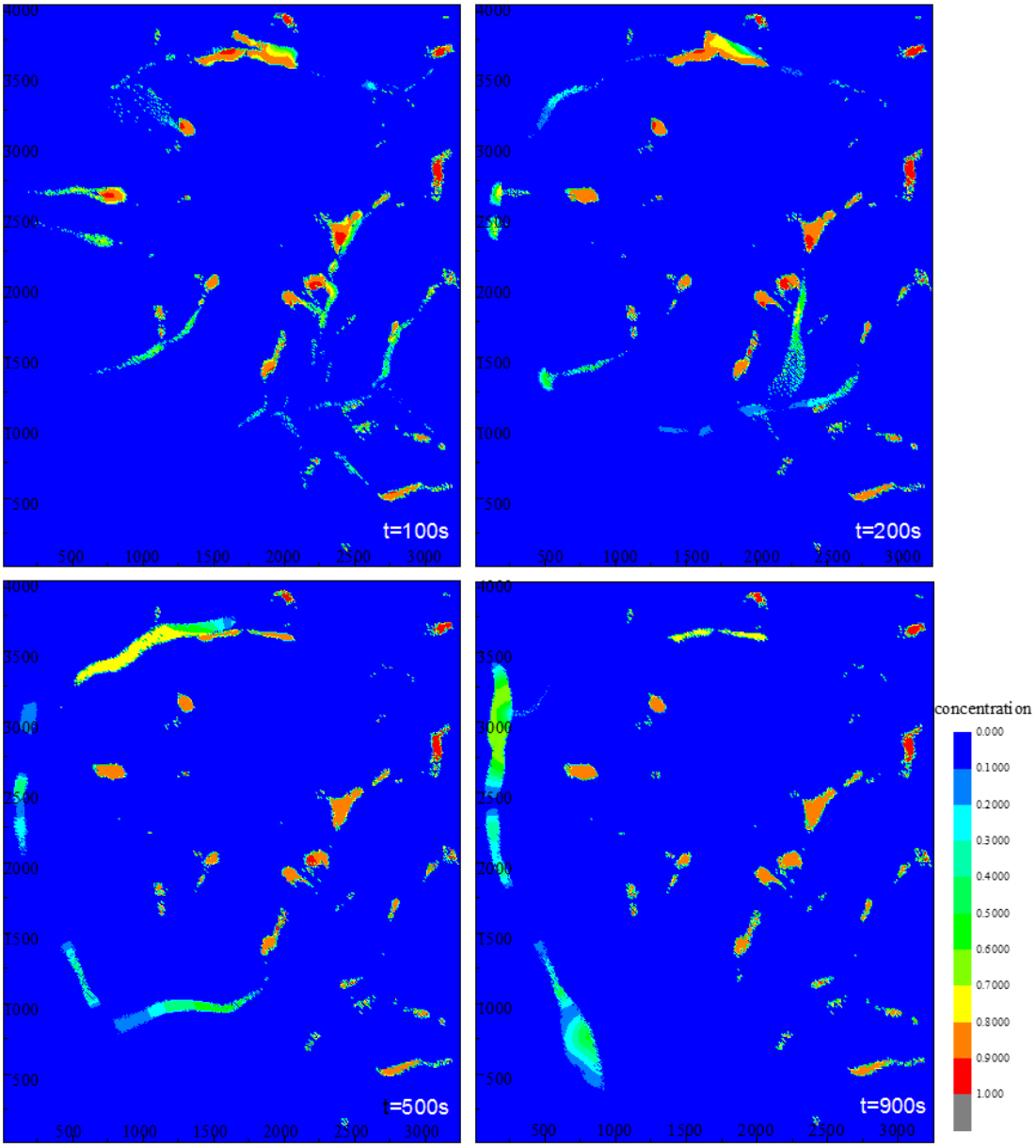

Fig.5.40 Concentration distribution features varied with simulation time

In the actual debris flows, the diffusion effect between debris flow and river water is weak. Therefore, debris flows always blocked river and formed barrier lake. In the present study, the diffusion coefficient was set to the constant in the whole simulation process. To simulate the realistic concentration on the deposition fan, the distribution of water particles can be changed to avoid large amount of water particles in the river. In this case, it's assumed that the diffusion coefficient is extremely small between debris flow and river water. The entire distribution features of concentration are favor for analyzing the composition of sedimentation and further evaluate the time of be flooded away or the dam breach.

The hydrograph is often inputted to some models to evaluate the effects of surges in the damage

process of debris flows. In this areas, six cross-sections were measured the number of particles in both Hongchun and Mozi valleys (Fig.5.41). This work didn't separate debris flow particles and water particles to count. Actually, the mostly water particles were not pure water particles any more. They had mixed with the solid particles by the concentration distribution features in the figure 5.40. Four cross-sections were selected in the Hongchun valley while S05 and S06 located in the Mozi valley. Both S04 and S05 are situated near the mouth of valley, where weren't small braches to flow into the main flow channel. Combined the detailed simulation processes in the figure 5.39, the number of particles in S02 increased suddenly due to one of braches flowed into the main flow channel. Because many braches flowed into the main flow channel, the hydrograph in four cross-sections in Hongchun valley behaved complex with two peaks at least. The hydrograph reached to peak value in 200s and 600s in S04. And the maximum peak value arrived at 600s near the mouth of Hongchun valley. The braches in the Mozi valley are less than in the Hongchun valley, and the hydrograph is simpler. And both hydrographs have similar trends with 200s delay. The peak value of hydrograph generated in 600s from the initiation near the mouth of Mozi valley. Additionally, the peak value of hydrograph in Mozi valley is larger than in Hongchun valley.

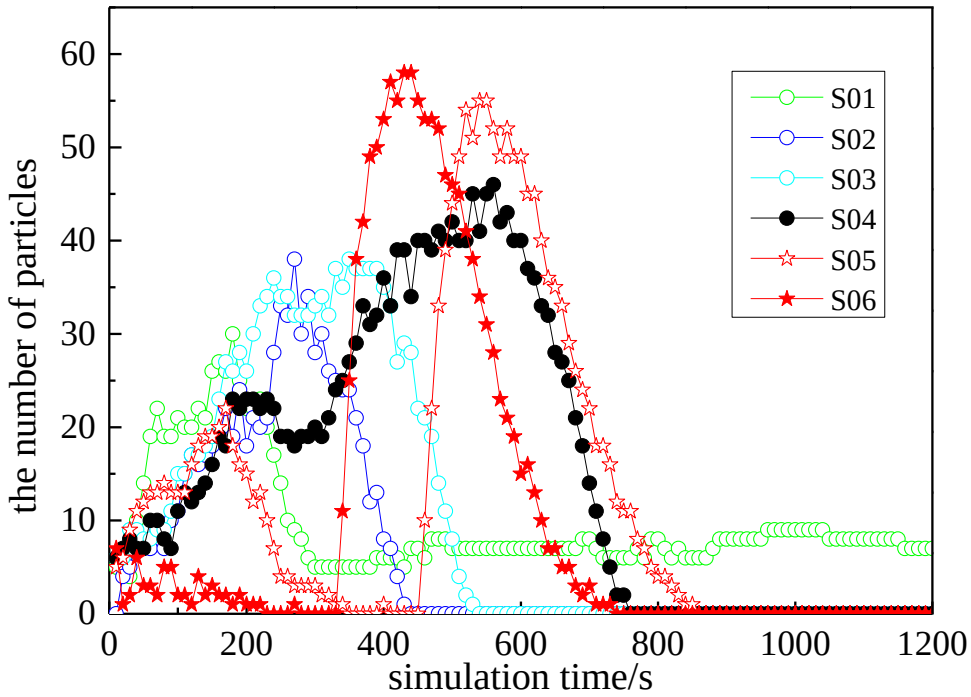

Fig.5.41 Hydrograph in six flow cross-sections of two valleys

As illustrated in the figure 5.42, the velocity distribution features along the width of flow cross-section varied with the simulation time. The velocity in S04 cross-section had small fluctuation with simulation time and the width of cross-section, and its value closed to 3.7m/s. However, the velocity in S05 cross-section ranged 3-6m/s and behaved complex along the width of cross-section. The discharge up to the peak value from 500s to 600s. The velocity also up to the maximum value at

t=500s and t=600s. It inferred that the discharge had some influence for the velocity. The simulation results of velocity in both cross-sections are in a realistic range.

The velocity usually determined the destructive power or impact force. Such simulation results are very useful to take reasonable measures in the prevention works to avoid large debris flows together to arrive at the main channel simultaneously.

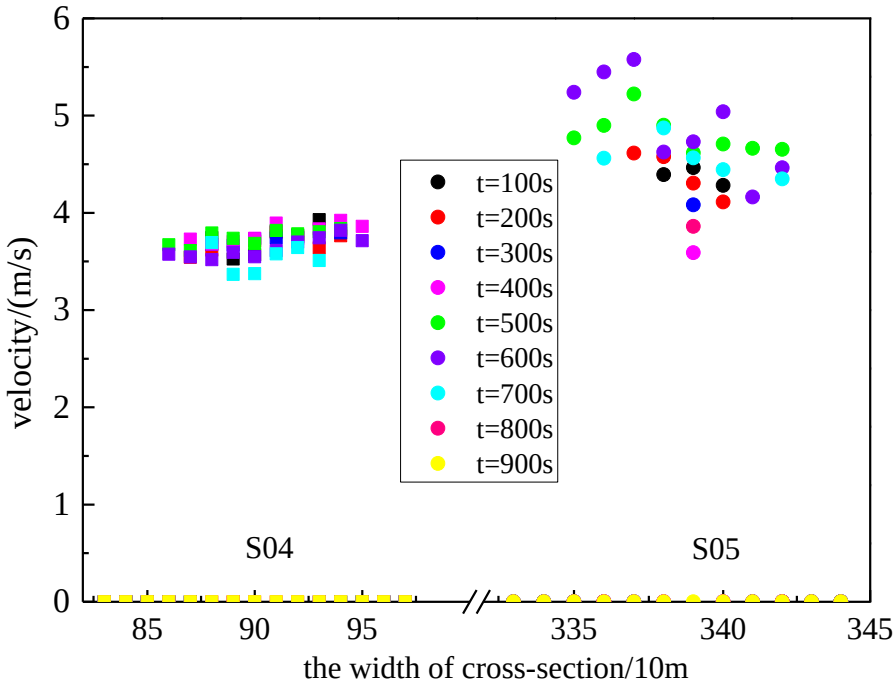

Fig.5.42 Velocity distribution features varied with the simulation time along the width of flow cross-section

Fig.5.43 The comparison simulation results with actual damage in term of affected areas

Due to the debris-dam generated by the Hongchun debris flow pushed the river water to the opposite side, the Yingxiu new town was flooded. As illustrated in the figure 5.43, the affected area extended to the resident zones and covered the whole riverbed. The agreement is good between simulation results and actual damage features.

Regarding simulation results, it's found that every flow path can generate debris flow even the catchment area is very small. This is a new phenomenon of debris flows in the earthquake-stricken zone. It's inferred that small valleys can't be ignored or underestimated in the evaluation works of debris flows, particularly in the seriously damaged zone. Furthermore, the upstream of smaller debris flows that are characterized by short channel length and large gradient, were earlier than larger debris flows to arrive and block the river. In such case, the discharge of river water for the downstream must be reduced rapidly. The discharge and velocity of river water are important factors to determine whether debris flow blocked the river or not. Therefore, it increased the possibility of blocking river for the downstream debris flows. It must be concerned before taking any measures to prevent. It's a very common phenomena that a single dam of debris flow might not cause any damage. However, multiple debris flow occurred simultaneously might further cause large damage due to kinds of coupling effects. It seems that the volume of three smaller dams of debris flows is smaller than the actual debris flows. It's demonstrated that there were not sufficient debris sources were generated if the critical failure slope was set to 38°. It's likely that the actual failure slope was smaller than 38° in so small catchment or the thickness of deposits was much larger than 1m. It's also revealed that it's not a good choice to simulate regional debris flows by setting a constant for critical failure slope to generate debris sources in different catchments.

(3) Simulation of two opposite debris flows

Noted that there is a special topographic feature that the distance of valley mouths of two opposite valleys is rather small. Several pairs of such valleys that behaved this special feature in this region. Here, one of pair-wise valley (Manianping and Daxi valley) was selected to evaluate such special debris flows. Both valleys are 40km away from the epicenter. They were caused differently damage in the earthquake. The basic parameters of both valleys showed in the table 5.8. A simulation was carried out to show two debris flows how to block river in the same rain event.

Table 5.8 Basic parameters of both Manianping valley and Daxi valley (modified by Liu et al. (2012) and Liu et al. (2004))

valley	catchment area/km^2	relative elevation/m	damaged area/km^2	cross-angle
Manianping	46.3	3257	12.82	78°
Daxi	15.76	3762	1.45	91°

Assumed the critical failure slope of both valleys is 38° and repose of angle is 30°, according to the existing research that the critical failure slope ranged 35°-45° in this region (Gan et al., 2010). Hence, the debris source particles were generated. It seems that the generated debris sources in Manianping valley are more than Daxi valley (Fig.5.44. Such distribution of debris source roughly matched well with the damaged area from the perspective of the amount. Therefore, averagely distributed water particles and simulated both debris flows. Manning coefficient and diffusion coefficient is set to 0.1 and 0.1 respectively.

The whole simulation processes showed in the figure 5.44 Solid particles were initiated by water particles which mostly confluence to the main channel after 100s. Due to the valley channel of Daxi valley is relatively straight, the first surge reached to the river after 280s from the initiation. At that time, solid particles blocking the valley channel in Manianping valley hadn't been initiated yet. Around 600s, the second surge flowed to river again in Daxi valley, while the large amount of solid particles were mixing with the sequence water particles from the upstream of Manianping valley. After 900s, the debris flow in Daxi valley finished the transportation process, while the debris flow was initiated completely in Manianping valley. Before the Manianping debris flow flowed into valley, the previous arrived debris flow particles from Daxi valley was flowing down along the riverbed with a small velocity. The concentration was larger than 0.4, and the largest concentration located in the center of deposits. At 900s, the concentration of front debris flow in Manianping was larger than 0.7. It's likely to completely block the river if the Manianping debris flow flowed into river with a fast velocity. At 1500s, large amount of debris flow from Manianping valley had flowed into river. The width of blocking river clearly increased, it's hard to cross for the water flow.

This simulation showed that river was not completely blocked by the Daxi debris flows. The debris flows narrowed the width of riverbed and pushed river to the opposite. This phenomenon is very common in post-earthquake debris flow events. This case often didn't further cause large damage, the sediments were washed away in short period. Certainly, a single large-scale debris flow usually completely blocked river and formed the barrier lake. Once the barrier lake was formed, the backwater would flood road, village, etc.

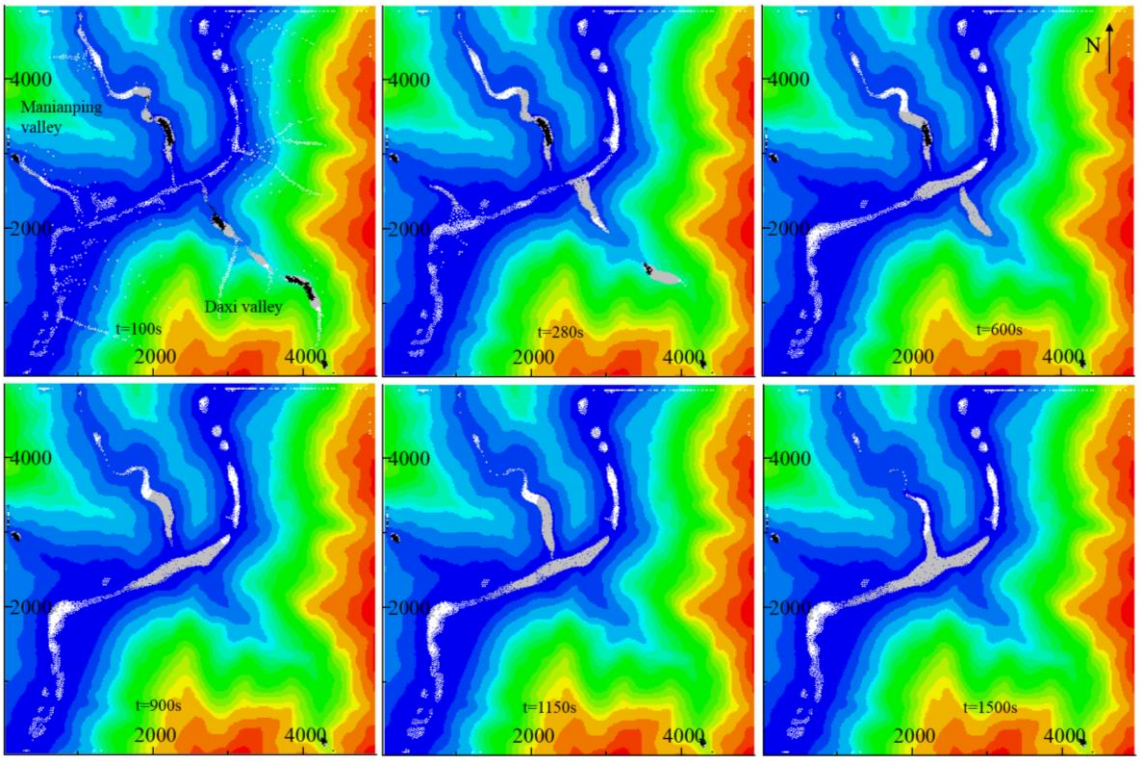

Fig.5.44 Simulation process of blocking river by both debris flows

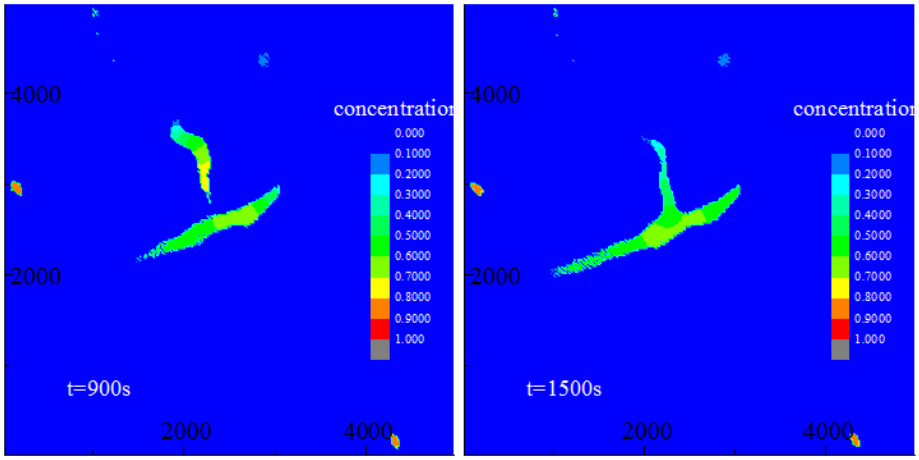

Fig.5.45 The concentration distribution features

Although both valleys haven't occurred such damage yet, both debris flow valleys had high-risk to block river by evaluating topographic features and debris sources (Liu et al., 2012). So far, none of the similar phenomenon was reported, but such phenomenon exists in this region (Fig.5.46). Considering the special topographic features in this region as well as extremely rich debris sources, it should be concerned on the prevention work.

Fig.5.46 The phenomenon of two opposite debris flows together block river by post-earthquake image

5.5.4 Countermeasure structures

To prevent and mitigate the disaster of debris flow, it's a very common way to build check dams in the valley channel as well as some drainage channels on the deposition fan. However, the designers rarely considered the failure effect if it can't bear enough strongly debris flow. With the development of expanding new city and building more roads, many kinds of check dams were built in the potential high-risk debris flow valley to prevent and mitigate the disasters since 90s' last century in China. Certainly, many kinds of check dams were also built in the valleys where were damaged seriously during the earthquake. However, a series of check dams were damaged one by one under strong debris flows, and finally the last dam failure clearly enlarged the disaster, such as Wenjia valley and Hongchun valley. This phenomenon urged us to consider all of effects of building dam before build it. Drainage channel also played a significant role in transporting debris flow on the deposition fan. It's important that what size of channels and where be adjust to build it. Therefore, some simulations about check dam and drainage channel were showed with the Hongchun valley as a case study.

Hongchun valley, located on the opposite of Yingxiu town. The Yingxiu-Beichuan fault crosses this valley along valley channel. The catchment area is 5.35km^2, the main channel length is 3.62km, and the relative height between valley mouth and summit is 1288m. The earthquake caused serious damage in this valley. On 13 Aug. 2010, the Hongchun valley occurred debris flow and formed a 100m wide and 350-400m length blocked dam, resulting from the Min river moved to the opposite of Hongchun valley and further led to flood flowed into the Yingxiu new town. Five days later, the Hongchun valley occurred debris flow again. Resulting in the Yingxiu new town was flooded again.

(1) Check dam

To show the effect of check dam in prevention debris flow, three cases were simulated. In case one (no dam), simulate debris flow on the original topography. Simulate debris flow on the topography with a dam which is about 500m far away from the river, the simulation was carried out keeping the dam well from the initial to finally in case three (keep dam well), while the dam was eliminated at some time in case two (dam breach).

The detailed simulation processes showed in the figure. At the initial state, case 1 is no dam, while case 2 and case 3 are the same and have dam near mouth of valley. From the simulation time at 200s, it's found that the flow behavior was changed by the dam in case 2 and case 3, while small debris flow had flowed out the mouth of valley. After 400s from initiation, the main debris flow began to flow out the mouth of valley, while debris flow continuously flowed down and stopped inside of the dam in the case 2 and case 3. After 400s, the dam was eliminated in the case 2, while the dam was kept in the case 3. After 450s from the initiation, the main debris flow flowed into river in case 1, large debris flow lateral spread and further flowed down in case 2, and small debris flow overflowed the dam in case 3. After 100s from the dam breach in case 2, debris flow reached river. The cross-section of flow in case 2 is clearly wider than case 1 before flowed into river. Finally, all of debris flow flowed out the valley in case 1 and case 2, while small debris flow overflowed the dam and flowed into river as well as most debris flow stopped inside of dam. It's clearly that check dam changed flow behavior in different time and also influenced the affected area.

The close-up of the affect area (Fig.5.48) on the downstream of valley and deposition fan showed that the dam breach increased the affect area by wider lateral damage (Fig.5.49). Although the dam kept well from initial state to final state, large debris flow overflowed out the dam and a small flow also overflowed from one sides of dam. Therefore, unexpected area is also possible to damage by overflowed debris flows under dam keeps well. Three sections were chosen and the width of affect areas were measured (table 5.9). The width of affect area gradually increased from the upstream to the downstream. Because the dam breach, the width averagely increased by 34.4% in comparison with the result of no dam. The main overflowed flow led to small damage along the flow path, and the width of affect area averagely reduced 18.3%. However, the small overflowed flow additionally caused 10% damage in comparison with the case of no dam.

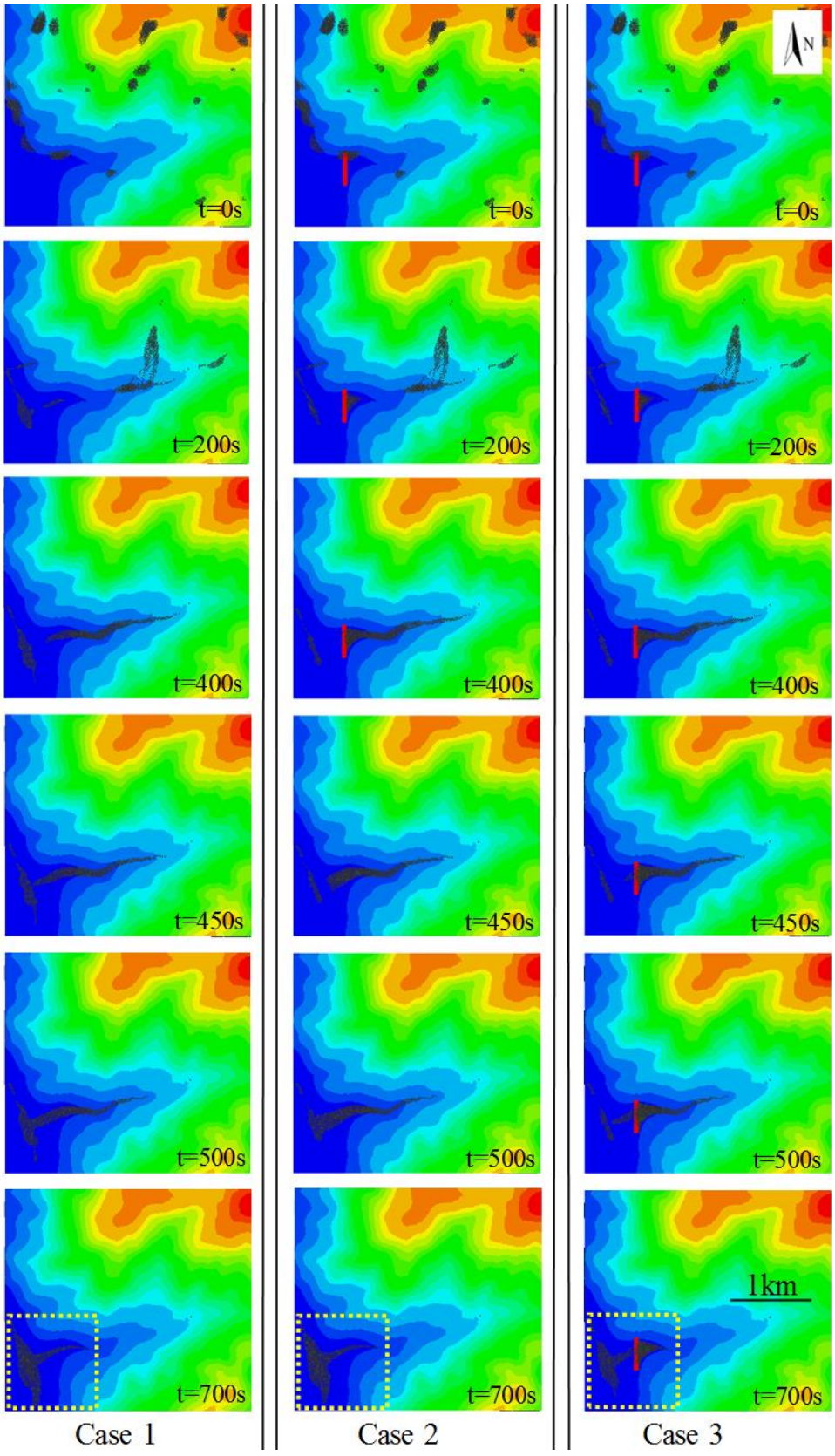

Fig.5.47 Simulation processes of three cases about check dam

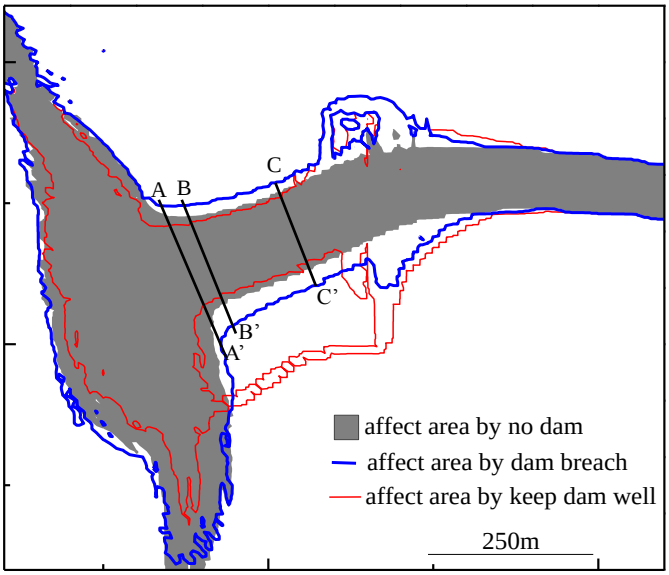

Fig.5.48 Affect areas under three cases of check dam

Table 5.9 The width of cross-section varied in three cases

cross-section	increase rate of damage width in comparison with the case of no dam		
	dam breach	main overflowed flow in case 3	small overflowed flow in case 3
A-A'	0.25594	-0.28419	0.07988
B-B'	0.4204	-0.15723	0.10568
C-C'	0.35785	-0.10684	0.11795
Mean value	0.34373	-0.18275	0.10117

According to the simulation results of velocity, it's found that the check dam also played an important role in changing the value of maximum velocity and mean velocity (Fig.5.48). After the dam breach, the maximum and mean velocity suddenly increased instantly. Due to the dam increased the height, the maximum velocity clearly increased for overflowed debris flows. Velocity has a closely relation with impact force which determined the destructive power. Therefore, the velocity suddenly increased would cause damage that is more serious.

Simple simulation showed that check dam played an important role in changing flow behavior and some parameters, such as occurrence time, affected area and velocity. The dam breach by strong debris flow can increase the affected area and velocity. Even though dam kept well during debris flow, large debris flow would fill the dam and overflow the dam. In that case, the velocity also increased due to higher elevation. Therefore, it must evaluate the effect of check dam before constructing it.

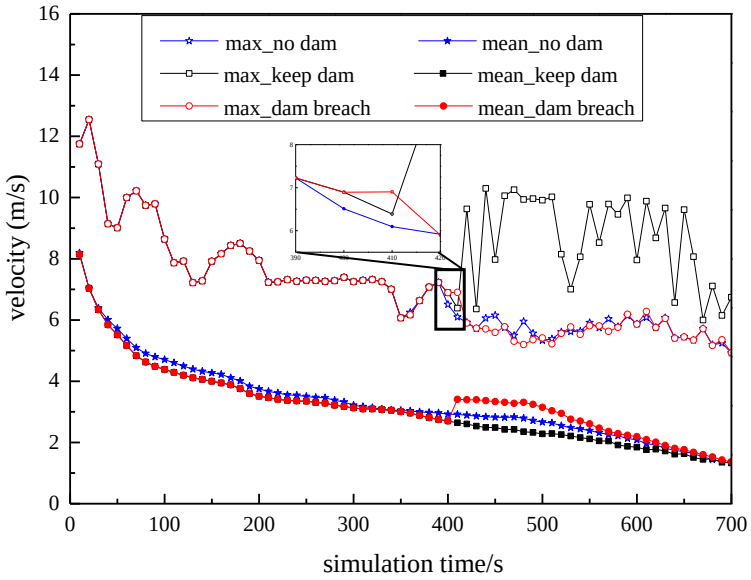

Fig.5.49 Simulation velocity under three cases of check dam

(2) Drainage channel

Drainage channels are also common built on the deposition fan to control the debris flow behavior. However, what size of channel to build and where are adjust to build, and what effects will be brought? A simple channel is built and four cases are simulated. In case 1, keep original topography in the whole simulation process and not add channel. In case 2, add a channel from valley mouth to river with the width of channel is 4 mesh size, while the width of channel is10 mesh size in case 3. In case 4, add a different channel with case 2 and case 3, with the width of channel is 9 mesh size (Fig.5.50). From the detailed simulation processes (Fig.5.50), the drainage channel not only changed the flow path and also influenced affect area and flow behavior. The debris flow had flowed into river in case 1, while only small debris flow just reached the river in both case 2 and case 3 and debris flow was transported to another place along drainage channel in case 4. After 400s from the initiation, small debris flow overflowed from the narrower channel in case 2 while all of debris flows moved along the channel in case 3. Finally, the debris flows were transported to the different place by two channels in different directions. The series of simulations showed that what size of channel to be built and where is adjust to build are very important to prevent debris flow. Design a reasonable drainage channel is also important to rebuild a new city in the earthquake-stricken zone.

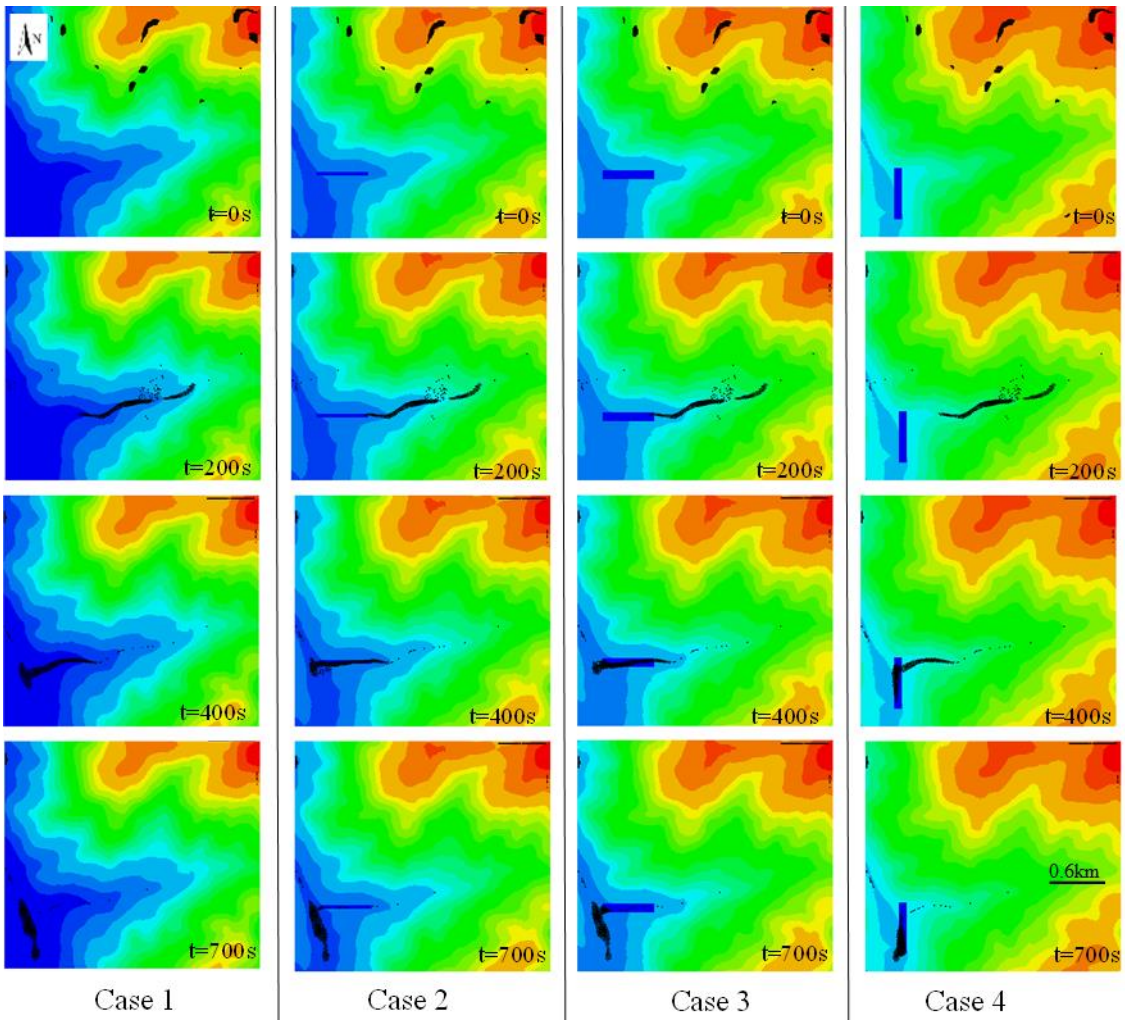

Fig.5.50 Simulation processes of four cases about drainage channel

5.6 Summary

The satellite image of ALOS is characterized by wide coverage area and high spatial resolution. The high quality images that are observed shortly after the earthquake can be used to efficient analyze the damaged features and further provide adequately and available rescue planning in time in the earthquake-stricken areas. Considering main damaged features, it showed mostly damages occurred along the Yingxiu-Beichuan fault, and more damages concentrated on the hanging-wall. The surface damage rate ranged 20% to 37% by analysis of three regions from Dujiangyan to An County. Various damage patterns are also observed by high quality images. However, it's hard to attain the relationship between damaged areas and slope only by satellite image. The high spatial resolution images that are observed shortly after the earthquake are precious data for the sequence evaluation of disasters and reconstruction in the earthquake-stricken areas.

The earthquake resulted in more than 10,000 km^2 were seriously damaged in the Longmen

mountainous zones. Advantage topographic conditions and extremely rich loose solid materials under rainy season is the most serious threaten for the earthquake-stricken areas in a long period. Actually, the earthquake-stricken areas have been heavy hit again in the last five years. The existing research demonstrated that more researchers concentrated on the prediction of rainfall. It's no doubt that the rainfall-related parameters will reduce because the new generated debris sources with the loose structures are more easier to initiate. However, the rainfall features varied with the different places and it's very hard to apply in a wide areas. Additionally, it's not enough to provide accurate rainfall parameters by the present distribution of rain gauge stations in the earthquake-stricken areas. The imperative work is the effective evaluation of debris flow hazards and further prevention.

The mixing model based on two-step evaluation scheme can well evaluate the post-earthquake debris flow hazards in the Wenchuan earthquake-stricken areas.

The distribution features of debris sources strongly influenced the distribution of debris flow. It's very hard to judge the location of debris sources by a constant for critical failure slope, due to the special features of earthquake-induced landslides. The simulation results showed the agreement is good between simulation results and actual debris flows in term of the number of debris flows in a wide region. The southern of Beichuan city is the most dangerous zone facing the threat of debris flows. The hydrograph, concentration and velocity are favor for providing useful parameters to prevent debris flow hazards. The deposition thickness is clearly smaller than the actual deposition thickness if the initial particle height is set to 1.0m.

Regarding the evaluation of blocking river by debris flow hazards in the region from Yingxiu to Wenchuan along the Min River, watershed features and special coupling effect of multiple debris flows are analyzed combining the satellite image and processed DEM. The topography is characterized by high density of valley and small or even no buffer zone between mouth of valley and river. The simulation results of rainwater showed there are more than 70 flow paths, and less than 20 for large valleys. The cross-angle concentrated on 80°-100° by measuring 78 flow paths. It inferred that it's extremely likely to block river by the debris flows in this region. By simulating multiple debris flows occur simultaneously near Yingxiu, the agreement is fairly well between simulation results and actual debris flow event on 13 Aug. 2010. It demonstrated that every flow path can transport debris flow even very short flow path. It means that the small valleys must be concerned in the evaluation work, particularly the catchment was seriously damaged in the earthquake. Detailed transportation processes, velocity and concentration distribution features varied simulation time can be used to analyze the actual disaster process. One more pattern of blocking river was carried out to show the coupling effect of two opposite debris flows. The simulation results indicated that two opposite debris flows occur at the same rain event would increase the possibility of blocking river. It need to take measures to avoid such disasters occur. The site survey demonstrated that there are landslide dams particularly in the large valleys, such as Fotangba,

Taoguan, Qipan valley, etc. The failure of landslide dams was considered an important cause for debris flow initiation. It must concern the valleys with large scale landslide dams and do a long period prevention work to avoid the disasters like Zhouqu.

A series of simple simulations about check dam and drainage channel showed theirs' effect in prevention and mitigation of debris flow. The effect of countermeasure structures must be comprehensive evaluated before building them. This region is and will be a high frequency occurrence zone of debris flows in a long period. Considering the limited deposition areas and security of infrastructures, it's better to keep the extremely rich debris sources in the valley. How to effective keep debris sources in the valley need to make a further evaluation.

CHAPTER 6 CONCLUSION

In the present study, the mixing model based on two-step evaluation scheme was proposed to quantitatively evaluate the debris flow hazards in Zhouqu and Wenchuan earthquake-stricken areas using depth-integrated particle method and satellite images. The conclusions are summarized from the depth-integrated particle method, the mixing model, satellite image, parametric studies, and quantitative evaluation of debris flow hazards in Zhouqu and Wenchuan earthquake-stricken areas.

The depth-integrated particle method is a very simple and efficient method with only two parameters (Manning coefficient and critical deposition slope) to simulate debris flows. The modified depth-integrated particle method was verified by two simple flows in 1-D. It can be applied to quantitatively evaluate debris flow hazards based on detailed DEM. The mixing model based on two-step evaluation scheme can efficiently evaluate the debris flows according to the diffusion equation. In the present model, diffusion coefficient was assumed to a constant in the whole simulation process. And one fitting coefficient was assumed to build the relationship between the critical deposition slope and concentration.

The satellite image of ALOS is characterized by wide coverage area and high spatial resolution. The images can be processed into detailed DEM with the resolution is less than 10m combined control points from the Google earth. The error of control points was evaluated in comparison with the topographic map, and it was assumed acceptable in this study. The high quality images that are observed shortly after the earthquake can be used to efficient analyze the damaged features and further provide adequately and available rescue planning in time in the earthquake-stricken areas. Considering main damaged features, it showed mostly damages occurred along the Yingxiu-Beichuan fault, and more damages concentrated on the hanging-wall. The surface damage rate ranged 20% to 37% by analysis of three regions from Dujiangyan to An County. Various damage patterns are also observed by high quality images. However, it's hard to attain the relationship between damaged areas and slope only by satellite image. The good quality images that were observed shortly after the earthquake are precious data for the sequence evaluation of disasters as well as reconstruction in the earthquake-stricken areas. It's available to check the location of debris sources by satellite image, but it's very hard to evaluate the volume of debris source only depending on satellite image.

By parametric studies, it's found that the accurate topographic data played a critical role in quantitative evaluating debris flow hazards in terms of affect area, travel distance, flow path. The discharge strongly governed the flow behavior on the deposition fan, while Manning coefficient determined the velocity of debris flow. The critical slope of deposition and flow volume significant influenced the travel distance and the extent of deposition.

The debris sources in Zhouqu debris flows were evaluated in terms of location and thickness

combined the post-event satellite image and filed survey. It's reasonable to evaluate debris sources in Zhouqu region by setting critical failure slope and repose of angle is 60º and 26º respectively. By assuming the initial particle height is 1.0m, the thickness of debris sources ranged 0-8m. Two models (re-initiation model and mixing model) were adopted to evaluate the debris flow hazard. It's found that the re-initiation model is very efficient with small particles (only solid particles), while the mixing model is rather time-consuming because of more than 2 or 3 times of solid particles were increased as water particles to initiate debris flow. The re-initiation model is suitable to evaluate the extent of deposition area and flow path on the deposition fan with only two parameters (Manning coefficient and critical deposition slope). Although two more additional parameters (diffusion coefficient and fitting coefficient for the relationship between critical deposition slope and concentration) were taken into account in the mixing model, it's reasonable to evaluate debris flow hazard to consider the physical properties of particles. Moreover, more local concentration-related phenomenon is also described in the mixing model. Affected area was evaluated using re-initiation model, the agreement is good on SYY and LJY deposition fan if the critical failure slope is set to 60º and 61.5º. The debris sources were initiated when the mean rainfall was 29.03mm at the upstream of valley and the diffusion coefficient was set to 0.1. A series of simulation results showed the difference of discharge on both valleys strongly influenced the debris flow hazard on deposition fan. Advantage topographic features, rich debris sources and rainstorm together triggered this debris flow event. The failure of some countermeasure structures and high population density enlarged the destructive nature to large extent.

Quantitative evaluation of debris flow hazards in the Wenchuan earthquake-stricken areas, it's found that almost every valley has potential high-risk to occur debris flow. The evaluation of earthquake-induced debris sources was focused on the Beichuan region. It's hard to evaluate debris sources by a single critical failure slope in a wide region, particularly, an active fault crosses the research area. The evaluation results of debris sources strongly influenced the evaluation of regional debris flow hazards. The simulation concentrated on blocking river in the area from Yingxiu to Wenchuan along the Min river. The topographic features determined the debris flows in this region are easy to flow the river and the watershed features demonstrated that the debris flows are extremely easy to block river to form barrier lake due to 60% cross-angles of all of flows ranged 80°-100°. Many small valleys together with larger valleys occurred debris flow simultaneously increased the destructive degree. Two patterns of blocking river were simulated and the coupling effect of multiple debris flows and two opposite debris flows occurred simultaneously are also evaluated. The simulation results indicated that such phenomenon would increase the possibility of blocking river. It must take measures to avoid such disasters to occur. Detailed transportation processes, velocity and concentration distribution features varied simulation time can be used to analyze the actual disaster process.

Simple simulation results of both check dam and drainage channel can be used to evaluate the effect of countermeasure structures in the prevention and mitigation works. The forecast work of debris flow by monitoring rainfall is now developing in the mostly rural mountainous areas in China because of wide regions and limited technology. It's very essential to do prevention and mitigation works by building necessary countermeasure structures in the potential debris flow valley and deposition fan. The parameters of quantitative evaluation of debris flow in terms of velocity, hydrograph, the extent of deposition and flow path can contribute to provide adequately protective measures to prevent and mitigate the disasters in practical engineering.

ACKNOWLEDGEMENT

During these three years in University of Tsukuba, I not only study some major knowledge, and also learn more things about how to be a person and how to do a thing. Firstly, I must thanks my advisor, professor Takashi Matsushima to give me the opportunity to study here under his guidance. His warm-hearted, patience and mild characteristic let me have a pleasure and relax study in Geotechnical Engineering group. His creativity, insight and passion for research always inspire to me. He taught me how to consider problem and how to resolve problem, and how to study a scientific problem. I have also greatly benefited from conferences I attended, thanks to his financial support. You are the great advisor in my life, and I'd love to express my deepest appreciation to you again!

I also would like to express sincere gratitude to professor Yasuo Yamada for giving me creative advice and comments on my research. His kind and happy lets me feel relax and happy in this group. I have also greatly benefited from conferences I attended, thanks to his financial support.

Thanks associate professor Yamamoto for guiding us to attend conference in Shanghai, and doing a lot of things for us. As well as all of helps in my study.

Thanks professor Kazuo Konagai, professor Shoji for providing useful advice and comments in my preliminary defense to improve my research. Thanks professor Kazuo Konagai again for introducing the research sources to me.

I express my sincere thanks to everybody in Geotechnical Engineering group. Thanks to doctor Ueda for picking me up in Narita Airport on 30 Aug. 2012, and providing much help to me. Thanks doctor Toyota for teaching me how to use the software of MapMatrix and resolving kinds of problems for many times. Miss Ayumi Suzuki is a kind and warm-hearted girl, thanks for providing kinds of help to me. It's you let me adjust the live in Japan easily, feel the kind and warm-hearted of the Japanese. I'd love to express my deepest appreciation to you again! Thanks to doctor Nakata, for providing kinds of help to me and accompanying me in three years. You make me not feel lonely any more, and not hurry to do one thing. Thanks to Kundo-kun, Ikezawa-kun, Abe-kun, Ito-kun, Otake-kun as well as all of members in Geotechnical engineering group, theirs' kind, warm-hearted, let me enjoy a safe, relax and happy life in three years here. Thanks all of members in Geotechnical engineering group for understanding and help during my preliminary defense and move.

I am grateful thanks to doctor Wenli Huang, doctor Wei Zhang, doctor Guoling Li,

doctor Xia Hao, doctor Junping Liu, doctor Shaohua Guo, doctor Shenghao Wang, doctor Qing Shi, doctor Ningbo Peng as well as all of my friends who gave me great help and happy in three years.

My heartfelt and deepest appreciation goes to my parents and sisters. Thanks theirs' daily encouragement and support.

Finally, thanks doctor Xiaowei Liu and doctor Faguo He to guarantee for me and China Scholarship Council for sponsoring me three years to study in Japan.

REFERENCE

An P.J., Li L., Zhang Z.Q. A bibliometrical analysis of international landslide research. Advances in Earth Science, 2011, 26(10): 1116-1124. (in Chinese)

Chen H., Lee C.F. Numerical simulation of debris flows. Canadian geotechnical journal, 2000, 37(1):146-160

Chen, N.S., Zhang, F. Movement and deposit characteristic of typical catastrophic debris flows by rainstorm in the mountainous area of southwestern China in 2003, Scientia geographica sinica, 2006, 26(26):701-705 (in Chinese).

Cui P., Chen X.Q., Wang Y.Y., et al. Jiangjia ravine debris flow in south-western China. Debris flow hazards and related phenomena, 2005, 22:565-594

Cui P., Zhou G.D., Zhu X.H., Zhang J.Q. Scale amplification of natural debris flows caused by cascading landslide dam failures. Geomorphology, 2013, 182:173-189

Davies T.R.H. Large debris flow: a macro-viscous phenomenon. Acta mechanica, 1986, 63:161-178.

Davies T.R.H. Debris-flow surges-experimental simulation. Journal of hydrology, 1990, 29(1):18-46.

Du R.H., Li H.L., Tang B.X., etc. Research on debris flow for thirty years in China. Journal of natural disasters, 1995, 4(1): 64-73. (in Chinese)

Fei X.J., Shu A.P. Movement mechanism and disaster control for debris flow. Tshinghua university press, 2004.

Fannin R.J., Wise M.P. An empirical-statistical model for debris flow travel distance. Canadian geotechnical journal, 2001, 38: 982-994.

Fukuoka H., Cui P., Hong Y. Mechanism of landslides triggered by the 2008 Wenchuan earthquake and subsequent rainstorm-induced debris flow. Investigation report of the 2008 Wenchuan Earthquake, China, Grant-in-Aid for Special Purposes of 2008, MEXT, No. 20900002, 75-84

Hakuno M., Uehida Y. Application of the Distinct Element Method to the numerical analysis of debris flows. Structural Eng./EarthquakeEng,1991,8(2),5-85, Proe, Japan Society of Civil Engineers,1991.

Han J.L., Wu S.R., He S.J., etc. Basal characteristics and formation mechanisms of geological hazards triggered by the May 12, 2008 Wenchuan earthquake with a moment magnitude of 8.0. Earth Science Frontiers, 2009, 16(3): 306-326

Huttcr K., Svendsen B., Rickenmann D. Debris flow modeling: A review, Continuum Mech. Thermodyn. 1996, 8:1-35

Hu K.H., Ge Y.G., Cui P., Guo X.J., Yang W. (2010) Preliminary Analysis of extra-large scale debris flow disaster in Zhouqu County of Gansu Province, J. Mountain Sci., 28: 628-634, (in Chinese).

Suwa H., Okano K., Kanno T. Forty years of debris -flow monitoring at Kamikamihorizawa Creek, Mount Yakedake, Japan, 2011, DOI: 10.4408/IJEGE.2011-03.B-066

Hoang, G.Q., Matsushima, T., Yamada, Y., Debris flow simulation by particle method using PRISM-DSM, Proceedings of 6th Geo-Kanto conference (in Japanese).

Huttcr K., Svendsen B., Rickenmann D. Debris flow modeling: a review. Continuum mechanics and thermodynamics, 1996, 8:1-35

Hübl J., Steinwendtner H. Two-dimensional simulation of two viscous debris flows in Austria. Physics and Chemistry of the Earth, Part C: Solar, Terrestrial & Planetary Science, 2001, 26(9): 639-644.

Huggel C., Schneider D., Miranda P.J., Granados H.D., Kääb A. Evaluation of ASTER and SRTM DEM data for lahar modeling: a case study on lahars from Popocatépetl volcano, Mexico. J Volcanol Geotherm Res, 2008, 170:99-110

Huang R.Q. After effect of geohazards induced by the Wenchuan Earthquake. Journal of engineering geology, 2011, 19(2):145-151 (in Chinese)

Huang R.Q., Fan X.M. The landslide story. Nature geoscience, 2013, 6: 325-326.

Huang R.Q., Li W.L. Research on development and distribution rules of geohazards induced by Wenchuan earthquake on 12 May 2008. Chinese journal of rock mechanics and engineering, 2008, 27(12):2585-2592 (in Chinese)

Iverson R.M. Debris-flow mechanics. Debris-flow hazards and related phenomena, 2005,105-134.

Iverson RM. The physics of debris flows. Rev. Geophys., 1997, 35(3): 245-296

Iverson, R.M.; Costa, J.E.; LaHusen, R.G. Debris-flow flume at HJ. Andrews experimental forest, Oregon. Open-file report, 1992, 92-483

Iverson RM. Debris flows: behavior and hazard assessment. Geology today, 2014, 30(1):15-20

Gan J.J., Huang R.Q., Li Q.Y., etc. Formation mechanism of geo-hazards triggered by Wenchuan MS 8.0 earthquake along Dujiangyan-Wenchuan highway. Journal of geomechanics, 2010, 16(2): 146-158 (in Chinese)

Gorum T. Fan X.M., Westen C.J., et al. Distribution pattern of earthquake-induced landslides triggered by the 12 May 2008 Wenchuan Earthquake. Geomorphology 2011, 133, 152-167

Gan J.J., Sun H.Y., Huang R.Q., etc. Study on mechanism of formation and river blocking of Hongchungou giant debris flow at Yingxiu of Wenchuan county. Journal of catastrophology, 2012, 27(1): 5-16 (in Chinese)

Ge Y.G., Chen X.Z., Zhuang J.Q., Zhu X.H. Characteristics, impacts and risks of dammed lakes induced by debris flows at the Wenchuan earthquake areas. Journal of Water Resource and Protection, 2014, 6, 1574-1588

Ge Y.G., Cui P., Zhang J.Q., Zeng C., Su F.H. Analysis and Management of Changing Risks for Natural Hazards, International conference, Padua, Italy. 2014, 6, 1574-1588

Guo X.J., Cui P., Ma L., Kong Y.D. Triggering rainfall characteristics for debris flows along Dujiangyan-Wenchuan highway of Sichuan. Journal of mountain research, 2014, 32(6):739-746

(in Chinese)

Konagai K., Ishikawa Y., Tsuchiya S., et al. Geotechnical issues caused by the May 12th2008, Wenchuan earthquake, China. Investigation report of the 2008 Wenchuan Earthquake, China, Grant-in-Aid for Special Purposes of 2008, MEXT, No. 20900002, 85-94

Li R.D., Wang G.L., Zhao C. et al. Analysis of Material Sources Derived from Sanyanyu Debris Flow in Zhouqu County, northwestern geology, 2011, 44(3):21-29. (in Chinese)

Lin L.J., Fang C., Li X.J., Xu J.Y., Liu C.Z. Preliminary investigation of geo-hazards in 5.12 Wenchuan earthquake zone. Hydrogeology & Engineering Geology, 2008, 1-5 (in Chinese)

Liu C.Z., Miao T.B., Chen H.Q. et al. (2011) Basic feature and origin of the "8・8" mountain torrent-debris flow disaster happened in Zhouqu County, Gansu, China, 8 Aug. 2010. Geological Bulletin of China, 30(1):141-150(in Chinese)

Liu Q.H., Tang C., Chang M., Yu B. Risk of debris flow in epicenter of Wenchuan earthquake, Yingxiu of Sichuan. Journal of mountain research, 2012, 30(5):592-598 (in Chinese)

Liu, G.R. and Liu, M.B.: Smoothed particle hydrodynamics, World Scientific Publishing, 2003.

Logan, M., and Iverson, R.M., 2007, revised 2013, Video documentation of experiments at the USGS debris-flow flume 1992–2006 (amended to include 2007-2013): U.S. Geological Survey Open-File Report 2007-1315 v. 1.3., http://pubs.usgs.gov/of/2007/1315/.

Major J.J. Experimental Studies of Deposition at a Debris Flow Flume. USGS Open-field report: 1990, 0-28.

Major J.J. Depositional processes in large-scale debris-flow experiments. The journal of geology, 1997, 105:345-366.

Major J.J., Iverson R.M. Debris flow deposition: effects of pore-fluid pressure and friction concentrated at flow margins. Geological society of America bulletin, 1999, 111(10): 1424-1434.

Matthias J., Scott M., Hamish W., Neil R. Debris-flow simulations on Cheekye river, British Columbia. Landslides, 2013, 10:685-699

Mergili M., Fellin W., Moreiras S.M., etc. Simulation of debris flows in the Central Andes based on Open Source GIS: possibilities, limitations, and parameter sensitivity, Nat Hazards, 2012, 61:1051-1081

Ma, D.T., Qi, L. 1997. Study on comprehensive controlling of debris flow hazards in Sanyanyu Gully, Bulletin of Soil and Water Conservation, 17, 26-31 (in Chinese).

Nakata, A.M., Matsushima, T., Yamada, Y. Risk mapping of landslides due to torrential rain in Brazil. Proceedings of 9th GeoKanto conference, 2012

Nakamura H., Tsuchiya S., Inoue K., et al. Sabo against earthquakes. Kokon shoin, Tokyo, Japan, 200, 190-220

Pastor M., Haddad B., Sorbino G., etc. A depth-integrated, coupled SPH model for flow-like landslides and related phenomena. Int.J. Numer.Anal.Meth.Geomech. 2009, 33:143-172

Pastor, M. et al., Application of a SPH depth-integrated models to landslide run-out analysis, Landslides, 11, 793-812, 2014.

Qi S.W., Xu Q., Lan H.X., et al. Spatial distribution analysis of landslides triggered by 2008.5.12 Wenchuan earthquake, China. Engineering geology, 2010, 116(1-2):95-108

Rickenmann D. Empirical relationships for debris flows. Natural hazards, 1999, 19: 47-77.

Rickenmann D., Laigle D., Mcardell B.W., Hubl J. Comparison of 2D debris-flow simulation models with field events. Computational geosciences, 2006, 10:241-264.

Stevens NF, Manville V, Heron DW. The sensitivity of a volcanic flow model to digital elevation model accuracy: experiments with digitised map contours and interferometric SAR at Ruapehu and Taranaki volcanoes, New Zealand. J Volcanol Geotherm Res, 2002, 119:89-105

Stolz A., Huggel C. Debris flows in the Swiss National Park: the influence of different flow models and varying DEM grid size on modeling results. Landslides, 2008, 5:311-319

Takahashi T. Debris flow mechanics, prediction and countermeasures. Taylor & Francis/Balkema, 2007.

Takahashi T. Progress in debris flow modeling. Progress in landslide science, 2007, 59-77.

Takahashi, T. Estimation of potential debris flows and their hazard zones; soft countermeasures for a disaster. Natural Disaster So. 1981b, 13, 57-89

Takahashi, T., Ashida, K., Sawai, K.: Delineation of debris flow hazard areas, in: Erosion and sediment transport in Pacific rim steeplands (Davies, T. R. H., Pearce, A. J., eds.) IAHS Publ. No. 1981, 132, 589-603

Takahahi T. A review of Japanese debris flow research. International journal of erosion control engineering, 2009, 2(1):1-14

Tang C, Rengers N, Van Asch TWJ, Yang YH, Wang GF. Triggering conditions and depositional characteristics of a disastrous debris flow event in Zhouqu city, Gansu Province, northwestern China. Nat Hazards Earth Syst Sci, 2011, 11(11):2903-2912

Tang C., Liang J.T. Characteristics of debris flows in Beichuan epicenter of the Wenchuan Earthquake triggered by rainstorm on September 24, 2008. Journal of Engineering Geology. 2008, 16 (2): 751-758. (in Chinese)

Tang C. A J. Zhu A W. L. Li A J. T. Liang Rainfall-triggered debris flows following the Wenchuan Earthquake. Bull Eng Geol Environ, 2009, 68:187-194

Tang C., Zhu J., Ding J., et al. Catastrophic debris flows triggered by a 14 August 2010 rainfall at the epicenter of the Wenchuan earthquake. Landslides, 2011, 8:485-497

Tang C., Li W.L., Ding J., etc. Field investigation and research on giant debris flow on 14 August 2010 in Yingxiu town, epicenter of Wenchuan earthquake. Earth science-Journal of China University of geosciences, 2011, 36(1):172-180 (in Chinese)

Tang C. Ding J., Liang J.T. Remote sensing images based observation analysis on characters of

debris flow source areas in Beichuan county of Wenchuan earthquake epicenter region. Journal of engineering geology, 2010, 18(1):1-7(in Chinese)

Tang C., Zhu J., Qi X., Ding J. Landslides induced by the Wenchuan earthquake and the subsequent strong rainfall. Engineering geology, 2011, 122:22-33

Tang C., Zhu J., Chang M., et al. An empirical-statistical model for predicting debris-flow runout zones in the Wenchuan earthquake area. Quaternary international, 2012, 250:63-73

Tang Y.J. '5.12' Wenchuan earthquake Sichuan zaiqu gonglu yingji diaocha yu qiangtong. China communication press, 2008.

Theule J.I., Liebault F., Loye A., etc. Sediment budget monitoring of debris-flow and bedload transport in the Manival Torrent, SE France. Natural hazards and earth system sciences, 2012, 12:731-749

Tu G.Q., Cheng Z.L., Liu J.K., Huang J.H. Assessment of debris flow danger in high-intensity earthquake area after intense earthquake-a case study of the Yingxiu-Chediguan section of G213 highway hit by the Wenchuan Earthquake. Journal of mountain research, 2013, 31(4):391-398 (in Chinese)

Vandine F., Bovis M. History and goals of Canadian debris flow research, a review. Natural Hazards, 2002, 26: 69-82.

Wang G.L., Li J., Yu G.Q. et al. Analysis on the Development Trend of Sanyanyu Valley Debris Flow, northwestern geology, 2011, 44(3):128-133. (in Chinese)

Wu J., Chen G.Q., Zheng L., etc. GIS-based numerical simulation of Amamioshima debris flow in Japan. Front. Struct. Civ. Eng. 2013, 7(2): 206-214

Xie H., Zhong D.L., Jiao Z., Zhang J.S. Debris flow in Wenchuan quake-hit area in 2008. Journal of mountain research, 2009, 501-509 (in Chinese)

Xu Q. The 13August 2010 catastrophic debris flows in Sichuan province: characteristics, genetic mechanism and suggestions. Journal of engineering geology, 2010, 18(5):596-608(in Chinese)

Xu Q., Li W.L. Distribution of large-scale landslides induced by the Wenchuan earthquake. Journal of engineering geology, 2010, 18(6):818-826(in Chinese)

Xu Q., Zhang S., Li W. L., Asch Th.W. J. The 13 August 2010 catastrophic debris flows after the 2008 Wenchuan earthquake, China. Nat. Hazards Earth Syst. Sci., 2012, 12, 201-216,

Yin Y.P., Wang F.W., Sun P. Landslide hazards triggered by the 2008 Wenchuan earthquake, Sichuan, China. Landslides, 2009, 6:139-151

Yu B, Yang YH, Su YC, Huang WJ, Wang GF. Research on the giant debris flow hazards in Zhouqu County, Gansu Province on August 7, 2010. J Eng Geol, 2010, 04:437-444

You Y., Liu J.F., Chen X.Z. Disaster characteristics and optimal design of drainage canal of debris flow following Wenchuan earthquake in Weigou gully in Beichuan county, Sichuan province, China. Italian Journal of Engineering Geology and Environment, 2011 Casa Editrice Università

La Sapienza, DOI: 10.4408/IJEGE.2011-03.B-088

Zhao YC, Cui CG. A study of rainstorm process triggering Zhouqu extremely mudslide on 8 August 2010. Torrential Rain Disaster, 2010, 9:289-295 (in Chinese)

Zhang N., Matsushima T., Yamada Y. Efficient numerical simulation of debris flow with erosion and sedimentation. Proceedings of 14th IACMAG, 2014,1529-1534

Zhang Y.S., Cheng Y.L., Yao X., etc. The evolution process of Wenchuan earthquake-landslide-debris flow geohazard chain. Geological bulletin of China, 2013, 32(12):1900-1910 (in Chinese)

Zou Q., Guo X.J., Zhu X.H., Kong Y.D. Hazard characteristics and causes of "7・10" debris flow along highways in the upper reaches of Minjiang River. Journal of mountain research, 2014, 32(6):747-753

Zhuang J.Q., Cui P., Ge Y.G., Pei L.Z.Hazard assessment of debris flow valleys along Dujiangyan Wenchuan highway after '5.12' Wenchuan devastating earthquake. Journal of Sichuan University (engineering science edition). 2009, 41(3): 131-139 (in Chinese)

Zhu L.F., Zhao C., Yu G.Q. etc. Accumulation characteristics of Sanyanyu extremely big debris flow, northwestern geology, 2011, 44(3):30-37. (in Chinese)

http://vulcan.wr.usgs.gov/

http://www.preventionweb.net/english/

User handbook, Earth observation research center, Japan aerospace exploration agency

PUBLICATIONS

N. Zhang, T. Matsushima, Y. Yamada. Review on depositional behavior of viscous debris flow. Proceedings of the international conference on advances in civil, structural and environmental engineering, doi:-10.3850/978-981-07-7965-8_31, 2013, 57-66

Ni Zhang, Takashi Matsushima, Yasuo Yamada. Simulation of large-scale debris flow with particle method. COMPSAFE 2014, 394-396

N. Zhang, T. Matsushima, Y. Yamada. Efficient numerical simulation of debris flow with erosion and sedimentation. 14th IACMAG Conference, 2014, 1529-1534

Ni Zhang, Takashi Matsushima, Yasuo Yamada. Simulation of debris flow deposition by depth-integrated particle method. The Twenty-seventh KKHTCNN Symposium on Civil Engineering